Aus dem Bereich Physiologie
Theoretische Medizin und Biowissenschaften
der Medizinischen Fakultät
der Universität des Saarlandes, Homburg/Saar

GnRH-induced calcium signals and spike activity in GnRHR neurons: Change in activity during reproductive cycle?

Dissertation zur Erlangung des Grades eines Doktors der Naturwissenschaften

der Medizinischen Fakultät
der UNIVERSITÄT DES SAARLANDES
2014

vorgelegt von Christian Lothar Schauer
geboren. am 24. Mai 1977 in München

Tag des Prüfungskolloquiums: _____

Dekan: _____

Vorsitzender: _____

Berichterstatter: _____

_____

_____

To my marvelous parents and my beloved wife

and

to all persons who don't take themselves too seriously…

Index

List of figures I

Abbreviations III

Zusammenfassung VII

Abstract IX

1. Introduction 1

1.1. The Hypothalamic-Pituitary-Gonadal-Axis 1

1.2. GnRH 2

1.2.1. Structure of GnRH 2

1.2.2. GnRH synthetizing and releasing neurons 3

1.2.3. GnRH receptor 3

1.2.4. Activation of GnRHR expressing neurons 4

1.3. Distribution of GnRHR neurons in the brain 6

1.4. GnRHR related pathologies 8

1.5. Aims 9

1.6. References 11

2. Materials & Methods 18

2.1. Materials 18

2.1.1. Chemicals and enzymes 18

2.1.2. Solutions and buffers 19

2.1.3. Consumables 20

2.1.4. Equipment 21

2.1.5. Software 23

2.2. Methods 24
2.2.1. Animals 24
2.2.2. Assessment of the reproductive stages 24
2.2.3. Ca^{2+} Imaging of τGFP-tagged GnRHR neurons 25
2.2.4. Loose patch clamp method 27
2.2.5. Analysis of data acquired from loose patch clamp recording 28
2.2.6. Statistics 29

2.3. References 30

3. A method to measure Ca^{2+} responses in GFP-tagged hypothalamic GnRHR neurons by confocal microscopy ____ 32

3.1. Abstract 32

3.2. Protocol 33
3.2.1. Preparation of solution and agarose gel 33
3.2.2. Dissection of the mouse brain 33
3.2.3. Slicing coronal hypothalamic sections of the mouse brain 35
3.2.4. Preparation of the Ca^{2+} indicator dye loading solution 36
3.2.5. Microscopy and analysis 37
3.2.6. Representative results 40

3.3. Discussion 42

3.4. References 43

4. A new model for studying neural circuits underlying reproductive physiology in the mouse brain ____ 45

4.1. Abstract 45

4.2. Introduction 45

4.3. Results 46
4.3.1. Visualization of fluorescently labeled GnRHR neurons 46
4.3.2. τGFP labelled GnRHR neurons express a functional GnRH receptor 47
4.3.3. Quantification of GnRH induced Ca^{2+} signals in GnRHR neurons 49

4.3.4. GnRH-induced Ca^{2+} signals are not dependent on network activity or voltage-activated channels 49

4.4. Discussion 50

4.5. References 52

5. Endogenous GnRH determines GnRHR neuron spike code activity during female cyclicity 55

5.1. Abstract 55

5.2. Introduction 55

5.3. Results 57

5.3.1. GnRHR neurons are spontaneously active and change their spike activity patterns depending on the female's reproductive stage 57

5.3.2. Dose-dependent modulation of action potential firing by GnRH 62

5.3.3. Endogenous GnRHR activity regulates the neuronal spike code 64

5.4. Discussion 66

5.4.1. Involvement of GnRH or estradiol 67

5.4.2. Possible role of receptor expression or internalization during the estrous cycle 68

5.4.3. Mechanisms underlying GnRHR-induced spike code modulation 69

5.5. References 70

6. Discussion 76

6.1. References 79

7. Publications 81

7.1. Permission of use 82

8. Acknowledgements _____ **84**

9. Curriculum Vitae _____ **85**

List of figures

Chapter 1

Figure 1 The Hypothalamic-Pituitary-Gonadal axis 1

Figure 2 Schematic representation of hypothalamic GnRH (GnRH type I) 2

Figure 3 The murine GnRH receptor 4

Figure 4 Possible intracellular signal pathways in hypothalamic GnRHR neurons 5

Figure 5 GnRHR expression in different brain areas 7

Chapter 2

Figure 6 Cytological assessment of reproductive stage 25

Figure 7 Preparation of a multi-barrel pipette 28

Chapter 3

Figure 8 Tools, material and steps for excising a mouse brain 34

Figure 9 Slicing of coronal hypothalamic sections of the mouse brain 36

Figure 10 Brain slice positioned in recording chamber 38

Figure 11 Gravity drive multi-channel bath application 38

Figure 12 Ca^{2+} signals in τGFP neurons of mouse hypothalamic brain slices 41

Chapter 4

Figure 13 Visualization of τGFP expressing GnRHR neurons in acute brain slice preparations 47

Figure 14 GnRHR-τGFP cell loaded with fura-red/AM 47

Figure 15 Examples of somatic Ca^{2+} responses from individual GnRHR neurons located in (A) the Pe, (B) the Arc, and (C) the PAG 48

Figure 16 Average Ca^{2+} responses (AUC) in GnRHR neurons of the Pe, the Arc, the DM, and the PAG 49

Figure 17 Somatic Ca^{2+} responses from an individual GnRHR neuron located in (A) the Pe and (B) the DM 50

Chapter 5

Figure 18 Coronal brain slice showing the location of the periventricular nucleus 56

Figure 19 Overlay of a fluorescence image on top of an infrared-differential interference contrast (IR-DIC) micrograph of a live brain tissue slice identifying a GnRHR neuron in the Pe, which is located next to the third ventricle 57

Figure 20 Example recordings of trains of extracellularly recorded, action-potential-driven capacitive currents of three different GnRHR neurons (n1 – n3) 58

Figure 21 Distribution of GnRHR neurons plotted in a two- (A-C) and three-dimensional (D) space using the first three principal components..... 59

Figure 22 Bar histogram of the CV_{ISI} (A), the MSiB (B) and the PSiB (C) dependent on the spike activity classification of GnRHR neurons 59

Figure 23 GnRHR neurons change their spontaneous spike activity pattern during the reproductive cycle..... 60

Figure 24 Distribution of firing pattern in GnRHR neurons depends on reproductive stage..... 61

Figure 25 GnRH modulates the neuronal activity of GnRHR neurons dose-dependently..... 62

Figure 26 GnRHR neurons possess long-lasting changes in spike activity after a brief GnRH stimulation 63

Figure 27 Long-term application of GnRH changes the firing pattern of GnRHR neurons 64

Figure 28 Effect of GnRH long-term application depends on reproductive state 65

Figure 29 GnRHR induced changes of the firing pattern is reversible in GnRHR neurons 66

Abbreviations

129SvJ	Mouse strain
2D	Two-dimensional
3D	Three-dimensional
3V	Third ventricle (*ventriculus teritius*)
αT3	Human pituitary cell line
AC	Adenylate cyclase
AM	Acetoxymethyl ester
ANOVA	Analysis of variance
Arc	Arcuate nucleus of the hypothalamus
ART	Assisted reproductive technology
ATPase	Adenosinetriphosphatase
BES	N,N-Bis(2-hydroxyethyl)-2-aminoethanesulfonic acid
°C	Degree Celsius
C57BL/6J	Mouse strain
Ca^{2+}	Calcium ion
CAGS	Cytomegalovirus early enhancer chicken beta actin rabbit Beta-globulin gene sequence promoter
cAMP	Cyclic adenosine monophosphate
Ca_v	Voltage dependent calcium channel
CBP	Calcium-binding protein
CNG channel	Cyclic nucleotide-gated ion channels
COOH terminus	Carboxyl terminus
CV_{ISI}	Coefficient of the variation of the interspike interval
dB	Decibel
[D-TRP^6]-LHRH	GnRH analog
DAG	Diacyl-glycerol
DF	Dark field
DM	Dorsomedial hypothalamic nucleus
DMSO	Dimethyl sulfoxide
EGTA	Ethylene glycol tetraacetic acid
ER	Endoplasmic reticulum

eROSA26	Enhanced Rosa26
et al.	*et alii / et aliae*
F	Fluorescence intensity
F_0	Starting/ base line fluorescence intensity
ΔF	Change in fluorescence intensity
F_{max}	Maximum of fluorescence intensity
F_{min}	Minimum of fluorescence intensity
$F_{n,m}$	Degrees of freedom
FSH	Follicle-stimulating hormone
G protein	Guanosine nucleotide-binding protein
G_α	Alpha subunit of the guanosine nucleotide-binding protein
G_β	Beta subunit of the guanosine nucleotide-binding protein
$G\gamma$	Gamma subunit of the guanosine nucleotide-binding protein
$G\alpha i$	Inhibiting subtype of alpha subunit of the guanosine nucleotide-binding protein
$G\alpha q/11$	Ca^{2+} increasing subtype of alpha subunit of the guanosine nucleotide-binding protein
$G\alpha s$	Stimulating subtype of alpha subunit of the guanosine nucleotide-binding protein
GFP	Green fluorescent protein
τGFP	Tau-green fluorescent fusion protein
GnRH	Gonadotropin releasing hormone
GnRHR	Gonadotropin releasing hormone receptor
GPCR	G-protein coupled receptor
GRIC	GnRHR-internal ribosome entry site-Cre
GRIC/eR26-τGFP	Mouse strain
HEK	Human embryonic kidney cell line
HPG	Hypothalamic-pituitary-gonadal
Hz	Hertz
i	Symbol for running counter
ICSI	Intracytoplasmic sperm injection
id	Inner diameter
IHH	Idiopathic hypogonadotropic hypogonadism
IP_3	Inositol trisphosphate

IP_3R	Inositol trisphosphate receptor
IR-DIC	Infrared-differential interference contrast
ISI	Interspike interval
IVF	*In vitro* fertilization
K^+-channels	Voltage dependent potassium channel
$K_{1/2}$	Statistic half maximum value
KCl	Potassium chloride
K_d	Dissociation constant
L	Liter
LH	Luteinizing hormone
LHRH	Luteinizing hormone releasing hormone synonym for GnRH
LSD	Least significant difference
m	Meter
M	Molar
mf	Mean frequency
min	Minute
mRNA	Messenger ribonucleic acid
MSiB	Mean spikes in burst
n	Sample number
Na_v	Voltage dependent sodium channel
NCX	Sodium-calcium exchanger
NIH	National Institutes of Health
NH_2-terminus	Amino-terminus
Ω	Ohm
od	Outer diameter
Osm	Osmole
p	p-value
PAG	Periaqueductal gray
PBS	Phosphate buffered saline
Pe	Periventricular nucleus of the hypothalamus
pH	*potentium hydrogenii*
PIP_2	Phosphatidylinositol 4,5-bisphosphate
PLC	Phospholipase C
PSiB	Percentage of spikes in bursts

R26	Rosa26
ROI	Region of interest
RyR	Ryanodine receptor
s	Seconds
S1	Extracellular solution 1
S2	Extracellular solution 2
SD	Standard deviation
SERCA	Sarco/endoplasmic reticulum Ca^{2+}-ATPase
t_0	Time of the onset of stiumulus
TRP channel	Transient receptor potential
TTX	Tetrodotoxin
UV	Ultraviolet
VARiF	Variance of the instantaneous spike frequency
VNO	Vomeronasal organ
w/v	Mass concentration, mass/volume
YPF	Yellow fluorescent protein

Amino acids

Arg	Arginine
Glu	Glutamic acid
Gly	Glycine
Pro	Proline
Ser	Serine
Trp	Tryptophne
Tyr	Tyrosine
Val	Valine

Zusammenfassung

Das Hormon Gonadoliberin (engl. Gonadotropine releasing hormone, GnRH) spielt eine entscheidende Rolle in der Reproduktionsphysiologie und wird daher auch „Master molecule of reproduction“ (engl. sinngemäß: Hauptmolekül der Fortpflanzung) genannt. GnRH ist ein entscheidender Faktor in der sexuellen Entwicklung, ebenso spielt es eine wichtige Rolle in der Regulierung unterschiedlicher endokrinologischer und physiologischer Signale im Gehirn. Welche Funktion es jedoch in der neuronalen Aktivierung hat ist weiterhin unklar, da die Möglichkeiten einzelne Neurone, welche von GnRH aktiviert werden – GnRH-Rezeptor (GnRHR) exprimierende Neurone, in lebenden Gehirnschnitten zu identifizieren sehr eingeschränkt sind.

Eine derartige Identifizierung GnRHR exprimierender Neurone in einer Lebendpräparation ist nur mittels genetischer Markierung, in diesem Fall durch die Kopplung von GnRHR mit dem grün fluoreszierendem Protein (τGFP), möglich (GnRHR/eR26-τGFP Mauslinie). Unter Verwendung dieser speziellen Mäuse konnte ein neuartiges Versuchsprotokoll für konfokales Kalzium-Imaging entwickelt werden. Mit diesem Verfahren konnte gezeigt werden, dass τGFP markierte Neurone einen funktionierenden GnRH Rezeptor exprimieren. GnRHR Neurone können reproduzierbar durch extrazelluläre Stimulierung mit GnRH oder einem GnRH-Analog, [D-TRP6]-LHRH, aktiviert werden. Diese Aktivierung ist netzwerkunabhängig da sie unter der Wirkung des Natriumkanalblockers Tetrodotoxin, welcher die synaptische Aktivität des Netzwerkes stark reduziert, weiterhin auftritt. Interessanterweise zeigen GnRHR Neurone eine, in Bezug auf Dauer und Form, individuelle Antwort auf Stimulierung, welche in den verschiedenen Nuklei sehr unterschiedlich, jedoch nukleusspezifisch gleichförmig ausfällt. Dies legt nahe, dass GnRH abhängige Signale in verschieden Bereichen des Gehirns unterschiedlich verarbeitet werden und damit vielfältigen Einfluss, beispielsweise auf den Reproduktionserfolg, haben können.

Um genauere Informationen über die Aktivität der GnRHR Neurone zu erhalten, wurden GnRHR Neurone des hypothalamischen periventrikulären Nukleus in lebenden Gehirnschnitten mit der minimal invasiven Loose-Patch-Clamp Methode untersucht. Diese Neurone zeigten eine dauerhaft vorhandene Aktionspotentialgrundaktivität, welche sich in unterschiedlichen Aktivitätsmustern – gleichförmig (tonic), hochfrequent-blockartig (bursting) oder ungleichmäßig (irregular) – manifestiert. Mittels verschiedener physikalischer Parameter konnten die verschieden Aktivitätsmuster eindeutig kategorisiert werden. Die

Wahrscheinlichkeit für das Auftreten der einzelnen Aktivitätsmuster ändert sich in Abhängigkeit und korreliert mit den Phasen des Sexualzyklus, was auf die Änderungen des endogenen GnRH-Spiegels im Verlauf des Sexualzyklus zurückgeführt werden kann. Dies konnte erfolgreich durch die Stimulation von GnRHR Neurone währen unterschiedlicher Phasen des Sexualzyklus in *in vivo* Experimenten simuliert werden. Hochfrequente blockartige Aktivitätsmuster, welche typisch für Burst-Aktivität sind, treten insbesondere in Anwesenheit von GnRH auf, wohingegen die Anwendung eines GnRH-Antagonist (Cetrorelix) eine Verschiebung zu tonischen Aktivitätsmustern verursacht. Kurzzeitige gepulste Stimulation mit unterschiedlichen Konzentrationen verursacht eine temporär erhöhte Aktivität der Neurone, bei welcher die Latenzzeit und die Dauer der Aktivierung sich als konzentrationsabhängig erwiesen. Durch Dauerstimulation konnte eine vollständige Änderung des Aktivitätsmusters induziert werden, was der physiologischen Modulation des GnRH-Spiegels über die verschiedenen Phasen des Sexualzyklus entspricht. Damit konnte gezeigt werden, dass GnRH über ein starkes neuromodulatorisches Potenzial verfügt.

Zusammenfassend kann gesagt werden, dass GnRHR exprimierende Neurone eine hohe Sensibilität für Veränderungen des GnRH-Spiegels während des Sexualzyklus aufweisen und mit einer Änderung ihrer Aktivitätsmuster reagieren. Dies dürfte zu einer verbesserten Transmitterfreisetzung und einer damit einhergehenden verbesserten Signalübertragung zwischen im neuronalen Netzwerk führen, was im Endeffekt zu einer Optimierung der Reproduktionswahrscheinlichkeit führt.

Abstract

Gonadotropin releasing hormone (GnRH) plays an essential role in reproductive physiology. As the so called master molecule of reproduction, it plays a key role in the regulation of the estrus cycle as well as in sexual maturation. It has been postulated to be implicated in the regulation of different hormonal and physiological signals in the brain. However, its function in neuronal excitation remains mainly unclear due to the difficulty in identifying direct GnRH signaling targets, the GnRH receptor (GnRHR) neurons in live brain tissue.

Mice, expressing τGFP with the GnRHR, allow identifying GnRH receptor (GnRHR) single neurons in acute mouse brain slices. Using a novel protocol for confocal Ca^{2+} imaging it could be shown that τGFP labelled GnRHR neurons express a functional GnRH receptor in GnRHR/eR26-τGFP mice. GnRHR neurons respond reproducibly to extracellular application of GnRH or its analog [D-TRP^6]-LHRH. GnRH induced GnRHR responses remain present after the application of the sodium channel blocker tetrodotoxin indicating that these responses are network independent. Interestingly, the duration and shape of the Ca^{2+} responses were similar within and different between brain areas, suggesting that GnRH signaling may differentially influence brain functions to affect reproductive success.

To obtain detailed information about the activity of hypothalamic periventricular GnRHR neurons without influencing the intracellular environment too much loose patch clamp technique was used. Periventricular hypothalamic GnRHR neurons show a continuous basic spike activity with different firing pattern – tonic, bursting or irregular. These distinct basic spike activity modes could be classified using independent properties of firing. The probability of expressing each firing pattern changes depending on the stage of reproductive cycle of the mice. The effect of changing GnRH levels in the brain can be successfully simulated in *in vivo* experiments. High-frequency clusters of action potentials, characteristic of a burst firing mode, are observed in the presence of GnRH, simulating changing GnRH levels during the estrous cycle. Contrary, the discharges change to a regular temporal pattern in the presence of a GnRHR antagonist. Information regarding the GnRH concentration to a pulsed stimulation is encoded in the response latency to the first spike, indicating that GnRHR neurons can respond timely to GnRH changes and more substantially with a long-lasting conversion in spike activity detected by the latency and duration of the modified variance in instantaneous spike frequency. A complete transformation in action potential firing pattern as seen during the estrous cycle is triggered by prolonged GnRH stimulation, manifesting this regulatory hormone as a strong neuromodulator. Taken together, GnRHR neurons are ideally attuned to vascular changes in

GnRH during the estrous cycle firing with brief action potential bursts after GnRH stimulation, potentially to be more effective in transmitter release and therefore enhance communication between neurons to optimize reproductive success.

1. Introduction

The Gonadotropin releasing hormone (GnRH) is the key player in the neuroendocrine regulation of the reproductive function in vertebrates via the hypothalamic-pituitary-gonadal axis. It has been implicated to control hormonal and physiological signals in the brain.

1.1 The Hypothalamic-Pituitary-Gonadal-Axis

Reproductive success is crucial for the survival of a species. In vertebrates, the adaptive regulation of the Hypothalamic-Pituitary-Gonadal axis (HPG axis) regulates the sexual maturation and reproductive function (Figure 1). The hypothalamus on the apex of the HPG axis forms the integrative center. Neurons that synthesize the decapeptide gonadotropin releasing hormone (GnRH, LHRH) are located in the supraoptic and periventricular part of the hypothalamus (Hoffman and Gibbs, 1982). These neurons release GnRH at the axon terminal of the medial eminence to the hypothalamo-hypophyseal portal circulation in the anterior pituitary (Gore, 2002; Herbison, 2006). The release of GnRH occurs pulsatile and with a substantially elevated surge during the late phase of proestrus (Krsmanovic et al., 2009; Sisk et al., 2001; Stojilkovic et al., 1994). In the anterior pituitary, following the HPG axis, GnRH binds to the GnRH receptor (GnRHR) of gonadotrope cells. This induces the liberation of the luteinizing hormone (LH) and follicle-stimulating hormone (FSH) into the bloodstream (Harris, 1964; Clayton and Catt, 1981). When LH and FSH bind to their respective receptor in the gonads, the synthesis of steroid hormones is stimulated. These steroid hormones are released to the circulatory system and transported into different target tissues including the brain (Beato and Klug,

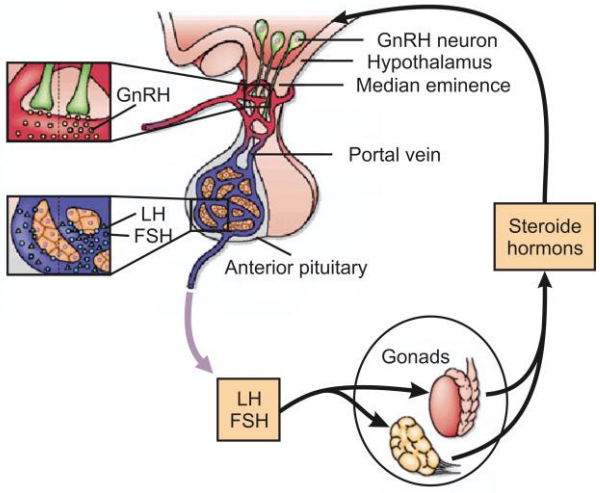

Figure 1. The Hypothalamic-Pituitary-Gonadal axis. GnRH is synthesized by neurons in the hypothalamus and released via the hypothalamo-hypophyseal portal circulation. In the anterior pituitary, it binds to GnRH receptors of the gonadotrope cells and stimulates the release of LH and FSH to the bloodstream. LH and FSH reaching the gonads induce the production and release of steroid hormones to the circulatory system. Transported by the bloodstream to the hypothalamus and the hypophysis, they can act excitatory or inhibitory on GnRH neurons. Adapted from Sisk and Foster (Sisk and Foster, 2004)

2000). Steroid hormones are cholesterol derived and therefore highly lipophilic, what permits them to pass easily the blood-brain barrier and reach the hypothalamus (Woolley and Schwartzkroin, 1998). There they can act stimulatory or inhibitory on the production of GnRH in the hypothalamus and LH/FSH in the pituitary (Shupnik, 1996).

1.2 GnRH, a primary regulator of reproduction

1.2.1 Structure of GnRH

The neuropeptide GnRH is the central regulator of the reproductive hormonal cascade (Millar et al., 2004). The identity and structure of GnRH was first clarified from porcine hypothalami 1971 as a decapeptide (pGlu-His-Trp-Ser-Tyr-Gly-Leu-Arg-Pro-Gly.NH_2) (Schally et al., 1971; Baba et al., 1971; Matsuo et al., 1971). The NH_2 and COOH termini are involved in the receptor binding, whereas only the NH_2 ending is involved in the receptor activation (Figure 2) (Millar et al., 2004). GnRH is conserved in all mammals except the guinea pig (*Cavia porcellus*), where substitutions of the amino acids 2 and 7 were identified (pGlu-Tyr-Trp-Ser-Tyr-Gly-Val-Arg-Pro-Gly.NH_2) (Jimenez-Linan et al., 1997). Three different forms of GnRH have been identified, which are highly homologous, but have differences concerning particular amino acids in the decapeptide sequence (White et al., 1998; Miyamoto et al., 1984; Baba et al., 1971; Matsuo et al., 1971; Schally et al., 1971). GnRH type I expressing neurons are mainly present in hypothalamic areas, whereas GnRH type II is located in the midbrain. GnRH type III, located in the forebrain exclusively can be found in teleost fish (Vizcarra, 2013). Normally at least two forms of GnRH are present in the majority of vertebrate species (Millar et al., 2004). Neither GnRH type II nor GnRH type III have been identified in mice so far (Pawson et al., 2003; Morgan and Millar, 2004), therefore if not indicated otherwise GnRH refers to GnRH I in this work.

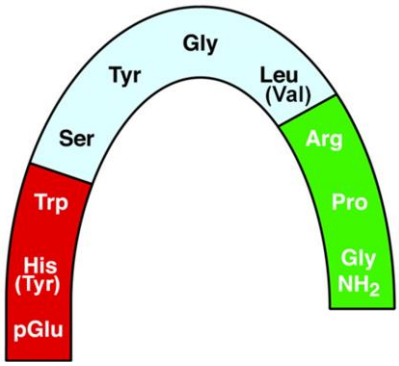

Figure 2. Schematic representation of hypothalamic GnRH (GnRH type I). GnRH consists of ten amino acids (mammalian amino acid sequence, in parenthesis substitutions in guinea pig). The NH_2 and COOH termini are involved in the receptor binding, only the NH_2 ending is involved in the receptor activation Adapted from Millar et al. (Millar et al., 2004).

1.2.2 GnRH synthetizing and releasing neurons

GnRH synthetizing and releasing neurons are mainly localized in hypothalamic nuclei of the brain. Apart of the hypothalamic, other small populations of GnRH neurons have been identified in several brain areas (Merchenthaler et al., 1984). All GnRH neurons (~800 neurons in mice (Wray et al., 1989)) have a common origin, namely the nasal placode. During the embryonic development, they migrate to the brain (Schwanzel-Fukuda and Pfaff, 1989; Schwanzel-Fukuda, 1999). Interestingly, GnRH neurons in sexually mature animals remain connected to the olfactory system (Boehm et al., 2005; Yoon et al., 2005), which processes a variety of sensory signals (Del Punta et al., 2002; Haga et al., 2010; Leinders-Zufall et al., 2000; Leinders-Zufall et al., 2004; Leinders-Zufall et al., 2009; Munger et al., 2010) influencing numerous behaviors, including reproduction (Insel and Fernald, 2004; Tirindelli et al., 2009). Signals of GnRH neurons are transmitted to more than 20,000 neurons in 31 brain areas and likely influence numerous brain functions (Boehm et al., 2005; Sherwood et al., 1993), but the individual neurons and neural circuits that mediate these behavioral effects have not been elucidated. Female reproductive behaviors such as lordosis can be facilitated by GnRH infusion into hypothalamus (arcuate nucleus and medial preoptic area), periaqueductal gray or spinal subarachnoid space (Sirinathsinghji, 1983; Moss and Foreman, 1976; Sakuma and Pfaff, 1980). In males GnRH application decreases the latency to intromission and ejaculation (Moss and McCann, 1973). Vaccination induced antibodies against GnRH have been shown to be in male an effective immunocontraceptive in different species (Levy et al., 2004; Dunshea et al., 2001).

1.2.3 GnRHR receptor

The GnRH receptor (GnRHR) was identified in the pituitary first, but subsequently GnRHR expression could be identified in several types of tissues of the reproductive system (i.e. gonads, prostate, breast, placenta) (Stojilkovic et al., 1994; Kakar et al., 1994), as well as in non-reproduction related tissues (i.e. heart, muscle, liver, kidney) (Kakar and Jennes, 1995), several tumor tissues (Kakar et al., 1994) and different areas of the brain (Badr and Pelletier, 1987).

GnRHR was first cloned from the pituitary αT3 gonadotrope cell line (Reinhart et al., 1992; Tsutsumi et al., 1992) and consists of 327 amino acids (Sealfon et al., 1997). It is a member of the rhodopsin-like seven-transmembrane G protein-coupled receptor superfamily (Sealfon et al., 1997). Three GnRHR types have been described, type III occurs mainly in non-mammalians, whereas types I and II can be found in most vertebrates. In rodents and hominid

species only GnRHR type I is functionally expressed. Out of mice these species express the gene for GnRHR type II, but lack the receptor due to a frame shift and a stop codon (Millar, 2005). Therefore, if not indicated otherwise GnRHR refers to the GnRH type I receptor in this work. Although all types of GnRHR share the common structural architecture of GPCRs within the rhodopsin subfamily, the mammalian GnRHR type I possesses as a unique feature, the complete absence of the carboxyl-terminus (Sealfon et al., 1997). The lack of the carboxyl-terminus in the GnRHR is supposed to result in the inability of the receptor to undergo agonist-dependent phosphorylation. It correlates directly with a resistance of the receptor to rapid desensitization (Willars et al., 1999). In mammals, GnRHR can be activated by both, GnRH type I as well as by GnRH type II (Millar, 2003).

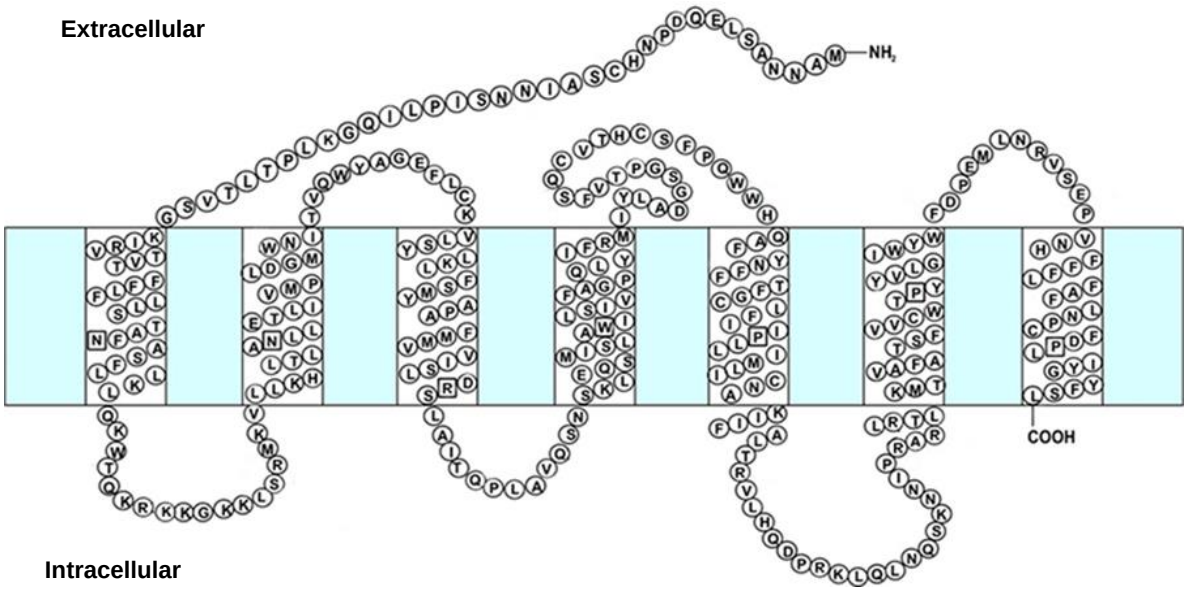

Figure 3. The murine GnRH receptor. The murine GnRHR consists of 327 amino acids and 7 transmembranes. The carboxyl-terminus is completely absent, what makes it having a unique structural architecture in the GPCRs. Adapted from (Millar et al., 2004).

1.2.4 Activation of GnRHR expressing neurons

The binding of GnRH to the GnRHR activates G-protein (guanosine nucleotide-binding proteins) mediated intracellular signaling. Hypothalamic GnRHR can be coupled to different Gα subunit types ($G\alpha_{q/11}$, $G\alpha_i$, $G\alpha_s$), and a G_β/G_γ complex (Krsmanovic et al., 2003). The different signal transducers subunits induce distinct pathways of intracellular signaling (Gilman, 1984). The $G\alpha_{q/11}$ signaling pathway is can be activated by calcium-mobilizing hormones. Phospholipase C (PLC) gets activated, causing a hydrolization of phosphatidyl-inositol-bisphosphate (PIP_2) into the second messengers inositol trisphosphate (IP_3) and

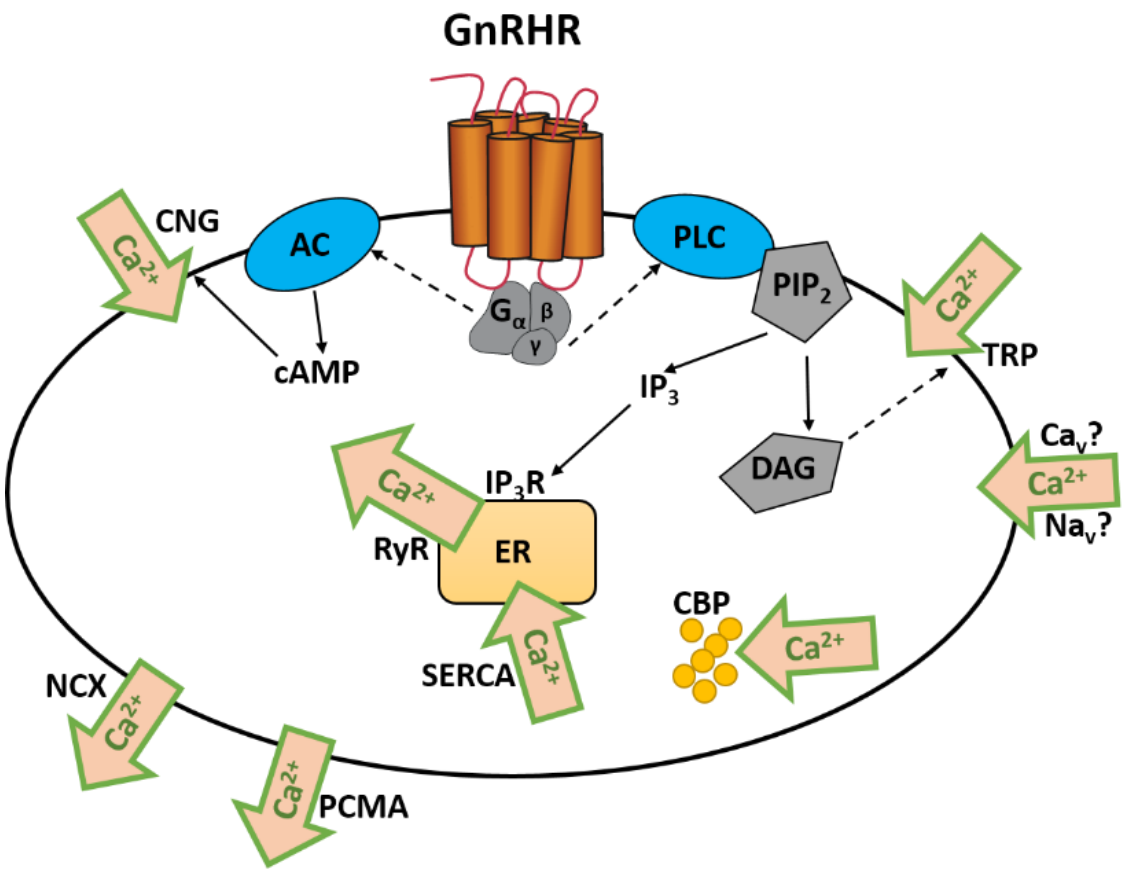

Figure 4. Possible intracellular signal pathways in hypothalamic GnRHR neurons. GnRHR (hypothalamic gonadotropin releasing receptor), Ca^{2+} (calcium), $G_{\alpha\beta\gamma}$ (G-protein subunits), AC (adenylate cyclase), cAMP (cyclic adenosine monophosphate), CNG (cyclic nucleotide-gated ion channels), NCX (sodium-calcium exchanger), PLC (phospholipase C), PIP_2 (phosphatidyl-inositol-bisphosphate), DAG (diacyl-glycerol), PCMA (plasma membrane calcium ATPase), TRP (transient receptor potential channels), ER (endoplasmic reticulum), IP_3 (inositol trisphosphate), IP_3R (inositol trisphosphate receptor), RyR (ryanodine receptor), SERCA (sarco/endoplasmic reticulum calcium-ATPase), CBP (calcium binding protein), Ca_v voltage gated calcium channel.

diacylglycerol (DAG) (Dickson et al., 2013). DAG could induce via transient receptor potential (TRP) channel activation a Ca^{2+} influx (Qiu et al., 2010). IP_3 triggers the activation of the IP_3 receptor (IP_3R) and thereby the release of calcium (Ca^{2+}) from intracellular stores of the endoplasmic reticulum (ER) (Falkenburger et al., 2013). An increase of Ca^{2+} levels close to the ER may activate ryanodine receptors (RyR) which than as well transport Ca^{2+} from the ER to the cytoplasm (Zucchi and Ronca-Testoni, 1997) The sarco-endoplasmic reticulum calcium ATPase (SERCA) functions to decrease the intracellular calcium concentration and to restore normal calcium levels in the ER (Syntichaki and Tavernarakis, 2003). The G_β/G_γ complex directly interacts with several proteins of importance in both effector as well as regulator function in the intracellular signaling (e.g. PLC (Park et al., 1993), AC (Tang and Gilman, 1991), IP_3 (Zeng et al., 2003)) (Smrcka, 2008).

The induced changes of the intracellular Ca^{2+} level in GnRHR neurons lead to a modulation of the membrane potential. By passing an individual threshold of depolarization, a short discrete electrical current - an action potential (or spike) is generated (Gerstner et al., 1997). Via axodentritic connection points (synapses), electric currents can transport signals and information to different brain areas, rapidly and over large distance. The rate and time coding of action potentials as binary signals allows a highly complex communication system in neuronal network of the brain which contains over 10^{11} neurons, each can have more than 10000 synaptic connections to other neurons (Izhikevich, 2000). Information transported by this network is encoded by variations of frequency, timing and the pattern of spiking, single spike and high frequency spike clusters (burst) (Gerstner et al., 1997). Bursting firing behavior, which is common in sensory input, is thought to encode high amounts of information, facilitate the release of neurotransmitter and provide a higher reliability in synaptic information transport (Lisman, 1997). Understanding the neuronal coding might permits the step from a local functional to a systemic analysis of signal transmission and the induced behavior. Neuronal networks and circuits integrate by electrical and chemical transmission most of the information processed in the brain and as a downstream result induces, regulates and inhibits physiologic functions and behavior.

1.3 Distribution of GnRHR neurons in the brain

GnRHR expression could be identified in several areas of the brain using receptor binding studies with radiolabeled GnRH and in situ hybridization studies. GnRH binding sites and GnRHR mRNA are present in several brain regions including the hypothalamus (Badr and Pelletier, 1987; Jennes et al., 1988; Jennes et al., 1997). However, these methods only allow localization studies in fixed tissue but not the identification of live primary GnRHR neurons nor the analysis of GnRH signaling in the central nervous system. To avoid this problem the group of Prof. Dr. Ulrich Boehm generated a new mouse model which provides the possibility of genetic identification of GnRHR expressing neurons (Wen et al., 2008). First, GnRHR-internal ribosome entry site-Cre (GRIC) mice were generated (Wen et al., 2008), which then were crossbred to a Rosa26-YFP (YPF, yellow fluorescent protein) reporter mouse line (Srinivas et al., 2001). The offspring (GRIC/R26-YFP) of these mice showed an irreversible Cre-mediated activation of the YFP reporter in GnRHR positive cells. The fluorescently marked neurons report the history of activity of the GnRHR promoter in GRIC/R26-YFP mice. In this way, the GRIC/R26-YFP mouse line could provide for the first time the possibility to

investigate the distribution of GnRHR expressing neurons in the brain (Wen et al., 2011). Using this mouse line the functionality of GnRHR could be shown in gonadotrope cells of the pituitary (Wen et al., 2008).

To facilitate the functional analysis in live brain slices a GnRHR/eR26-τGFP (GFP, green fluorescent protein) was generated by crossbreeding GRIC mice to eRosa26-τGFP reporter mice (eR26-τGFP) (Wen et al., 2011). The GnRHR/eR26-τGFP shows a sufficient high level of fluorescence that allows identifying the GnRHR positive cells in live brain slices (Wen et al., 2011). GnRHR neurons could be localized in several brain areas, including areas implicated in sexual behavior like the ventromedial hypothalamus, medial preoptic area and periaqueductal gray (Figure 4) (Wen et al., 2011). Using calcium imaging as well as electrophysiological recording techniques the functionality of GnRHR could be demonstrated in brain tissue of GnRHR/eR26-τGFP mice ((Wen et al., 2011); result section of these thesis).

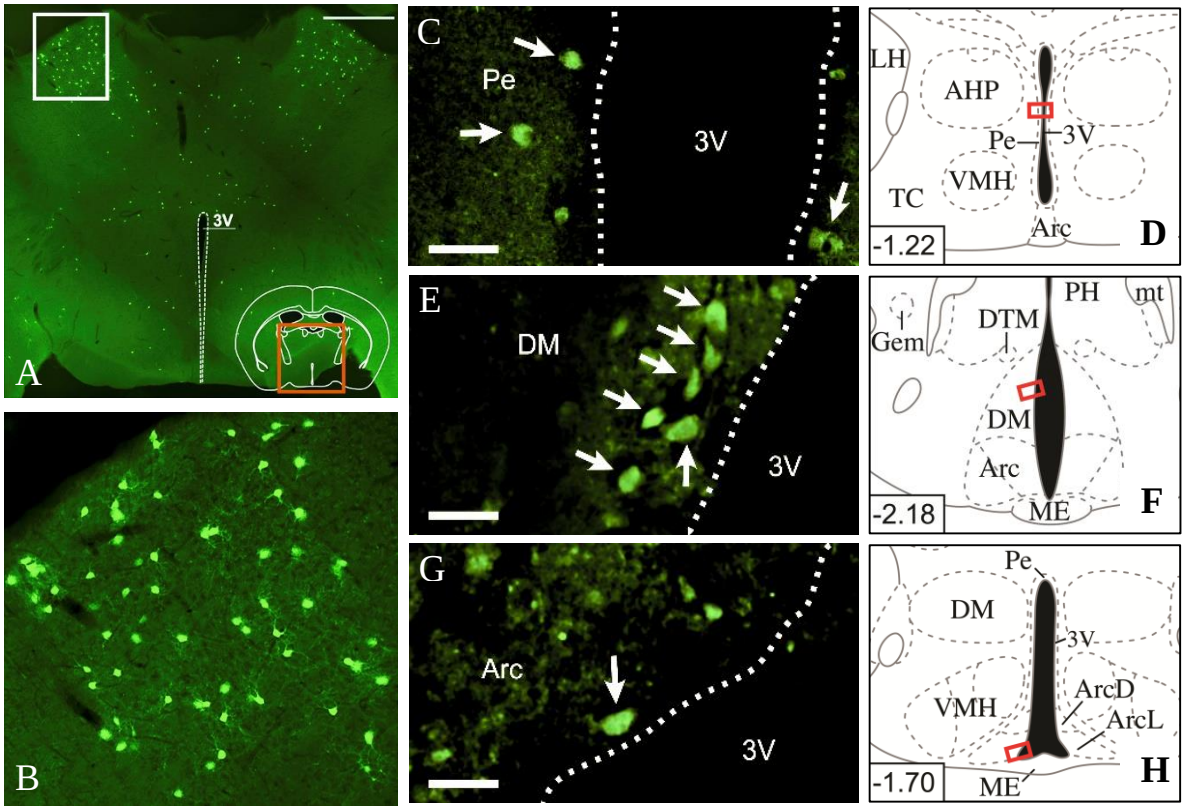

Figure 5. GnRHR expression in different brain areas. A, Immunostaining of a GRIC/R26-YFP mouse brain slice shows GnRHR expression in different brain areas. B, Magnified image (white square) of the thalamus. C, E, and G, Individual GnRHR neurons displaying robust τGFP fluorescence (arrows) are easily visible in 250 µm thick coronal brain tissue slices prepared from (C) the Pe, (E) the Arc, and (G) the DM of GRIC/eR26-τGFP mice. Scale bars, 20 µm. D, F, and H, Schematic diagrams indicating the imaged area (red box) shown in C, E, and G, respectively. Diagrams are adapted from Paxinos and Franklin (20). 3V, third ventricle. Lower left corner numbers indicate the distance (mm) from bregma. AHP, anterior hypothalamic area, posterior. Adapted from (Wen et al., 2011).

1.4 GnRHR related pathologies

Mutations of the gene coding the GnRHR can cause different pathologies. The most common is hypo-/hypergonadism where numerous mutations in the GnRHR have been described (de Roux et al., 1997). Up to 40% of familial cases of idiopathic hypogonadotropic hypogonadism (IHH) have been related to GnRHR mutations (Karges et al., 2003). In male patients GnRHR mutation induced hypogonadism pathologies like microphallus and undescended testes in childhood, failure of pubertal development in adolescence and infertility in adults have been reported (Karges et al., 2003). Women with GnRHR mutations typically have delayed puberty and primary amenorrhea (Karges et al., 2003).

The presence of GnRHR has been described in several cancer tissues, either tissues related to the reproductive system (i.e. prostate, breast, ovarian and endometrial cancers) or unrelated (i.e. melanoma, glioblastoma, lung, and pancreatic cancers) to the reproductive system (Limonta et al., 2012). Surprisingly, the activation on the GnRHR shows an inhibitory effect on cancer tissues, such as strong antiproliferative, antimetastatic and antiangiogenic effects. The activation of GnRHR by GnRH and its analogs offers a powerful therapeutic strategy in cancer treatment due to combination of inhibitory effects and a widespread expression over several tissues. Furthermore, GnRH analogs are used as carrier for potent anticancer drugs (GnRH analog-based cytotoxic hybrids, GnRH analog-based nutraceutic hybrids, and GnRHR-targeted nanoparticles, which specifically deliver cytotoxic compounds to cancer cells) (Limonta et al., 2012).

A dysfunction in GnRH/GnRHR can influence the reproductive success negatively as well as an optimization of the GnRH/GnRHR signaling can increase the chance of reproductive success. Assisted reproductive technologies (ART) offer the possibility to enhance the chance of positive reproductive outcome. The most common treatments in ART are *in vitro* fertilization (IVF) and intracatoplasmatic sperm injection (ICSI) (van Loenen et al., 2002). A crucial step in ART is GnRH agonist and antagonist induced controlled, ovarian hyperstimulation. The adequate application of GnRH agonists/antagonists leads to an increased live birth rate (Kyrou et al., 2011), as well as a decreased probability to develop ovarian hyperstimulation syndrome (OHSS), the most common and major complication of ovarian stimulation (van der Linden et al., 2012).

1.5 Aims

Knowledge regarding hypothalamic GnRHR neurons is restricted to expression/localization and behavioral investigations, the latter especially after GnRH injection into hypothalamic areas. The main goal of this thesis was to investigate for the first time the effect of GnRH on GnRHR expressing hypothalamic neurons in brain slices using physiological techniques. The following questions were addressed:

1) Do GnRHR/eR26-τGFP mice express a functional GnRHR in hypothalamic neurons? Due to the breeding scheme, it is not clear if these genetically marked neurons still express the receptor for GnRH. GnRHR could have been expressed during development and just due to the original activation of the promoter Cre is being expressed, activating the expression of τGFP. Normally, antibody staining could have been used, but unfortunately, the antibody against GnRHR is very unreliable. Therefore, we opted for a functional assay like calcium imaging.

2) If the genetically tagged neurons do indeed respond to GnRH confirming the existence of GnRHR expression, do all GnRHR neurons respond similarly and independent of the brain area? Therefore, we wondered if GnRHR neurons differ in their responsivity. GnRH neurons have various fibers reaching a multitude of brain areas. This suggests that many areas should also contain cells expressing GnRHR. Indeed, the data from (Wen et al., 2010) indicate that GnRHR seems to be expressed in neurons all over the brain. However, modulating the brain with a primary regulator like GnRH relies on the role and function of its target neurons. This suggests that these neurons may differ in their GnRH-induced activity.

3) Endogenous GnRH level likely changes in the brain during the estrous cycle influencing the activity of GnRHR neurons. In what way may GnRH induce any effect in GnRHR neurons? GnRH is released in a pulsatile way, but before estrus GnRH release intensifies. This increase in GnRH is needed for the induction of ovulation. It is however not clear, whether GnRH changes the activity of target neurons in the brain and in what manner. Using a non-invasive electrophysiological technique, we investigated the action potential activity of GnRHR neurons during the estrous cycle.

Understanding how GnRH influences the activity of GnRHR expressing neurons opens the way to a deeper understanding of intracerebral GnRH signaling mechanisms. This may help to

determine adverse effects of GnRH treatment in assisted reproductive techniques and hypogonadotropism treatment to improve therapeutic strategies.

1.6 References

1 BABA, Y., MATSUO, H. & SCHALLY, A. V. 1971. Structure of the porcine LH- and FSH-releasing hormone. II. Confirmation of the proposed structure by conventional sequential analyses. Biochem Biophys Res Commun, 44, 459-63.

2 BADR, M. & PELLETIER, G. 1987. Characterization and autoradiographic localization of LHRH receptors in the rat brain. Synapse, 1, 567-71.

3 BEATO, M. & KLUG, J. 2000. Steroid hormone receptors: an update. Human Reproduction Update, 6, 225-236.

4 BOEHM, U., ZOU, Z. & BUCK, L. B. 2005. Feedback loops link odor and pheromone signaling with reproduction. Cell, 123, 683-95.

5 CLAYTON, R. N. & CATT, K. J. 1981. Gonadotropin-releasing hormone receptors: characterization, physiological regulation, and relationship to reproductive function. Endocr Rev, 2, 186-209.

6 DE ROUX, N., YOUNG, J., MISRAHI, M., GENET, R., CHANSON, P., SCHAISON, G. & MILGROM, E. 1997. A Family with Hypogonadotropic Hypogonadism and Mutations in the Gonadotropin-Releasing Hormone Receptor. New England Journal of Medicine, 337, 1597-1603.

7 DEL PUNTA, K., LEINDERS-ZUFALL, T., RODRIGUEZ, I., JUKAM, D., WYSOCKI, C. J., OGAWA, S., ZUFALL, F. & MOMBAERTS, P. 2002. Deficient pheromone responses in mice lacking a cluster of vomeronasal receptor genes. Nature, 419, 70-4.

8 DICKSON, E. J., FALKENBURGER, B. H. & HILLE, B. 2013. Quantitative properties and receptor reserve of the IP(3) and calcium branch of G(q)-coupled receptor signaling. J Gen Physiol, 141, 521-35.

9 DUNSHEA, F. R., COLANTONI, C., HOWARD, K., MCCAULEY, I., JACKSON, P., LONG, K. A., LOPATICKI, S., NUGENT, E. A., SIMONS, J. A., WALKER, J. & HENNESSY, D. P. 2001. Vaccination of boars with a GnRH vaccine (Improvac) eliminates boar taint and increases growth performance. J Anim Sci, 79, 2524-35.

10 FALKENBURGER, B. H., DICKSON, E. J. & HILLE, B. 2013. Quantitative properties and receptor reserve of the DAG and PKC branch of G(q)-coupled receptor signaling. J Gen Physiol, 141, 537-55.

11 GERSTNER, W., KREITER, A. K., MARKRAM, H. & HERZ, A. V. M. 1997. Neural codes: Firing rates and beyond. Proceedings of the National Academy of Sciences, 94, 12740-12741.

12 GILMAN, A. G. 1984. Guanine nucleotide-binding regulatory proteins and dual control of adenylate cyclase. J Clin Invest, 73, 1-4.

13 GORE, A. C. 2002. GnRH: The master molecule of reproduction, Kluwer Academic Publishers.

14 HAGA, S., HATTORI, T., SATO, T., SATO, K., MATSUDA, S., KOBAYAKAWA, R., SAKANO, H., YOSHIHARA, Y., KIKUSUI, T. & TOUHARA, K. 2010. The male mouse pheromone ESP1 enhances female sexual receptive behaviour through a specific vomeronasal receptor. Nature, 466, 118-22.

15 HARRIS, G. W. 1964. Sex Hormones, Brain Development and Brain Function. Endocrinology, 75, 627-48.

16 HERBISON, A. E. 2006. Chapter 28 - Physiology of the Gonadotropin-Releasing Hormone Neuronal Network. In: NEILL, J. D., PLANT, T. M., PFAFF, D. W., CHALLIS, J. R. G., KRETSER, D. M. D., RICHARDS, J. S. & WASSARMAN, P. M. (eds.) Knobil and Neill's Physiology of Reproduction (Third Edition). St Louis: Academic Press.

17 HOFFMAN, G. E. & GIBBS, F. P. 1982. LHRH pathways in rat brain: 'deafferentation' spares a sub-chiasmatic LHRH projection to the median eminence. Neuroscience, 7, 1979-93.

18 INSEL, T. R. & FERNALD, R. D. 2004. How the brain processes social information: searching for the social brain. Annu Rev Neurosci, 27, 697-722.

19 IZHIKEVICH, E. M. 2000. Neural excitability, spiking and bursting. International Journal of Bifurcation and Chaos, 10, 1171-1266.

20 JENNES, L., DALATI, B. & CONN, P. M. 1988. Distribution of gonadrotropin releasing hormone agonist binding sites in the rat central nervous system. Brain Res, 452, 156-64.

21 JENNES, L., EYIGOR, O., JANOVICK, J. A. & CONN, P. M. 1997. Brain gonadotropin releasing hormone receptors: localization and regulation. Recent Prog Horm Res, 52, 475-90; discussion 490-1.

22 JIMENEZ-LINAN, M., RUBIN, B. S. & KING, J. C. 1997. Examination of guinea pig luteinizing hormone-releasing hormone gene reveals a unique decapeptide and existence of two transcripts in the brain. Endocrinology, 138, 4123-30.

23 KAKAR, S. S., GRANTHAM, K., MUSGROVE, L. C., DEVOR, D., SELLERS, J. C. & NEILL, J. D. 1994. Rat gonadotropin-releasing hormone (GnRH) receptor: tissue expression and hormonal regulation of its mRNA. Mol Cell Endocrinol, 101, 151-7.

24 KAKAR, S. S. & JENNES, L. 1995. Expression of gonadotropin-releasing hormone and gonadotropin-releasing hormone receptor mRNAs in various non-reproductive human tissues. Cancer Lett, 98, 57-62.

25 KARGES, B., KARGES, W. & DE ROUX, N. 2003. Clinical and molecular genetics of the human GnRH receptor. Hum Reprod Update, 9, 523-30.

26 KRSMANOVIC, L. Z., HU, L., LEUNG, P. K., FENG, H. & CATT, K. J. 2009. The hypothalamic GnRH pulse generator: multiple regulatory mechanisms. Trends Endocrinol Metab, 20, 402-8.

27 KRSMANOVIC, L. Z., MORES, N., NAVARRO, C. E., ARORA, K. K. & CATT, K. J. 2003. An agonist-induced switch in G protein coupling of the gonadotropin-releasing hormone receptor regulates pulsatile neuropeptide secretion. Proc Natl Acad Sci U S A, 100, 2969-74.

28 KYROU, D., KOLIBIANAKIS, E. M., FATEMI, H. M., TARLATZI, T. B., DEVROEY, P. & TARLATZIS, B. C. 2011. Increased live birth rates with GnRH agonist addition for luteal support in ICSI/IVF cycles: a systematic review and meta-analysis. Human Reproduction Update, 17, 734-740.

29 LEINDERS-ZUFALL, T., BRENNAN, P., WIDMAYER, P., S, P. C., MAUL-PAVICIC, A., JAGER, M., LI, X. H., BREER, H., ZUFALL, F. & BOEHM, T. 2004. MHC class I peptides as chemosensory signals in the vomeronasal organ. Science, 306, 1033-7.

30 LEINDERS-ZUFALL, T., ISHII, T., MOMBAERTS, P., ZUFALL, F. & BOEHM, T. 2009. Structural requirements for the activation of vomeronasal sensory neurons by MHC peptides. Nat Neurosci, 12, 1551-8.

31 LEINDERS-ZUFALL, T., LANE, A. P., PUCHE, A. C., MA, W., NOVOTNY, M. V., SHIPLEY, M. T. & ZUFALL, F. 2000. Ultrasensitive pheromone detection by mammalian vomeronasal neurons. Nature, 405, 792-6.

32 LEVY, J. K., MILLER, L. A., CYNDA CRAWFORD, P., RITCHEY, J. W., ROSS, M. K. & FAGERSTONE, K. A. 2004. GnRH immunocontraception of male cats. Theriogenology, 62, 1116-1130.

33 LIMONTA, P., MONTAGNANI MARELLI, M., MAI, S., MOTTA, M., MARTINI, L. & MORETTI, R. M. 2012. GnRH receptors in cancer: from cell biology to novel targeted therapeutic strategies. Endocr Rev, 33, 784-811.

34 LISMAN, J. E. 1997. Bursts as a unit of neural information: making unreliable synapses reliable. Trends in Neurosciences, 20, 38-43.

35 MATSUO, H., BABA, Y., NAIR, R. M., ARIMURA, A. & SCHALLY, A. V. 1971. Structure of the porcine LH- and FSH-releasing hormone. I. The proposed amino acid sequence. Biochem Biophys Res Commun, 43, 1334-9.

36 MERCHENTHALER, I., GORCS, T., SETALO, G., PETRUSZ, P. & FLERKO, B. 1984. Gonadotropin-releasing hormone (GnRH) neurons and pathways in the rat brain. Cell Tissue Res, 237, 15-29.

37 MILLAR, R. P. 2003. GnRH II and type II GnRH receptors. Trends Endocrinol Metab, 14, 35-43.

38 MILLAR, R. P. 2005. GnRHs and GnRH receptors. Animal Reproduction Science, 88, 5-28.

39 MILLAR, R. P., LU, Z. L., PAWSON, A. J., FLANAGAN, C. A., MORGAN, K. & MAUDSLEY, S. R. 2004. Gonadotropin-releasing hormone receptors. Endocr Rev, 25, 235-75.

40 MIYAMOTO, K., HASEGAWA, Y., NOMURA, M., IGARASHI, M., KANGAWA, K. & MATSUO, H. 1984. Identification of the second gonadotropin-releasing hormone in chicken hypothalamus: evidence that gonadotropin secretion is probably controlled by two distinct gonadotropin-releasing hormones in avian species. Proc Natl Acad Sci U S A, 81, 3874-8.

41 MOSS, R. L. & FOREMAN, M. M. 1976. Potentiation of lordosis behavior by intrahypothalamic infusion of synthetic luteinizing hormone-releasing hormone. Neuroendocrinology, 20, 176-81.

42 MOSS, R. L. & MCCANN, S. M. 1973. Induction of mating behavior in rats by luteinizing hormone-releasing factor. Science, 181, 177-9.

43 MUNGER, S. D., LEINDERS-ZUFALL, T., MCDOUGALL, L. M., COCKERHAM, R. E., SCHMID, A., WANDERNOTH, P., WENNEMUTH, G., BIEL, M., ZUFALL, F. & KELLIHER, K. R. 2010. An olfactory subsystem that detects carbon disulfide and mediates food-related social learning. Curr Biol, 20, 1438-44.

44 PARK, D., JHON, D. Y., LEE, C. W., LEE, K. H. & RHEE, S. G. 1993. Activation of phospholipase C isozymes by G protein beta gamma subunits. Journal of Biological Chemistry, 268, 4573-4576.

45 QIU, J., FANG, Y., RONNEKLEIV, O. K. & KELLY, M. J. 2010. Leptin excites proopiomelanocortin neurons via activation of TRPC channels. J Neurosci, 30, 1560-5.

46 REINHART, J., MERTZ, L. M. & CATT, K. J. 1992. Molecular cloning and expression of cDNA encoding the murine gonadotropin-releasing hormone receptor. J Biol Chem, 267, 21281-4.

47 SAKUMA, Y. & PFAFF, D. W. 1980. LH-RH in the mesencephalic central grey can potentiate lordosis reflex of female rats. Nature, 283, 566-7.

48 SCHALLY, A. V., ARIMURA, A., BABA, Y., NAIR, R. M. G., MATSUO, H., REDDING, T. W., DEBELJUK, L. & WHITE, W. F. 1971. Isolation and properties of

the FSH and LH-releasing hormone. Biochemical and Biophysical Research Communications, 43, 393-399.

49 SCHWANZEL-FUKUDA, M. 1999. Origin and migration of luteinizing hormone-releasing hormone neurons in mammals. Microsc Res Tech, 44, 2-10.

50 SCHWANZEL-FUKUDA, M. & PFAFF, D. W. 1989. Origin of luteinizing hormone-releasing hormone neurons. Nature, 338, 161-4.

51 SEALFON, S. C., WEINSTEIN, H. & MILLAR, R. P. 1997. Molecular mechanisms of ligand interaction with the gonadotropin-releasing hormone receptor. Endocr Rev, 18, 180-205.

52 SHERWOOD, N. M., LOVEJOY, D. A. & COE, I. R. 1993. Origin of mammalian gonadotropin-releasing hormones. Endocr Rev, 14, 241-54.

53 SHUPNIK, M. A. 1996. Gonadal hormone feedback on pituitary gonadotropin genes. Trends Endocrinol Metab, 7, 272-6.

54 SIRINATHSINGHJI, D. J. 1983. GnRH in the spinal subarachnoid space potentiates lordosis behavior in the female rat. Physiol Behav, 31, 717-23.

55 SISK, C. L. & FOSTER, D. L. 2004. The neural basis of puberty and adolescence. Nat Neurosci, 7, 1040-7.

56 SISK, C. L., RICHARDSON, H. N., CHAPPELL, P. E. & LEVINE, J. E. 2001. In vivo gonadotropin-releasing hormone secretion in female rats during peripubertal development and on proestrus. Endocrinology, 142, 2929-36.

57 SMRCKA, A. V. 2008. G protein betagamma subunits: central mediators of G protein-coupled receptor signaling. Cell Mol Life Sci, 65, 2191-214.

58 SRINIVAS, S., WATANABE, T., LIN, C. S., WILLIAM, C. M., TANABE, Y., JESSELL, T. M. & COSTANTINI, F. 2001. Cre reporter strains produced by targeted insertion of EYFP and ECFP into the ROSA26 locus. BMC Dev Biol, 1, 4.

59 STOJILKOVIC, S. S., KRSMANOVIC, L. Z., SPERGEL, D. J. & CATT, K. J. 1994. Gonadotropin-releasing hormone neurons: intrinsic pulsatility and receptor-mediated regulation. Trends Endocrinol Metab, 5, 201-9.

60 SYNTICHAKI, P. & TAVERNARAKIS, N. 2003. The biochemistry of neuronal necrosis: rogue biology? Nat Rev Neurosci, 4, 672-84.

61 TANG, W. J. & GILMAN, A. G. 1991. Type-specific regulation of adenylyl cyclase by G protein beta gamma subunits. Science, 254, 1500-3.

62 TIRINDELLI, R., DIBATTISTA, M., PIFFERI, S. & MENINI, A. 2009. From pheromones to behavior. Physiol Rev, 89, 921-56.

63 TSUTSUMI, M., ZHOU, W., MILLAR, R. P., MELLON, P. L., ROBERTS, J. L., FLANAGAN, C. A., DONG, K., GILLO, B. & SEALFON, S. C. 1992. Cloning and functional expression of a mouse gonadotropin-releasing hormone receptor. Mol Endocrinol, 6, 1163-9.

64 VAN DER LINDEN, M., BUCKINGHAM, K., FARQUHAR, C., KREMER, J. A. M. & METWALLY, M. 2012. Luteal phase support in assisted reproduction cycles. Human Reproduction Update, 18, 473.

65 VAN LOENEN, A. C. D., HUIRNE, J. A. F., SCHATS, R., HOMPES, P. G. A. & LAMBALK, C. B. 2002. GnRH Agonists, Antagonists, and Assisted Conception. Semin Reprod Med, 20, 349-364.

66 VIZCARRA, J. 2013. Contribution of Chicken GnRH-II and Lamprey GnRH-III on Gonadotropin Secretion.

67 WEN, S., AI, W., ALIM, Z. & BOEHM, U. 2010. Embryonic gonadotropin-releasing hormone signaling is necessary for maturation of the male reproductive axis. Proc Natl Acad Sci U S A, 107, 16372-7.

68 WEN, S., GOTZE, I. N., MAI, O., SCHAUER, C., LEINDERS-ZUFALL, T. & BOEHM, U. 2011. Genetic identification of GnRH receptor neurons: a new model for studying neural circuits underlying reproductive physiology in the mouse brain. Endocrinology, 152, 1515-26.

69 WEN, S., SCHWARZ, J. R., NICULESCU, D., DINU, C., BAUER, C. K., HIRDES, W. & BOEHM, U. 2008. Functional characterization of genetically labeled gonadotropes. Endocrinology, 149, 2701-11.

70 WHITE, R. B., EISEN, J. A., KASTEN, T. L. & FERNALD, R. D. 1998. Second gene for gonadotropin-releasing hormone in humans. Proc Natl Acad Sci U S A, 95, 305-9.

71 WILLARS, G. B., HEDING, A., VRECL, M., SELLAR, R., BLOMENROHR, M., NAHORSKI, S. R. & EIDNE, K. A. 1999. Lack of a C-terminal tail in the mammalian gonadotropin-releasing hormone receptor confers resistance to agonist-dependent phosphorylation and rapid desensitization. J Biol Chem, 274, 30146-53.

72 WOOLLEY, C. S. & SCHWARTZKROIN, P. A. 1998. Hormonal effects on the brain. Epilepsia, 39 Suppl 8, S2-8.

73 WRAY, S., GRANT, P. & GAINER, H. 1989. Evidence that cells expressing luteinizing hormone-releasing hormone mRNA in the mouse are derived from progenitor cells in the olfactory placode. Proc Natl Acad Sci U S A, 86, 8132-6.

74 YOON, H., ENQUIST, L. W. & DULAC, C. 2005. Olfactory inputs to hypothalamic neurons controlling reproduction and fertility. Cell, 123, 669-82.

75 ZENG, W., MAK, D.-O. D., LI, Q., SHIN, D. M., FOSKETT, J. K. & MUALLEM, S. 2003. A New Mode of Ca2+ Signaling by G Protein-Coupled Receptors: Gating of IP3 Receptor Ca2+ Release Channels by Gβγ. Current Biology, 13, 872-876.

76 ZUCCHI, R. & RONCA-TESTONI, S. 1997. The sarcoplasmic reticulum Ca2+ channel/ryanodine receptor: modulation by endogenous effectors, drugs and disease states. Pharmacol Rev, 49, 1-51.

2. Materials & Methods

2.1 Materials

2.1.1 Chemicals and enzymes

Agar-Agar	Carl Roth GmbH & Co. KG
Agarose DNA Grade ELECTRAN®, low gelling	VWR International
N,N-Bis(2-hydroxyethyl)-2-aminoethanesulfonic acid (BES) BioXtra, for molecular biology, ≥99.5% (T)	Sigma-Aldrich Corp.
Albumin from bovine serum	Sigma-Aldrich Corp.
Calcium chloride dihydrate for analysis EMSURE® ACS,Reag. Ph Eur	Merck KGaA
Cetrorelix acetat C5249	Sigma-Aldrich Corp.
D(+)-Glucose monohydrate for microbiology	Merck KGaA
[D-Trp^6]-Luteinizing Hormone Releasing Hormone L-9761	Sigma-Aldrich Corp.
Dimethyl Sulfoxide (DMSO)	Fisher Scientific Inc.
Fura-red/AM, cell permanent	Invitrogen AG
Isoflurane	Baxter International Inc.
Ionomycin	Sigma-Aldrich Corp.
Gonadotropin releasing hormone (GnRH), Luteinizing Hormone releasing Hormone, L7134)	Sigma-Aldrich Corp.
Magnesium sulfate, anhydrous, ReagentPlus®, ≥99.5%	Sigma-Aldrich Corp.
Pluronic® F-127, powder, BioReagent, suitable for cell culture	Sigma-Aldrich Corp.
Potassium chloride for analysis EMSURE® ACS,Reag. Ph Eur	Merck KGaA
Sodium chloride AnalaR NORMAPUR	VWR International
Sodium hydrogen carbonate for analysis EMSURE® ACS, Reag. Ph Eur	Merck KGaA
Tetrodotoxin 1078	Tocris Bioscience

2.1.2 Solutions and buffers

Extracellular solution (oxygenated with 95% O_2 / 5% CO_2) (S1)

120 mM NaCl, 25 mM $NaHCO_3$, 5 mM KCl, 5 mM BES, 1 mM $CaCl_2$, 1 mM $MgSO_4$, 10 mM Glucose, pH 7.3, 300 mOsm/L

Extracellular solution (S2)

145 mM NaCl, 5 mM KCl, 1 mM $CaCl_2$, 1mM $MgCl_2$, 10 mM HEPES titrated with NaOH to pH 7.27, 300 mOsm/L

High potassium solution

60 mM KCl, 90 mM NaCl, 1 mM $CaCl_2$, 1 mM $MgCl_2$, 10 mM HEPES titrated with NaOH to pH 7.27, 300 mOsm/L

Zero Ca^{2+} extracellular solution

125 mM KCl, 10 mM HEPES, KOH 2 mM, EGTA 1mM titrated with KOH to pH 7.3, 300 mOsm/L

Manganese (II) Chloride extracellular solution

145 mM NaCl, 5 mM KCl, 1 mM $MgCl_2$, 10 mM HEPES titrated with NaOH to pH 7.27, 300 mOsm/L

Diethylene Triamine Pentaacetic Acid (DTPA) extracellular solution

145 mM KCl, 10 mM HEPES, KOH 2 mM, EGTA 0.45mM titrated with KOH to pH 7.27, 300 mOsm/L

Tetrodotoxin blocking solution

120 mM NaCl, 25 mM $NaHCO_3$, 5 mM KCl, 5 mM BES, 1 mM $CaCl_2$, 1 mM $MgSO_4$, 10 mM Glucose, 10 µM tetrodotoxin (TTX), pH 7.3, 300 mOsm/L

Agar-Agar (4%) solution

4 g low gelling agarose / 100 mL double distilled water

Agarose (3%) solution

3 g low gelling agarose / 100 mL oxygenated extracellular solution (S1)

20% Pluronic F127-DMSO Solution

0.02 mg Pluronic F-127 / 100 µL DMSO

Fura-red/AM Loading solution

1526 µL oxygenated extracellular solution (S1), Fura-red/AM 50 µg, DMSO 0.33%, Pluronic F127 0.065%

GnRH stimulation solution (Ca^{2+} imaging)

10 mL oxygenated extracellular solution (S1), 0.1% BSA, concentration dependent GnRH (0.3 nM, 1nM; 3 nM; 10 nM; 100 nM)

[D-Trp^6)]-LH-RH stimulation solution

10 mL oxygenated extracellular solution (S1), 0.1% BSA, concentration dependent [D-Trp^6)]-LH-RH (0.3 nM, 1 nM; 3 nM; 10 nM; 100 nM)

KCl stimulation solution

10 mL oxygenated extracellular solution (S1), 0.1% BSA, concentration dependent [D-Trp^6)]-LH-RH (0.3 nM, 1 nM; 3 nM; 10 nM; 100 nM)

GnRH stimulation solution (Patch clamp)

10 mL oxygenated extracellular solution (S1), concentration dependent GnRH (0.3 nM, 1nM; 3 nM; 10 nM; 100 nM)

Phosphate buffered saline solution

137 mM NaCl, 2.7 mM KCl, 10.1 mM Na_2HPO_4, 1.9 mM KH_2PO_4 titrated with HCl to pH 7.4

2.1.3 Consumables

6-well Cell Culture Plates	Becton Dickinson AG
Capillary Glass, TW100-F4	World Precision Instruments Inc.
Capillary Glass, 8250, Filament, 1.50/0.86, 75 mm	A-M Systems Inc.
Disposable Pasteur Pipettes	Kimble Chase LLC
Filter Holder Swinnex®, 25 mm	EMD Millipore
Glassware, made of Borsilicate 3.3	VWR International
Heat-shrinking tubing, DERAY Set-2000	DSG-Canusa GmbH
Infusion Set with micro adjustment	Becton Dickinson AG
Liquid Blocker Pen, Super PAP	Ted Pella Inc.
Membrane Filter 0.2 µm, Supor® 200 PES, 47 mm	Pall Corporation

Membrane Filter 0.2 µm, HT Tuffryn® HPS, 25 mm	Pall Corporation
Microscope slides	VWR International
Pipette Tip 20 µL, 200 µL, 1 mL	Sarstedt AG
Safe-seal micro tube 1.5 mL, 2 mL	Sarstedt AG
Single Edge Carbon Steel Razorblade	Electron Microscopy Sciences
Sterile Syringe 10 mL, 50 mL, 60 mL Luer-Lok	Becton Dickinson AG
Super glue, Loctite 406TM	Henkel AG
Transfer pipette 3.5 mL	Sarstedt AG

2.1.4 Equipment

Ca^{2+} Imaging Set Up

Vibration Isolation Table VH3036W-OPT	Newport Corporation
Upright Microscope Olympus BX-51WI	Olympus GmbH
Confocal Laser Scanning System Radiance 2100	Carl Zeiss AG (former Bio-Rad)
PH-6 platform for Series 20 chambers	Warner Instruments LLC
Large Rectangular Open Bath Chamber RC-27	Warner Instruments LLC
Platinum-iridium harp, 1.5 mm spacing	Own construction
Vibration Vacuum Pump SP302SA-V	Schwarzer Precision GmbH & Co. Kg

Patch Clamp Set Up

Vibration Isolation Table VH3048W-OPT	Newport Corporation
Upright Microscope Olympus BX-51WI	Olympus GmbH
Imaging Station cell^R	Olympus GmbH
Digital CCD Camera ORCA-R^2	Hamamatsu Photonics

Workstation: 2 Micromanipulators Mini 25 Shifting Table 380FM-2P Platform LN Bridge 500 Remote Control Keypad SM-7 Control Box SM-7	Luigs & Neumann Feinmechanik und Elektrotechnik GmbH
EPC 10 USB Double Patch Clamp Amplifier	HEKA Elektronik GmbH
Low-pass Bessel Filter (LPF-8)	Warner Instruments LLC
Audio Monitor AM10, Grass Technologies	Astro-Med GmbH
Digital Storage Oscilloscope VC-6523	Hitachi Ltd.
Picospritzer® II	Parker Hannifin Corp.
PM-6 platform for Series 20 chambers	Warner Instruments LLC
Large Rectangular Open Bath Chamber RC-27	Warner Instruments LLC
Platinum-iridium harp, 1.5 mm spacing	Own construction
Vibration Vacuum Pump SP302SA-V	Schwarzer Precision GmbH & Co. Kg

General

CO_2 Incubator, CB210-UL	Bochem Instrumente GmbH
Double spatulas, spoon shape	Binder GmbH
Filter Funnel with Clamp DS0315	Thermo Fisher Scientific Inc.
Gastight Microliter Syringe #1710	Hamilton Bonaduz AG
Gravity flow controller	Becton Dickinson AG
Hazardous material workplace Basic AP 014590	Denios AG
Heating Bath Circulator 66557	Precision Scientific Corp.
Large Rectangular Open Bath Chamber (RC-27)	Warner Instruments LLC
Light Microscope	Ernst Leitz Wetzlar
Magnet stirrer, Thermolyne Cimarec 2	Thermo Fisher Scientific Inc.
Medical Forceps, Dumont 7b	Fine Science Tools Inc.
Microforge MF-830	Narishige International
Microgrinder EG-400	Narishige International

Multi-pipette Puller PMP-107	Microdata Instrument Inc.
Micro spoon spatulas, spoon shape	Bochem Instrumente GmbH
Microwave Midea MWGED 9025 E	Midea Europe GmbH
Modular Syringe Holder 10mL, Add on Bracket	Warner Instruments LLC
Modular Syringe Holder 60mL, Base Mount	Warner Instruments LLC
Osmometer OM-815	Vogel GmbH & Co. KG
Perfusion Mini Manifold, 8 to 1 ports	Warner Instruments LLC
pH Meter PHM240	Radiometer Analytical
Precision Balance 572	Kern & Sohn GmbH
Single Channel Pipettes (0.5-10 µL/10-100 µL/100-1000 µL)	VWR International
Vertical Glass Microelectrode Puller PP-830	Narishige International
Spring Scissors, 7 mm and 3 mm Blades	Fine Science Tools Inc.
Stopcocks with Luer Connections	Cole-Parmer
Ultrapure Water System Direct-Q 5	EMD Millipore
Ultrasonic Bath Aquasonic 50T	VWR International
Vacuum pump Air Admiral® diaphragm	Cole-Parmer
Vibrating-Blade Microtome HM 650V with Cooling Device CU65	Thermo Fisher Scientific Inc.
Vortex Genie 2	Scientific Industries Inc.
Wagner Scissors	Fine Science Tools Inc.
Water Bath TW 20	JULABO Labortechnik GmbH

2.1.5 Software

Software LaserSharp 2000	Carl Zeiss AG (former Bio-Rad)
xcellence rt	Olympus GmbH
Patchmaster	HEKA Elektronik GmbH
NeuroExplorer	Nex Technologies

IGOR Pro	WaveMetrix Inc.
SPSS Statistics	IBM Corp
NCSS Statistical Software	NCSS, LLC
GraphPad PRISM	GraphPad Software Inc
Microsoft Excel	Microsoft Corp.
ImageJ	Wayne Rasband, NIH
Photoshop	Adobe Systems Inc.
CorelDraw	Corel Corp.

2.2 Methods

2.2.1 Animals

Animal care and experimental procedures were performed in accordance with the guidelines established by the animal welfare committee of the University of Saarland, School of Medicine. Mice were kept under standard light/dark cycle with food and water ad libitum. GnRHR-IRES-cre (GRIC) mice (Wen et al., 2008) were bred to eR26-τGFP reporter mice (Wen et al., 2011) to express τGFP in GnRHR neurons. Mice were kept in a mixed (129/SvJ and C57BL/6J) background.

2.2.2 Assessment of reproductive stages

The identification of the stages of the estrous cycle was done by cytological analysis of the vaginal secretion of the mouse as described previously by (Caligioni, 2009).

Briefly, the tip of a glass pipette - previously smoothed by fire polishing to inhibit injuries - filled with 10 μL phosphate buffered saline (PBS) warmed to body temperature was placed into the vagina of the mouse. The vagina was flushed gently three to five times. The PBS containing the vaginal secretion was placed on a microscope slide and reviewed under a light microscope, where the cells could be easily differentiated (Caligioni, 2009) and digitalized. The stage of the estrous cycle was determined based on the presence or absence of leukocytes, cornified epithelia cells and nucleated epithelial cells (Felicio et al., 1984).

Metestrus (Figure 6A) is characterized by a mix of cell types with a predominance of leucocytes and a few nucleated epithelial and/or cornified squamous epithelial cells. In diestrus (Figure 6B) leukocytes are predominantly present. In proestrus (Figure 6C) nucleated epithelial cells are predominant, occasionally cornified cells may occur. Estrus (Figure 6D) is classifiable by the occurrence of mainly clusters of cornified squamous epithelial cells, which can be differentiated from nucleated epithelial cells by the absence of a visible nucleus, granular cytoplasm and irregular shape (Caligioni, 2009).

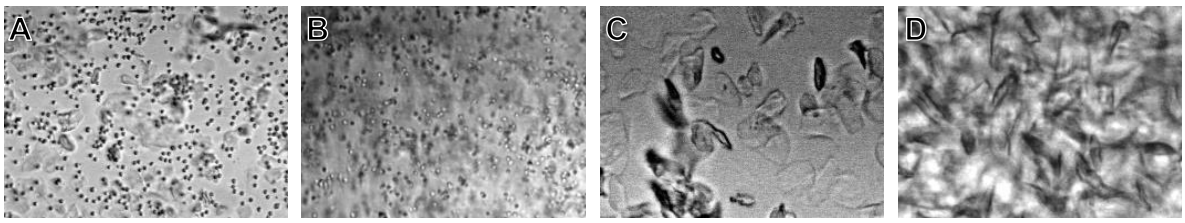

Figure 6. Cytological assessment of reproductive stage. Infrared-differential interference contrast (IR-DIC) micrographs of unstained vaginal secretion from female GRIC/eR26-τGFP mice in metestrus (A), diestrus (B), proestrus (C) and estrus (D).

2.2.3 Ca^{2+} Imaging of τGFP-tagged GnRHR neurons

Ca^{2+} imaging experiments were done in coronal brain tissue slices freshly prepared from GRIC/eR26-τGFP mice (2 to 6 months old, either sex) using the protocol described in Chapter 3. Brain structures were identified using a mouse brain atlas (Paxinos and Franklin, 2001).

Intracellular Ca^{2+} was monitored in τGFP-tagged GnRHR neurons of acute mouse brain slices loaded with fura-red, using a confocal scanning microscope and dedicated laser and filter systems (Radiance 2100, Zeiss) The acquisition frequency was in general 2.24 Hz. Therefore, a novel protocol was developed and published (Schauer and Leinders-Zufall, 2012; Wen et al., 2011). The precise steps can be found in chapter 3.

To analyze the change in Ca^{2+} signal over time in a particular neuron, the region of interest (ROI) of a GnRHR soma was identified and analyzed, using the software ImageJ (NIH). The somata of fura-red loaded τGFP-tagged neurons were marked in the respective image series as regions of interest (ROI). Mean values of the fluorescence intensity over a particular ROI can be saved for every time point of the image series.

Ca^{2+} signals are presented as arbitrary fluorescence units or as absolute values (ΔF/F) of the relative changes in fluorescence intensity (ΔF) normalized to baseline fluorescence (F). This procedure results in a positive deflection when the intracellular Ca^{2+} concentration rises, despite the fact that fura-red fluorescence decreases upon binding of Ca^{2+}.

To facilitate the analysis of huge amounts of data semi-automated routines were developed and applied to the dataset using IGORPro (Wavemetrics).

To quantify the change in the complex Ca^{2+} elevations and due to the impossibility to quantify the multiple peak Ca^{2+} responses, the area under the Ca^{2+} fluorescence response curve (AUC) was calculated (10 s before and 120 s after the start of the stimulus; total time: 130 s). The mean of the baseline before the stimulus start was calculated (F_0). All fluorescence values were normalized by this mean ($\Delta F/F_0$).

$$AUC = \int_0^t f(t)dt \approx \sum_{i=0}^{t} \frac{1}{2}(t_{i+1} - t_i)[(f(t_{i+1}) - f(t_0)) + (f(t_i) - f(t_0))]$$

f(t) represents the function of the measured intensity of the area of interest
$f(t_0)$ represents the function of the calculated mean of the baseline

This measurement for the amount of Ca^{2+} encompasses any initial Ca^{2+} transient, second phases and sustained elevated Ca^{2+} responses and oscillations. Control and wash periods were analyzed using the same method.

Some Ca^{2+} experiments were also performed in the presence of 10 μM tetrodotoxin (TTX). To ensure that TTX had thoroughly inhibited the network activity, 25 s pulses of 60 mM KCl were bath applied before and after TTX treatment (8 min). To ensure the capture of the depolarization-induced Ca^{2+} transients, images were acquired at a rate of 4.48 Hz.

For the calibration of fura-red, we relied on continuous perfusion of high- (1 mM Ca^{2+}) and zero-calcium (1 mM EGTA) solutions in the presence of 4 μM ionomycin, whereby F_{min} and F_{max} are the fluorescence intensity in the absence or presence of Ca^{2+}, respectively. The following equation was used to determine $[Ca^{2+}]_i$ at rest:

$$[\boldsymbol{Ca^{2+}}]_i = \boldsymbol{K_d}\frac{(\boldsymbol{F} - \boldsymbol{F_{min}})}{(\boldsymbol{F_{max}} - \boldsymbol{F})}$$

in which F is the measured baseline fluorescence intensity and K_d is the Ca^{2+}-fura-red dissociation constant (140 nM). To test for potential contribution of extracellular fura-red indicator solution, 0.1 mM $MnCl_2$ was added and then chelated after 20 s with 0.25 mM diethylene triamine pentaacetic acid (DTPA). There was no change in fluorescence, and thus a correction for extracellular fura-red solution was not necessary.

2.2.4 Loose patch clamp recording

All experiments were performed in coronal brain tissue slices freshly prepared from female GRIC/eR26-τGFP mice (2-4 months old). For the preparation of coronal hypothalamic mouse brain slices, an improved protocol of the fura-red/AM preparation protocol was used. Detailed steps can be found in chapter 3 and 4 (Schauer and Leinders-Zufall, 2012; Wen et al., 2011)).

Improvement and changes:

1. As an additional step after the decapitation (see 3.2.2.3), the whole mouse head was incubated for 240 s in ice cold oxygenated extracellular solution (S1) mixed with cubes of frozen oxygenated extracellular solution (S1).
2. Coronal hypothalamic brain slices were transferred to a beaker with cold oxygenated extracellular solution (S1) using a broad spoon spatula. The slices in oxygenated extracellular solution (S1) were incubated first for 30 min at 37° C followed by a 30 min incubation at room temperature being oxygenated all the time.

Extracellular solution S1 and S2 were prepared similar as (see Chapter 2.1.2. and 3.2.1). Stock solutions of GnRH were prepared in extracellular S2 solution and aliquots stored at -20 °C. GnRH was diluted in extracellular S2 solution immediately before use and focally ejected onto the epithelial surface using multi-barrel stimulation pipettes (see below). Cetrorelix, an antagonist of GnRHR (Halmos et al., 1996; Reissmann et al., 2000), was applied via microperfusion. Stock solution of Cetrorelix was prepared in extracellular S2 solution and aliquots stored at -20 °C and diluted in extracellular S2 solution immediately before use.

Patch pipette were pulled from thick wall borosilicate glass capillaries with filament (od 1.50 mm /id 0.86 mm). A vertical glass electrode puller (PP-830, Narishige International) which provides automated double mode function was used to pull the glass pipettes. All pipettes were fire-polished using a microforge (MF-830, Narishige International) after pulling to smooth the tip. The final resistance of pipettes produced by this protocol was around 4-7 MΩ. Pipettes were filled using a syringe with filtered oxygenated extracellular solution (S2).The multi-barrel pipette was made of glass capillaries (TW100-24) and pulled with a multi-pipette puller PMP-107 (Microdata Instrument Inc.). A bundle of tree glass capillaries kept together with heat-shrinking tubing (Figure 7A).

In the next step, the endings of the three pipettes were heated up and bent apart. As final step, the tip of the multi-barrel pipette was grinded with a micro grinder (EG-400, Narishige International) to an angle of 45° (Figure 7B). Barrels of the pipette were filled.

After mounting the filled patch pipette onto the headstage of the patch clamp amplifier (EPC-10, HEKA Elektronik, Lambrecht/Pfalz, Germany) and connecting the ground electrode, the pipette was moved by motorized micromanipulator to the cell.

Figure 7. Preparation of a multi-barrel pipette. A. Bundle of three glass capillaries kept together with heat-shrinking tubing. B. Ready to use three-barrel pipette.

To record action potential-driven capacitive currents (Leinders-Zufall et al., 2000; Leinders-Zufall et al., 2004; Leinders-Zufall et al., 2007) from the genetically identified neuron, a seal resistance of 20-80 MΩ was used. Spontaneous and GnRH-induced action potential discharges were monitored at a sampling rate of 10 kHz. The basic activity of the neuron was recorded over 180 s and the recording repeated several times.Stimuli were applied for 1 s with an inter-stimulus-interval of 9 min. Signals were low-pass filtered (analog 3- and 4-pole Bessel filters in series) with an effective corner frequency (-3 dB) of 3.0 kHz

The τGFP-tagged GnRHR neurons were visualized using an Olympus BX51WI fixed stage microscope equipped with infrared-optimized differential interference contrast (IR-DIC) optics. Before starting the setup of the Köhler illumination was checked and if necessary adjusted (Köhler, 1893; Köhler, 1894). The slice was first visually examined through the microscope at low magnification (10x) to exclude major damages and to identify the area of interest in the slice - the periventricular nucleus of the hypothalamus. The magnification was changed then to high (20x) to select a cell of interest which could be identified using τGFP. Cells near the surface might be damaged or dead, therefore only cells located at a depth of more than 10 µm were selected. Slices were continuously superfused with oxygenated S1 solution (~2 mL/min; gravity flow) at room temperature.

2.2.5 Analysis of data acquired from loose patch clamp recording

To analyze and classify the firing pattern of GnRHR neurons the four properties Coefficient of the Variation of the InterSpike Interval (CV_{ISI}), Percentage of Spikes in Bursts (PSiB) (Dahan et al., 2007; Grace and Bunney, 1984), Mean number of Spikes in each Burst (MSiB) (Jackson et al., 2004; Gariano and Groves, 1988) and mean spike frequency (mf) were used.

The CV_{ISI} as indicator for the regularity of firing (Selinger et al., 2007; Grace and Bunney, 1984) was calculated using the method of (Robin et al., 2009), in which the standard deviation

(SD) of the interspike interval (ISI) was divided by the mean ISI value. By plotting the CV_{ISI} a threshold, value to differentiate tonic and bursting firing pattern can be obtained (Hausser and Clark, 1997; Sigworth and Sine, 1987).

As criteria for defining a burst, an empirical method, which defines that a burst contains at least three spikes, was combined with an ISI threshold defined by the method of Selinger (Selinger et al., 2007). Plotting the PSiB logarithmically provides a threshold to distinguish between bursting and irregular firing pattern. MSiB and mf help to further distinguish the properties of the spiking pattern.

To determine changes in mean spike frequency in spontaneous active neurons after GnRH stimulation, the mean spike frequency ratio was calculated as the fraction of the mean frequency during the first 10 s after stimulation (t_0 + 10 s) and the frequency of action potentials during the 10 s before stimulation (t_0 - 10 s). The parameter t_0 indicates the start of the GnRH stimulation. The first-spike latency is defined as the time from the onset of the stimulus (t_0) to the time of the occurrence of the first action potential (Pawlas et al., 2010).

The variance of the instantaneous spike frequency (VARiF) is calculated over three periods: one period before stimulation and two periods after GnRH stimulation (total recording time: 180 s) (Miles et al., 2005; Plenz and Kital, 1999).

2.2.6 Statistics

Statistical analysis was done using GraphPad PRISM (GraphPad Software Inc., San Diego, USA) or SPSS (IBM Corporation, New York, USA).

In Ca^{2+} imaging, the Student's t-test was used for measuring the significance of difference between two distributions. Multiple groups were compared using a one-way or two-way analysis of variance (ANOVA). The Fisher's least significant difference (LSD) was used as a post hoc comparison of the ANOVA. If not otherwise stated, data are expressed as means ± SEM.

Loose patch clamp recording data were analyzed using NCSS 2004 statistical software (NCSS). The Student's t-test was used for measuring the significance of difference between two distributions. Multiple groups were compared using a two-way ANOVA with Tukey's Multiple Comparison test as a post hoc comparison.

2.3 References

1 CALIGIONI, C. S. 2009. Assessing reproductive status/stages in mice. Curr Protoc Neurosci, Appendix 4, Appendix 4I.

2 DAHAN, L., ASTIER, B., VAUTRELLE, N., URBAIN, N., KOCSIS, B. & CHOUVET, G. 2007. Prominent burst firing of dopaminergic neurons in the ventral tegmental area during paradoxical sleep. Neuropsychopharmacology, 32, 1232-41.

3 FELICIO, L. S., NELSON, J. F. & FINCH, C. E. 1984. Longitudinal studies of estrous cyclicity in aging C57BL/6J mice: II. Cessation of cyclicity and the duration of persistent vaginal cornification. Biol Reprod, 31, 446-53.

4 GARIANO, R. F. & GROVES, P. M. 1988. Burst firing induced in midbrain dopamine neurons by stimulation of the medial prefrontal and anterior cingulate cortices. Brain Research, 462, 194-198.

5 GRACE, A. A. & BUNNEY, B. S. 1984. The control of firing pattern in nigral dopamine neurons: burst firing. J Neurosci, 4, 2877-90.

6 HAUSSER, M. & CLARK, B. A. 1997. Tonic synaptic inhibition modulates neuronal output pattern and spatiotemporal synaptic integration. Neuron, 19, 665-78.

7 JACKSON, M. E., HOMAYOUN, H. & MOGHADDAM, B. 2004. NMDA receptor hypofunction produces concomitant firing rate potentiation and burst activity reduction in the prefrontal cortex. Proc Natl Acad Sci U S A, 101, 8467-72.

8 KÖHLER, A. 1893. Ein neues Beleuchtungsverfahren für mikrophotographische Zwecke. Zeitschrift für wissenschaftliche Mikroskopie und für Mikroskopische Technik, 10, 433-440.

9 KÖHLER, A. 1894. New Method of Illimination for Phomicrographical Purposes. Journal of the Royal Microscopical Society, 14, 261-262.

10 MILES, G. B., DAI, Y. & BROWNSTONE, R. M. 2005. Mechanisms underlying the early phase of spike frequency adaptation in mouse spinal motoneurones. J Physiol, 566, 519-32.

11 PAWLAS, Z., KLEBANOV, L. B., BENES, V., PROKESOVA, M., POPELAR, J. & LANSKY, P. 2010. First-spike latency in the presence of spontaneous activity. Neural Comput, 22, 1675-97.

12 PAXINOS, G. & FRANKLIN, K. B. J. 2001. The mouse brain in stereotaxic coordinates, San Diego, Academic Press.

13 PLENZ, D. & KITAL, S. T. 1999. A basal ganglia pacemaker formed by the subthalamic nucleus and external globus pallidus. Nature, 400, 677-82.

14 SCHAUER, C. & LEINDERS-ZUFALL, T. 2012. Imaging calcium responses in GFP-tagged neurons of hypothalamic mouse brain slices. J Vis Exp, e4213.

15 SELINGER, J. V., KULAGINA, N. V., O'SHAUGHNESSY, T. J., MA, W. & PANCRAZIO, J. J. 2007. Methods for characterizing interspike intervals and identifying bursts in neuronal activity. J Neurosci Methods, 162, 64-71.

16 SIGWORTH, F. J. & SINE, S. M. 1987. Data transformations for improved display and fitting of single-channel dwell time histograms. Biophys J, 52, 1047-54.

17 WEN, S., GOTZE, I. N., MAI, O., SCHAUER, C., LEINDERS-ZUFALL, T. & BOEHM, U. 2011. Genetic identification of GnRH receptor neurons: a new model for studying neural circuits underlying reproductive physiology in the mouse brain. Endocrinology, 152, 1515-26.

18 WEN, S., SCHWARZ, J. R., NICULESCU, D., DINU, C., BAUER, C. K., HIRDES, W. & BOEHM, U. 2008. Functional characterization of genetically labeled gonadotropes. Endocrinology, 149, 2701-11.

3. A method to measure Ca^{2+} responses in GFP-tagged hypothalamic GnRHR neurons by confocal microscopy

3.1 Abstract

Despite an enormous increase in our knowledge about the mechanisms underlying the encoding of information in the brain, a central question concerning the precise molecular steps as well as the activity of specific neurons in multi-functional nuclei of brain areas such as the hypothalamus remain. This problem includes identification of the molecular components involved in the regulation of various neurohormone signal transduction cascades. Elevations of intracellular Ca^{2+} play an important role in regulating the sensitivity of neurons, both at the level of signal transduction and at synaptic sites. New tools have emerged to help identify neurons in the myriad of brain neurons by expressing green fluorescent protein (GFP) under the control of a particular promoter. To monitor both spatially and temporally stimulus-induced Ca^{2+} responses in GFP-tagged neurons, a non-green fluorescent Ca^{2+} indicator dye needs to be used. In addition, confocal microscopy is a favorite method of imaging individual neurons in tissue slices due to its ability to visualize neurons in distinct planes of depth within the tissue and to limit out-of-focus fluorescence. The ratiometric Ca^{2+} indicator fura-2 has been used in combination with GFP-tagged neurons (Almholt et al., 1999). However, the dye is excited by ultraviolet (UV) light. The cost of the laser and the limited optical penetration depth of UV light hindered its use in many laboratories. Moreover, GFP fluorescence may interfere with the fura-2 signals (Bolsover et al., 2001). Therefore, we decided to use the red fluorescent Ca^{2+} indicator dye fura-red/AM (Invitrogen; AM, acetoxymethyl ester). The huge Stokes shift of fura-red permits multicolor analysis of the red fluorescence in combination with GFP using a single excitation wavelength. We had previously good results using fura-red in combination with GFP-tagged olfactory neurons (Leinders-Zufall et al., 2009). The protocols for olfactory tissue slices seemed to work equally well in hypothalamic neurons (Wen et al., 2011). Fura-red based Ca^{2+} imaging was also successfully combined with GFP-tagged pancreatic β-cells and GFP-tagged receptors expressed in HEK cells (Hara et al., 2006; Doherty et al., 1999). A little quirk of fura-red is that its fluorescence intensity at 650 nm decreases once the indicator binds Ca^{2+} (Kurebayashi et al., 1993). Therefore, the fluorescence of resting neurons with low Ca^{2+} concentration has relatively high intensity. It should be noted, that other red Ca^{2+}-indicator dyes exist or are currently being developed, that might give better or improved results in different neurons and brain areas.

3.2 Protocol

3.2.1 Preparation of solution and agarose ael

1. Prepare extracellular solution (see 2.1.2) with double distilled water. The pH will be ~7.3 after 10 min aeration with carbogen (95% O_2 / 5% CO_2), the osmolarity 300 mOsm (Heyward et al., 1993). If a higher osmolarity is required, it can be adjusted by adding more glucose (1 mM equals 1 mOsm). The solution is filtered twice using a 0.2 µm membrane filter to eliminate dust particles and possible bacterial contaminations.
2. The solution is stored at 4 °C, but should be aerated with carbogen (95% O_2 / 5% CO_2) for 10 min before use.
3. At this time, prepare also 1 cm^3 blocks of agar gel to stabilize the brain during the cutting procedure (see 3.2.3). First, dissolve 4% (w/v) agar (Sigma) in double distilled water by heating the solution to approximately 60 °C. The heated dissolved agar solution is poured into a square Petri dish to a height of 1 cm. After cooling and hardening, the 4% agar gel is cut into blocks of 1 cm^3. These blocks can be stored for up to 4 weeks at 4 °C.

3.2.2 Dissection of the mouse brain

Please make sure that all animal experimental procedures are performed in accordance with the guidelines established by the animal welfare committees of the respective institutions.

1. Before sacrificing the animal, make sure the agar gel blocks are ready for use.
2. Anesthetize the mouse with isoflurane (1-4% isoflurane in oxygen using a precision vaporizer for approximately 1 min). It is important to prevent hypoxia and therefore neuronal damage. A disadvantage of isoflurane is the cost and logistics of using precision vaporizers. A fatal overdose in an open system could be an alternative, since the mouse will be sacrificed. Occupational safety is in this case a serious concern. The isoflurane must be directly vented out of the room. Therefore, an overdose in an open system should be performed in a chemical fume hood.
3. Euthanize the mouse by decapitation after monitoring the depth of anesthesia by testing the rear foot reflex. This pedal or paw pinch reflex is performed by firmly pinching a paw or toe between one's fingers to elicit a withdrawal response by the

animal. An animal that shows a reflex is not at a surgical level of anesthesia and definitely not in a state to euthanize.

4. After decapitation, cut the scalp with a single edge razorblade centrally in sagittal direction, from the frontal bone to the external occipital protuberance. Move the two parts of the scalp, first from the medial caudal end in rostral lateral direction, then down in ventral direction (Figure 8A-C).

5. Make two lateral and one rostral cut in the foramen magnum with a small spring scissor (see for cutting direction the black dashed arrows in Figure 8C). Carefully cleave off the cranium from mediocaudal to lateral rostral with blunt forceps (see broad grey arrows in Figure 8C). In older animals a small cut at the sagittal suture is helpful and often necessary to avoid damaging cortical layers of the brain.

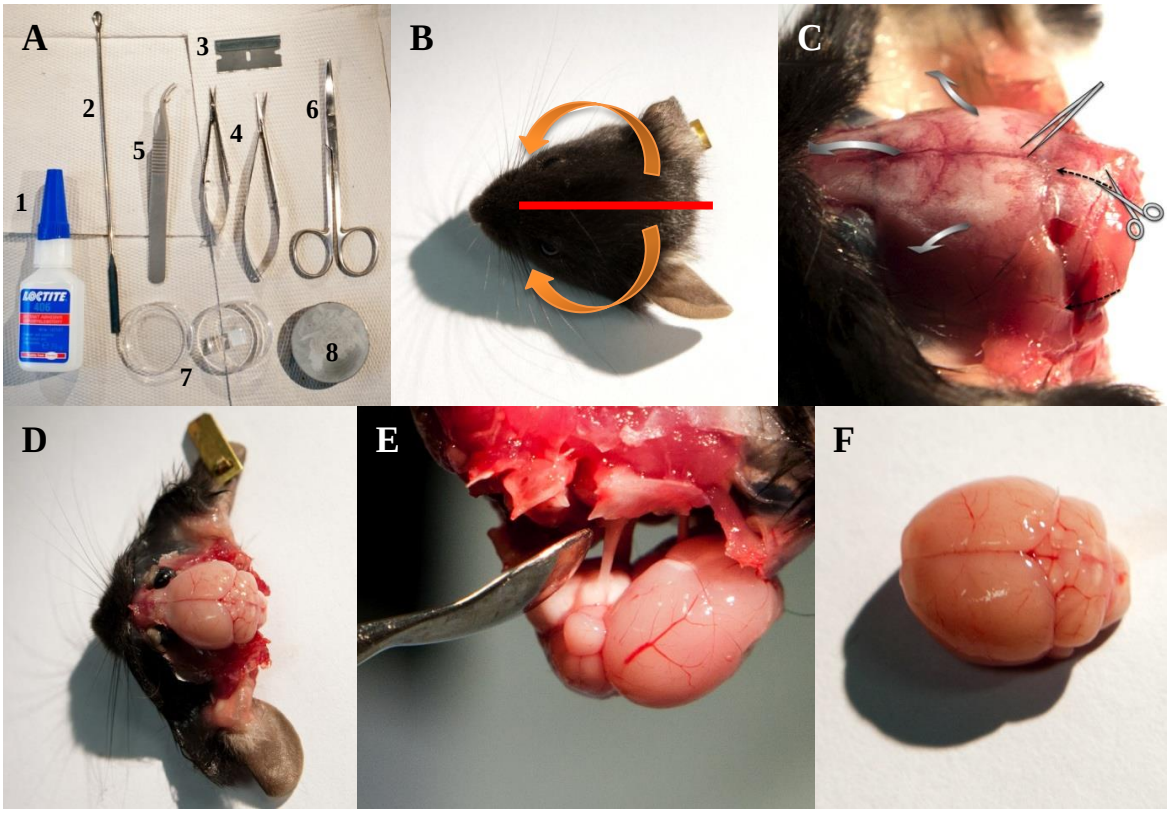

Figure 8. Tools, material and steps for excising a mouse brain. A. Tools and materials used for brain dissection: 1, Loctite 406 superglue; 2, micro spoon spatula; 3, single edge razor blade; 4, small and medium spring scissors; 5, blunt forceps; 6, scissors; 7, Petri dish containing agar gel block; 8, base plate for mounting brain into microtome. B-F. Images of some steps being described in point 3.2.2 of the protocol. B. Photograph of a mouse head indicating the cutting position of the scalp (red line) and arrows (orange) indicating the direction the skin should be pulled away from the bone. C. Photograph of the mouse head after the skin is pulled away showing the bone structures. Cutting direction of the scissor and the direction for breaking open the cranium with the blunt forceps is indicated with either the black dashed arrows or grey broad arrows, respectively. D. Photograph of the mouse brain after eliminating the various bone structures. E. Photograph of the removal of the brain still connected to the skull via the cranial nerves. F. Photograph of a relatively undamaged mouse brain.

6. At this moment the occipital, interparietal and parietal bones should be detached. If still present, the dura mater should be carefully removed using forceps to prevent damage to the brain in the next step.
7. Take away the squamosal bone, the anterior ethmoidal and frontal foramen (Figure 8D).
8. The brain can now easily be removed using an inverted micro spoon spatula and severing the cranial nerves (Figure 8E).

3.2.3 Slicing coronal hypothalamic sections of the mouse brain

1. Place the brain on its ventral side on a cut-resistant surface and remove the cerebellum with a single edge razor blade (Figure 9A). This straight cut surface will be the basis for mounting the brain on a plate to enable slicing of coronal brain sections.
2. Glue the brain with the cut section on the baseplate of the microtome (Zeiss, Hyrax V50) using low amounts of a fast curing high performance cyanoacrylate adhesive superglue (Loctite 406; Figure 8A). In addition, glue a 1 cm^3 agar gel block (see 3.2.1) at the ventral side of the brain (see 'v' in Figure 9B) onto the baseplate of the microtome (Zeiss, Hyrax V50) to support and fix the brain while slicing. Make sure not to use too much glue, to evade that glue traverses between brain and gel block causing problems in removing tissue slices after the cut. The gel block will be located at the opposite side of the cutting blade from the microtome (Figure 9B).
3. After a few seconds the bond has dried, put the plate into the bath of your microtome filled with 6 °C cold oxygenated (95% O_2 / 5% CO_2) extracellular solution (S1).
4. Use appropriate low slicing velocity and cut 300 µm thick slices. In case of our microtome, we use a frequency of 60 Hz, an amplitude of 0.8 mm and a velocity of 0.8 mm/s (Figure 9C). The coronal brain slices are either collected directly after each cut or can be left in the bath until the whole brain has been sectioned. The coronal brain slices are carefully transferred to a beaker with cold oxygenated extracellular solution (S1). Various tools have been designed to perform the transfer (e.g. cut broad plastic or glass Pasteur pipettes or broad spoon spatulas). It depends on the experimenter, which is being preferred. Most importantly, the slices should be handled appropriately to minimize damage.

5. If the microtome can be programmed to cut slices automatically, you can start to prepare the Ca^{2+} indicator dye loading solution at this moment. Otherwise, it is recommended that the preparation of this solution is performed before the brain slicing has ended to minimize delays for measuring Ca^{2+} responses in the neurons.

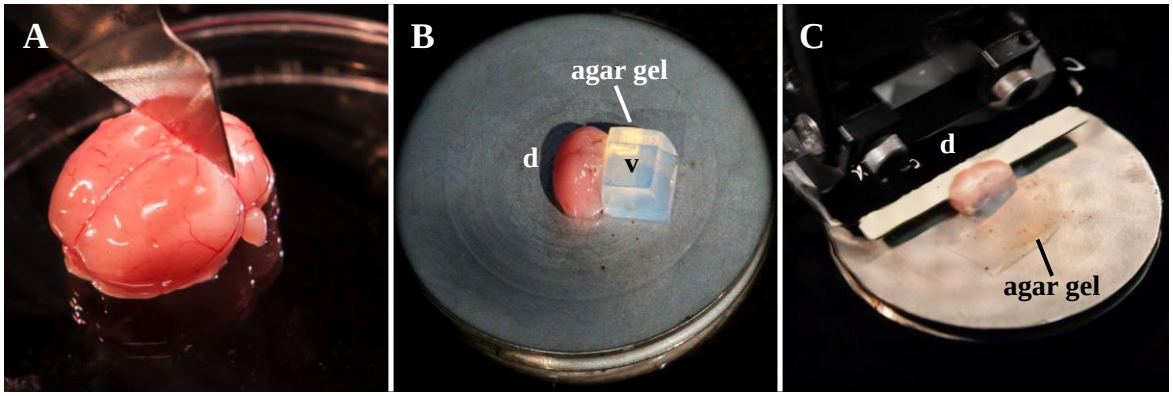

Figure 9. Slicing of coronal hypothalamic sections of the mouse brain. A. Photograph indicating the position of the single edge razor blade for eliminating the cerebellum (see step 3.2.3.1). B. Position of agar gel block in relation to the brain glued onto the baseplate of the microtome (see step 3.2.3.2). C. Cutting of coronal brain slice (note here the location of brain and gel block positions in regard to the cutting blade of the microtome; see step 3.2.3.4). d, dorsal; v, ventral.

3.2.4 Preparation of the Ca^{2+} indicator dye loading solution

A critical step in loading neurons remains often the health of the cells which depends on the amount of damage induced by and the speed of the dissection procedure. Another essential step seems to be the use of fresh Pluronic F-127 solution. It is being recommended to make this solution in the laboratory and not to use a premade solution from a vendor. Depending on the temperature, the humidity and the shelf lifetime of the Pluronic F-127 solution, we noted degradation of olfactory and brain neurons during the Ca^{2+} loading procedure.

1. Prepare the 20% (w/v) Pluronic F-127 (Sigma) in dimethyl sulfoxide (DMSO) by adding the Pluronic F-127 powder on top of the DMSO solution. Directly sonicate this solution without prior vortex or mixing. Within 2 min sonication the Pluronic F-127 will be dissolved. 100 µL Pluronic F-127 solutions are prepared fresh weekly.
2. Take one tube of 50 µg cell-permeable fura-red/AM and add 5 µL 20% Pluronic F-127 solution. Mix the solution using the tip of your pipette.
3. Add 45 µL extracellular solution to the mix and vortex it shortly.
4. Add an additional 325 µL extracellular solution and sonicate the tube for 3 min.

5. After sonication add 1.156 mL oxygenated (95% O_2 / 5% CO_2) extracellular solution to get your final Ca^{2+} indicator dye loading solution (30 μM fura-red, 0.33% DMSO and 0.065% Pluronic F-127). Store the tube in a dark place until use.
6. Transfer the coronal brain slices to a 6-well cell culture plate (BD Falcon) filled with oxygenated (95% O_2 / 5% CO_2) extracellular solution (up to six slices per well).
7. Suck off the oxygenated extracellular solution from the chambers of the 6-well plate taking care not to damage the brain slices.
8. Pipet directly 750 μL of the Ca^{2+} indicator dye loading solution to every well. The brain slices should be covered by the solution containing fura-red (immersion loading).
9. Incubate the slices in an O_2 / CO_2 cell culture incubator (O_2: 23.5%; CO_2: 5%) for 45 to 60 min at 37 °C.
10. At the end of the incubation time, replace the Ca^{2+} indicator dye loading solution by fresh oxygenated extracellular solution to prevent overloading the cells with fura-red and influencing in a subtle way the Ca^{2+} measurement via the chelating action of the dye. The slices are then being kept in the O_2 / CO_2 incubator (see previous point for settings) until use and are viable for up to 3-6 h.

3.2.5 Microscopy and analysis

In this protocol, the fluorescence intensity of GFP, which identifies the cell of interest, and of the Ca^{2+} indicator dye will be measured simultaneously in brain slices. Thus, the confocal microscope should be equipped with the correct laser, filters and two photomultiplier tubes to collect the two emission signals. GFP and the change in fluorescence intensity of fura-red can be measured using a single excitation wavelength of 488 nm. Emission fluorescence from the fluorophores can be collected using a 522/DF35 nm filter for GFP and a long-pass filter for wavelengths greater than 600 nm for fura-red.

1. To start monitoring stimulus-induced changes in the fluorescence signal, which are a measure of the intracellular Ca^{2+} concentration, one of the fura-red loaded brain slices is transferred to a recording chamber (i.e. Warner Instruments RC-27 Open Bath Chamber) that can be mounted on the confocal microscope setup (Figure 10A, B).

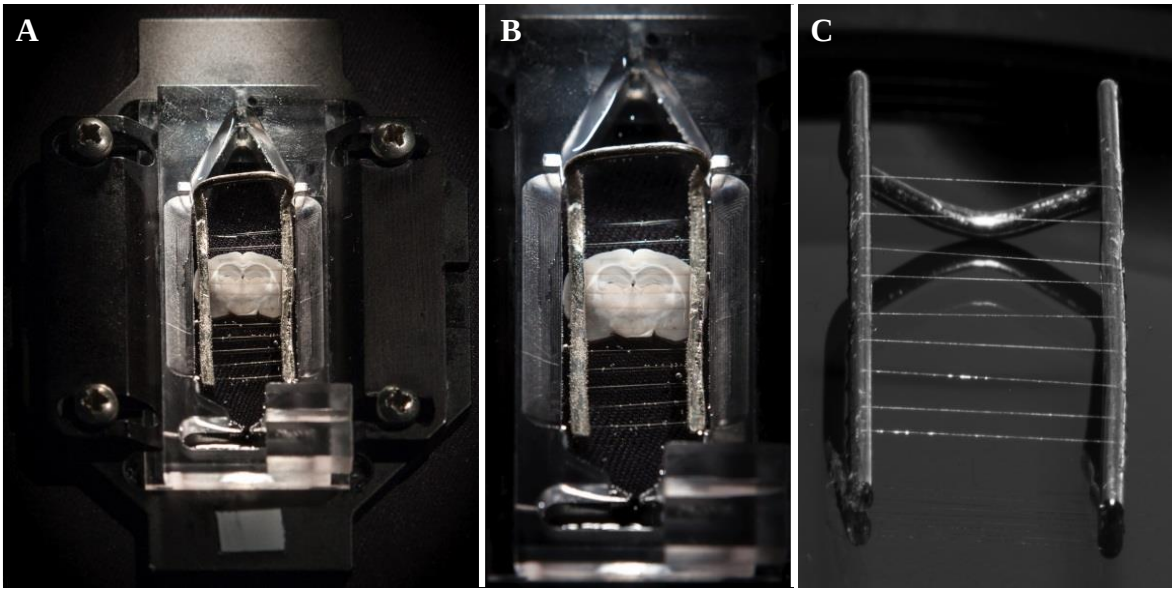

Figure 10. Brain slice positioned in recording chamber. A, B. Overview (A) and higher magnification (B) of a Warner Instruments RC-27 open bath recording chamber giving broad access to the hypothalamic areas of the coronal brain slice. C. U-shaped metal harp containing parallel arrays of nylon threads which will hold the slice in position in the recording chamber.

2. Secure the brain slice with a harp (Figure 10C) to prevent the slice to move due to the perfusion speed of the bath solution (oxygenated extracellular solution; see step 3.2.1.1). The harp (slice holder) is made of a parallel array of nylon threads (separated from each other by ~1 mm) strung on a U shape silver or platinum frame. The temperature of the bath solution at this step should be at least room temperature. If higher temperatures are required, appropriate care has to be taken to prevent condensation on microscope lenses and movement of the plane of focus due to shifting parts in the microscope.

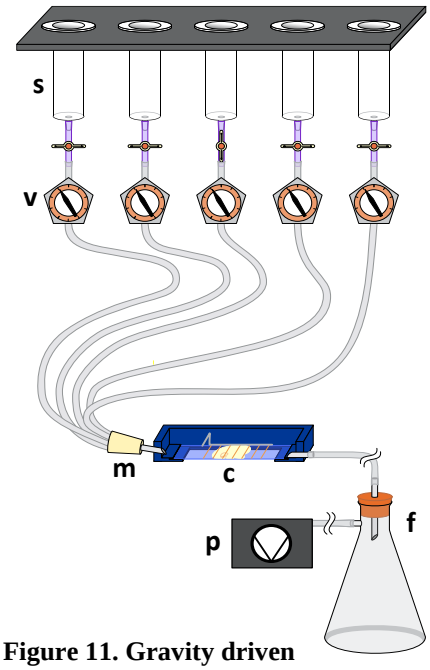

Figure 11. Gravity driven multi-channel perfusion system. s syringe, v valve (gravity flow controller), m manifold, c recording chamber, f side-arm flask, p vacuum pump.

3. Perfuse the slice for 10 min with oxygenated extracellular solution to remove any surplus of extracellular Ca^{2+} indicator dye. The flow rate of the perfusion should be adjusted to ~100 µL/s (tips regarding an appropriate perfusion system see (Leinders-Zufall, 1998)) (Figure 11).

4. Look at the slice through the microscope at low magnification, make a note of the orientation of the slice for your records and find your area of interest in the slice, in our case the hypothalamic area in the brain.

5. Change to high magnification and find the cell of interest in the slice by collecting GFP images and simultaneously checking the fluorescence intensity of the fura-red signal (Figure 12A-C). Cells near the surface could be damaged or dead. Therefore, cells located at a depth of more than 10 μm should be selected for imaging. We could reliably measure cells up to a depth of 40-50 μm, whereafter the signal strength started to drop. Remember that the fura-red signal of cells at rest with low Ca^{2+} concentration have relative high fluorescence intensities. This high fluorescence intensity is in this case not a sign of dead cells. The GFP signal can be used to detect any drift or movement of the tissue slice or as an indicator for changes in intracellular pH (Kneen et al., 1998).

6. Adjust the laser power to a value that allows measurements in the change of fura-red fluorescence intensity and prevents bleaching of the two fluorophores. Therefore, start with the lowest laser power and adjust to obtain a sufficient signal-to-noise ratio by changing black level (offset), detector aperture, gain and laser neutral density filters. Except for the laser power, the same should be done for the GFP signal.

7. Start to acquire images at rates between 0.5-2 Hz to collect the fura-red and GFP signals. The acquisition rate should be optimized to the expected rate of the Ca^{2+} signal. Voltage-dependent Ca^{2+} spikes may cause quicker and shorter transients than activation of some signal transduction cascades requiring activation of various second messengers. The length of the image acquisition should be appropriate for the purpose of the experiment. The GFP signal over time will help determine if any movement of the brain slice has occurred.

8. During the acquisition and the experiment, all scanning head settings have to be held constant to record reliable results that can be compared.

9. The changes in fluorescence over time can be analyzed using different mathematical programs, i.e. ImageJ (NIH, Bethesda, MD; http://rsb.info.nih.gov/ij/), Igor Pro (Wavemetrics) or MatLab (The MathWorks). By encircling the somata of a GFP-tagged neuron indicating the region of interest (ROI), this exact same region can be analyzed for changes in Ca^{2+} using the fura-red fluorescence signal over time.

Ca^{2+} signals can be presented as arbitrary fluorescence units or as values (ΔF/F) of the relative change in fluorescence intensity (ΔF) normalized to the baseline fluorescence (F). This procedure results in a negative deflection when the intracellular Ca^{2+} concentration increases using fura-red as the Ca^{2+} indicator dye. To ease the interpretation of the results, we recommend multiplying the ΔF/F values with -1 to obtain positive fluorescence signals to display a rise in Ca^{2+} (Figure 12C).

To compare results between neurons the amplitude and frequency of the Ca^{2+} signals are usually analyzed. Yet, some Ca^{2+} signals do not occur with a regular period or comparable amplitudes. Some signals might be strongly influenced by stochastic processes within the cell. Thus, to quantify the total change in Ca^{2+} in a given cell and to enable comparison of Ca^{2+} responses between neurons in different brain regions, analysis of the area-under-the-curve (AUC) is more appropriate. This measure for the amount of Ca^{2+} encompasses any initial Ca^{2+} transient, second phases and sustained elevated Ca^{2+} responses and oscillations. In this case care should be taken to analyze the same time period to enable the comparison between neurons.

3.2.6 Representative results

To start characterizing gonadotropin releasing hormone receptor (GnRHR) expressing neurons in the hypothalamus we made use of transgenic mice that express GFP after Cre-mediated excision in GnRHR-expressing neurons (Wen et al., 2011; Wen et al., 2008). GFP fluorescent neurons were identified in various brain areas, including the hypothalamus. To investigate the physiological properties of these GnRHR neurons, we first recorded Ca^{2+} signals in hypothalamic slices using a confocal microscope. First, we obtained coronal brain slices from these mice using the above-described protocol. Figure 8 illustrates the necessary tools, material and steps for excising a mouse brain. The coronal hypothalamic brain slices were cut (Figure 9) and then loaded according to the steps in point 4 of the protocol. Single brain slice of the appropriate area are placed in a recording chamber, secured with a harp (Figure 10) and then imaged using a confocal microscope (see steps 3.2.5.1 – 3.2.5.9). Figure 12 shows an example of two individual coronal brain slices identifying single GnRHR-τGFP cell bodies, the fluorescence at rest after loading the brain slice with fura-red and the merged confocal image indicating that the GFP neuron had taken up fura-red sufficiently to enable investigation of stimulus-induced Ca^{2+} signals in these cells. Using our protocol we initially tested whether GnRHR neurons utilize similar Ca^{2+} signals for stimulus detection in different areas of the hypothalamus in response to direct activation with GnRH (Figure 12E). However, these signals differed in their waveform depending on stimulus strength and brain area (Wen et al., 2011).

To quantify the change in the dynamics of the Ca^{2+} responses, the area-under-the-curve (AUC) can be calculated as a measure for the increase in intracellular Ca^{2+} (Figure 12E) (Wen et al., 2011). Studies are currently underway to investigate the molecular basis underlying the Ca^{2+} waves and oscillations, their dependence on sex and hormonal status of the animal, and whether they can be modulated by natural stimuli.

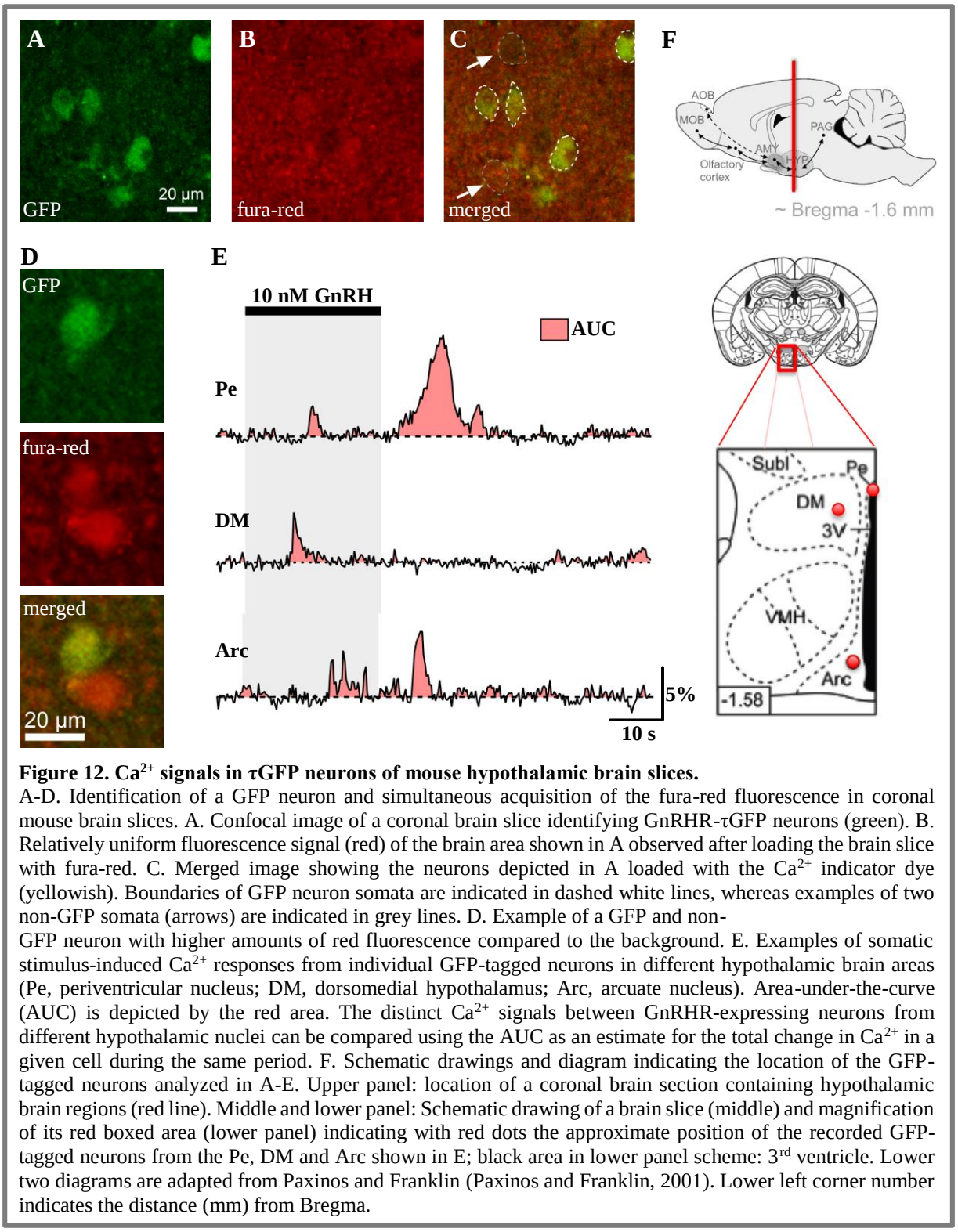

Figure 12. Ca^{2+} signals in τGFP neurons of mouse hypothalamic brain slices.
A-D. Identification of a GFP neuron and simultaneous acquisition of the fura-red fluorescence in coronal mouse brain slices. A. Confocal image of a coronal brain slice identifying GnRHR-τGFP neurons (green). B. Relatively uniform fluorescence signal (red) of the brain area shown in A observed after loading the brain slice with fura-red. C. Merged image showing the neurons depicted in A loaded with the Ca^{2+} indicator dye (yellowish). Boundaries of GFP neuron somata are indicated in dashed white lines, whereas examples of two non-GFP somata (arrows) are indicated in grey lines. D. Example of a GFP and non-
GFP neuron with higher amounts of red fluorescence compared to the background. E. Examples of somatic stimulus-induced Ca^{2+} responses from individual GFP-tagged neurons in different hypothalamic brain areas (Pe, periventricular nucleus; DM, dorsomedial hypothalamus; Arc, arcuate nucleus). Area-under-the-curve (AUC) is depicted by the red area. The distinct Ca^{2+} signals between GnRHR-expressing neurons from different hypothalamic nuclei can be compared using the AUC as an estimate for the total change in Ca^{2+} in a given cell during the same period. F. Schematic drawings and diagram indicating the location of the GFP-tagged neurons analyzed in A-E. Upper panel: location of a coronal brain section containing hypothalamic brain regions (red line). Middle and lower panel: Schematic drawing of a brain slice (middle) and magnification of its red boxed area (lower panel) indicating with red dots the approximate position of the recorded GFP-tagged neurons from the Pe, DM and Arc shown in E; black area in lower panel scheme: 3rd ventricle. Lower two diagrams are adapted from Paxinos and Franklin (Paxinos and Franklin, 2001). Lower left corner number indicates the distance (mm) from Bregma.

3.3 Discussion

A major question in neuroscience is to understand how the brain processes social information. A predominant source of information necessary for social recognition is encoded by olfactory or pheromonal signals. The detection of these signals by neuronal populations in the nose and the recognition of the signals in the brain, especially the hypothalamus, play a key role in many social processes and influence hormones and other neuroendocrine factors (Tirindelli et al., 2009; Kelliher and Wersinger, 2009; Yoon et al., 2005; Boehm et al., 2005). An essential obstacle of analyzing neuronal responses in brain areas like the hypothalamus containing multifunctional nuclei with multiple neurons is the identification of specific neurons of interest.

Many transgenic mouse lines have been developed, in which mainly GFP helps to identify neurons. Unfortunately, the fluorescent property of GFP complicates measurements using Ca^{2+} indicator dyes such as fluo-3 and fluo-4 (Wilson et al., 2007). We therefore started to investigate GFP-tagged neurons using a red-shifted Ca^{2+} indicator dye, like fura-red (Leinders-Zufall et al., 2009; Wen et al., 2011). Fura-red based Ca^{2+} imaging was previously combined with GFP-tagged pancreatic β-cells and GFP-tagged receptors expressed in HEK cells (Hara et al., 2006; Doherty et al., 1999). Like fura-2, some cross talk between fura-red and GFP has been reported (Bolsover et al., 2001). Yet, using high quality emission filter sets with specific bandwidths and dichromatic beamsplitter filters can limit the crosstalk/bleed-through between the dyes to some extent. It is wise to confirm the settings of a confocal microscope by measuring both channels (green and red fluorescence) at the same time using (1) brain slices with GFP-tagged neurons, but not loaded with the Ca^{2+} indicator dye, as well as (2) brain slices without GFP-tagged neurons but loaded with the red-shifted Ca^{2+} indicator. Using the same settings on the confocal microscope as with a regular experiment, the investigator can then note if any fluorescence is detected in the disparate channel, which should be avoided.

Some investigators use rhod-2 or recommend the use of X-rhod1 as an alternative red-shifted dye in combination with GFP-tagged cells (Bolsover et al., 2001; Hu et al., 2007; Perez et al., 2002). However, rhod AM dyes seem to have a tendency to concentrate in mitochondria (Trollinger et al., 1997) and have in many neurons low labeling efficiency (Wilson et al., 2007). Due to the need of improved red-shifted Ca^{2+}-indicators, investigators and companies are currently developing new probes with hopefully superior performance (Meshik, 2010).

Statement of copyright:
Figures 8 to 10 and figure 12 were adapted from (Schauer and Leinders-Zufall, 2012). Copyright 2012, The Journal of Visualized Experiments. Permission of usage see Chapter 7.

3.4 References

1 ALMHOLT, K., ARKHAMMAR, P. O., THASTRUP, O. & TULLIN, S. 1999. Simultaneous visualization of the translocation of protein kinase Calpha-green fluorescent protein hybrids and intracellular calcium concentrations. Biochem J, 337 (Pt 2), 211-8.

2 BOEHM, U., ZOU, Z. & BUCK, L. B. 2005. Feedback loops link odor and pheromone signaling with reproduction. Cell, 123, 683-95.

3 BOLSOVER, S., IBRAHIM, O., O'LUANAIGH, N., WILLIAMS, H. & COCKCROFT, S. 2001. Use of fluorescent Ca2+ dyes with green fluorescent protein and its variants: problems and solutions. Biochem J, 356, 345-52.

4 DOHERTY, A. J., COUTINHO, V., COLLINGRIDGE, G. L. & HENLEY, J. M. 1999. Rapid internalization and surface expression of a functional, fluorescently tagged G-protein-coupled glutamate receptor. Biochem J, 341 (Pt 2), 415-22.

5 HARA, M., DIZON, R. F., GLICK, B. S., LEE, C. S., KAESTNER, K. H., PISTON, D. W. & BINDOKAS, V. P. 2006. Imaging pancreatic beta-cells in the intact pancreas. Am J Physiol Endocrinol Metab, 290, E1041-7.

6 HEYWARD, P. M., CHEN, C. & CLARKE, I. J. 1993. Gonadotropin-releasing hormone modifies action potential generation in sheep pars distalis gonadotropes. Neuroendocrinology, 58, 646-54.

7 HU, J., ZHONG, C., DING, C., CHI, Q., WALZ, A., MOMBAERTS, P., MATSUNAMI, H. & LUO, M. 2007. Detection of near-atmospheric concentrations of CO2 by an olfactory subsystem in the mouse. Science, 317, 953-7.

8 KELLIHER, K. R. & WERSINGER, S. R. 2009. Olfactory regulation of the sexual behavior and reproductive physiology of the laboratory mouse: effects and neural mechanisms. ILAR J, 50, 28-42.

9 KNEEN, M., FARINAS, J., LI, Y. & VERKMAN, A. S. 1998. Green fluorescent protein as a noninvasive intracellular pH indicator. Biophys J, 74, 1591-9.

10 KUREBAYASHI, N., HARKINS, A. B. & BAYLOR, S. M. 1993. Use of fura red as an intracellular calcium indicator in frog skeletal muscle fibers. Biophys J, 64, 1934-60.

11 LEINDERS-ZUFALL, T. 1998. Technique for setting up the perfusion of a recording chamber for physiological studies with cultured and acutely dissociated cells. http://www.warneronline.com/pdf/whitepapers/perfusion_strategies.pdf.

12 LEINDERS-ZUFALL, T., ISHII, T., MOMBAERTS, P., ZUFALL, F. & BOEHM, T. 2009. Structural requirements for the activation of vomeronasal sensory neurons by MHC peptides. Nat Neurosci, 12, 1551-8.

13 MESHIK, X. A., HYRC, K.L., & GOLDBERG, M.P. 2010. Properties of Asante Calcium Red - a novel ratiometric indicator with long excitation wavelength. Neuroscience Meeting Planner, San Diego, CA, Society for Neuroscience.

14 PAXINOS, G. & FRANKLIN, K. B. J. 2001. The mouse brain in stereotaxic coordinates, San Diego, Academic Press.

15 PEREZ, C. A., HUANG, L., RONG, M., KOZAK, J. A., PREUSS, A. K., ZHANG, H., MAX, M. & MARGOLSKEE, R. F. 2002. A transient receptor potential channel expressed in taste receptor cells. Nat Neurosci, 5, 1169-76.

16 SCHAUER, C. & LEINDERS-ZUFALL, T. 2012. Imaging calcium responses in GFP-tagged neurons of hypothalamic mouse brain slices. J Vis Exp, e4213.

17 TIRINDELLI, R., DIBATTISTA, M., PIFFERI, S. & MENINI, A. 2009. From pheromones to behavior. Physiol Rev, 89, 921-56.

18 TROLLINGER, D. R., CASCIO, W. E. & LEMASTERS, J. J. 1997. Selective loading of Rhod 2 into mitochondria shows mitochondrial Ca2+ transients during the contractile cycle in adult rabbit cardiac myocytes. Biochem Biophys Res Commun, 236, 738-42.

19 WEN, S., GOTZE, I. N., MAI, O., SCHAUER, C., LEINDERS-ZUFALL, T. & BOEHM, U. 2011. Genetic identification of GnRH receptor neurons: a new model for studying neural circuits underlying reproductive physiology in the mouse brain. Endocrinology, 152, 1515-26.

20 WEN, S., SCHWARZ, J. R., NICULESCU, D., DINU, C., BAUER, C. K., HIRDES, W. & BOEHM, U. 2008. Functional characterization of genetically labeled gonadotropes. Endocrinology, 149, 2701-11.

21 WILSON, J. M., DOMBECK, D. A., DIAZ-RIOS, M., HARRIS-WARRICK, R. M. & BROWNSTONE, R. M. 2007. Two-photon calcium imaging of network activity in XFP-expressing neurons in the mouse. J Neurophysiol, 97, 3118-25.

22 YOON, H., ENQUIST, L. W. & DULAC, C. 2005. Olfactory inputs to hypothalamic neurons controlling reproduction and fertility. Cell, 123, 669-82.

4. A new model for studying neural circuits underlying reproductive physiology in the mouse brain

4.1. Abstract

GnRH signaling regulates reproductive physiology in vertebrates via the hypothalamic-pituitary-gonadal axis. In addition, GnRH signaling has been postulated to act on the brain. However, elucidating its functional role in the central nervous system has been hampered because of the difficulty in identifying direct GnRH signaling targets in live brain tissue. Using mice in which GnRHR expressing neurons can be visualized by their simultaneous expression of the fluorescent marker GFP (green fluorescent protein) we were able to investigate GnRHR neurons in various brain areas including areas influencing sexual behaviors.

GnRHR neurons respond reproducibly to extracellular application of GnRH or its analog [D-TRP^6]-LHRH, indicating that these neurons express functional GnRHR. Interestingly, the duration and shape of the Ca^{2+} responses were similar within and different between brain areas, indicating that GnRH signaling may differentially influence brain functions to affect reproductive success. The new mouse model sets the stage to analyze the next level of GnRH signaling in reproductive physiology and behavior.

4.2. Introduction

Understanding the regulation and signaling pathway of specific hormone-producing neurons is crucial to decode behavioral and endocrine responses. The functionality of a small subset of neurons, as in the case of GnRH expressing neurons, can be pivotal in the regulation of essential processes of an organism. In the case of GnRH, a restricted number of neurons, mainly expressed in the preoptic area of the hypothalamus, produces and secretes GnRH and thereby controls reproductive physiology and behavior in mammals (Gore, 2002; Herbison, 2006).

Multiple sensory inputs need to be processed and integrated to ensure reproductive success. In rodents, mainly olfactory cues assume this function. Once these inputs are recognized by receptors of chemosensory neurons in the olfactory system, signal transmission to higher brain regions is induced. During the integration and processing various signaling cascades can be activated which may influence social behavior as well as the endocrine status of the individual output (Tirindelli et al., 2009). It has been shown that GnRH neurons can be influenced by stimulation of the main and accessory olfactory system. The subcutaneous application of GnRH

as well as the intracerebral injection (third ventricle) has been shown affect directly reproductive behavior in rats (Moss and Foreman, 1976; Moss and McCann, 1973; Sirinathsinghji, 1983). Tracing studies showed that signals of GnRH neurons are transmitted to numerous neurons in several brain regions, influence different behaviors, including reproduction (Boehm et al., 2005; Yoon et al., 2005). This high number of neurons and brain areas influenced by the GnRH signaling indicate that additional to the well investigated effect of GnRH on the HPG axis (see Chapter 1.1) various other functions are influenced by GnRH signaling (Sherwood et al., 1993).

To analyze GnRH signaling in the central nervous system the identification of GnRH target cells is fundamental. Therefore, a genetic strategy to identify and characterize potential target neurons of GnRH signaling was developed (Wen et al., 2008). Crossbreeding the GRIC mouse line and the eR26-τGFP reporter mouse line leads to the generation of GnRHR/eR26-τGFP offspring. GnRHR/eR26-τGFP show an irreversible Cre-mediated activation of the τGFP reporter in GnRHR positive cells under the control of the enhanced ROSA26 promoter (Wen et al., 2011; Wen et al., 2008). Consequently, the fluorescently marked neurons report the history of activity of the GnRHR promoter in GRIC/eR26-τGFP mice. Fluorescent neurons may therefore be tagged due to transient GnRHR expression during development. GnRHR antibodies, which could have helped to confirm the expression of the receptor in the neurons, are unfortunately very unreliable. Therefore, we used a physiological technique to confirm the presence of functional GnRHR in the τGFP labelled neurons using acute brain slice preparations. Brain areas which are related to reproductive behavior and known to feature a high density of GnRH positive fibers, as the hypothalamic areas arcuate nucleus, dorsomedial nucleus and periventricular nucleus (Boehm et al., 2005), and the periaqueductal gray (Merchenthaler et al., 1984), were selected for this study.

4.3. Results

4.3.1. Visualization of fluorescently labeled GnRHR neurons

GnRHR neurons of various hypothalamic areas (periventricular nucleus (Pe), arcuate nucleus (Arc) and dorsomedial nucleus (DM of the hypothalamus) displayed a robust τGFP fluorescence in the acute coronal brain slices prepared from GRIC/eR26-τGFP mice. The neurons can be visualized easily using a confocal scanning microscope and dedicated laser and filter systems (Radiance 2100, Zeiss) (Figure 13A, C and E).

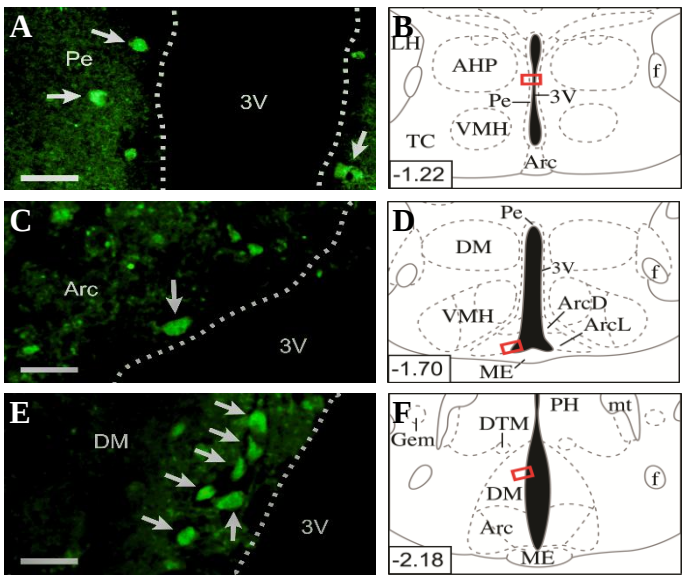

Figure 13. Visualization of τGFP expressing GnRHR neurons in acute brain slice preparations.
Individual GnRHR neurons displaying robust τGFP fluorescence (arrows) are easily visible in 250 µm thick coronal brain tissue slices prepared from (A) the Pe, (C) the Arc, and (E) the DM of GRIC/eR26-τGFP mice. Scale bars, 20 µm.
B, E, and F, Schematic diagrams indicating the imaged area (red box) shown in C, E, and G, respectively. Diagrams are adapted from (Paxinos and Franklin, 2001). 3V, third ventricle. Lower left corner numbers indicate the distance (mm) from bregma.

4.3.2. τGFP labelled GnRHR neurons express a functional GnRH receptor

To investigate whether the fluorescently tagged neurons express functional GnRHR in adult animals, we tested whether they could respond to GnRH. To enable us to monitor their stimulus-induced activity both spatially and temporally, we loaded the slices with fura-red/AM and used confocal microscopy to image the neurons at cellular resolution (Figure 14).

All τGFP/fura-red-labeled neurons (115 of 115 cells) responded with robust and reproducible Ca^{2+} increases (measured at the soma) to extracellular application of GnRH or its analog [D-Trp6]-LH-RH, although with different Ca^{2+} activity and sensitivity. During the experiments neither significant photobleaching nor any evidence of illumination-mediated damage of the cells under our experimental conditions was observed. Fluorescence changes showed full recovery to pre-stimulation levels.

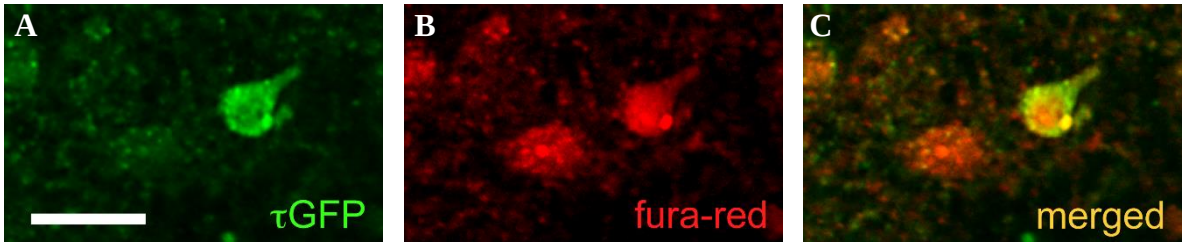

Figure 14. GnRHR-τGFP cell loaded with fura-red/AM. A, Confocal imaging in a coronal brain slice identifying a single GnRHR-τGFP cell body (green). Scale bar, 20 µm. B, Ca^{2+} fluorescence at rest (red) observed after loading the brain slice with fura-red/AM. C, Merged image shows that the GnRHR-τGFP neuron depicted in A took up the Ca^{2+} dye (yellow).

Within the Pe, we did not observe a noteworthy change in basic Ca^{2+} fluorescence at rest (Figure 15A), suggesting that GnRHR neurons do not receive direct input at the time of the recording or that their innervation by other neurons in the network did not change their basic Ca^{2+} concentration. However, stimulation with 25 s pulses of either GnRH or the GnRH analog [D-Trp^6]-LH-RH induced first a short followed by a broader Ca^{2+} transient.

In contrast, GnRHR neurons of the Arc displayed some basal Ca^{2+} activity (Figure 15B), which could be intrinsic or caused by the network of inputs onto these cells. The dynamics of the arcuate Ca^{2+} signal amplified with increasing GnRH concentration (Figure 15B and Figure 16; LSD, $p \leq 0.02$). Conversely, stimulation with [D-Trp^6]-LH-RH resulted in a short Ca^{2+} transient.

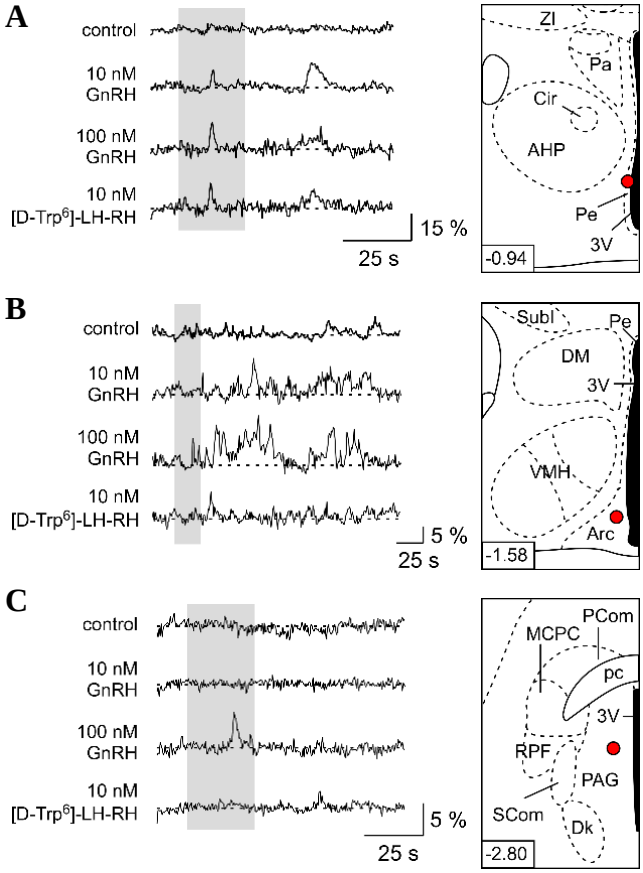

Figure 15. Examples of somatic Ca^{2+} responses from individual GnRHR neurons located in (A) the Pe, (B) the Arc, and (C) the PAG. Each neuron was subsequently stimulated with 0.1% BSA (control), 10 and 100 nM GnRH, as well as 10 nM [D-Trp^6]-LH-RH. Gray shaded area, start and end of bath application (duration, 25 s). Schematic diagram indicates the location of the recorded neuron (red dot). Lower left corner numbers indicate the distance (mm) from bregma.

GnRHR neurons within the PAG did not change their Ca^{2+} fluorescence at rest and were most of the time unable to respond to 10 nM GnRH (Figure 15C and Figure 16; LSD, $p = 0.29$). Interestingly, 10 nM [D-Trp^6]-LH-RH always caused a small Ca^{2+} transient in these cells (Figure 15C and Figure 16; LSD, $p < 0.01$). Responses to GnRH were consistently observed at the higher concentration of 100 nM (LSD, $p < 0.0001$). The duration and shape of these responses were similar within and different between areas. Spontaneous Ca^{2+} oscillations were seen in some GnRHR neurons depending on their location (Figure 15).

This result may reflect a difference in degradation rate of the two compounds or a difference in the combination of G protein coupling to the promiscuous GnRHR and its sensitivity to agonist stimulation (Naor, 2009; Tsutsumi et al., 2010).

4.3.3. Quantification of GnRH induced Ca^{2+} signals in GnRHR neurons

To quantify the change in the dynamics of the Ca^{2+} responses, we calculated the area under the curve (AUC) as a measure for the increase in intracellular Ca^{2+} (Figure 16). All tested GnRHR neurons raised their Ca^{2+} signals in response to GnRH or its analog [D-Trp^6]-LH-RH (ANOVA, F (3, 195) = 50.32; $p < 0.0001$), but differently between the measured areas (ANOVA, F (3, 195) = 23.85; $p < 0.0001$). Again, the arcuate GnRHR neurons seemed to have a slightly higher basal activity compared with those in other areas, although this was not statistically significant (Figure 16; LSD, $p = 0.30$ - 0.64).

The obvious differences in the basal activity of GnRHR neurons between the arcuate nucleus and the periventricular nucleus respectively the arcuate nucleus and the periaqueductal gray may be caused by distinct intracellular Ca^{2+} levels. To investigate this, a calibration of the Ca^{2+} signals of unstimulated GnRHR neurons was performed. The calibration of the Ca^{2+} signals in

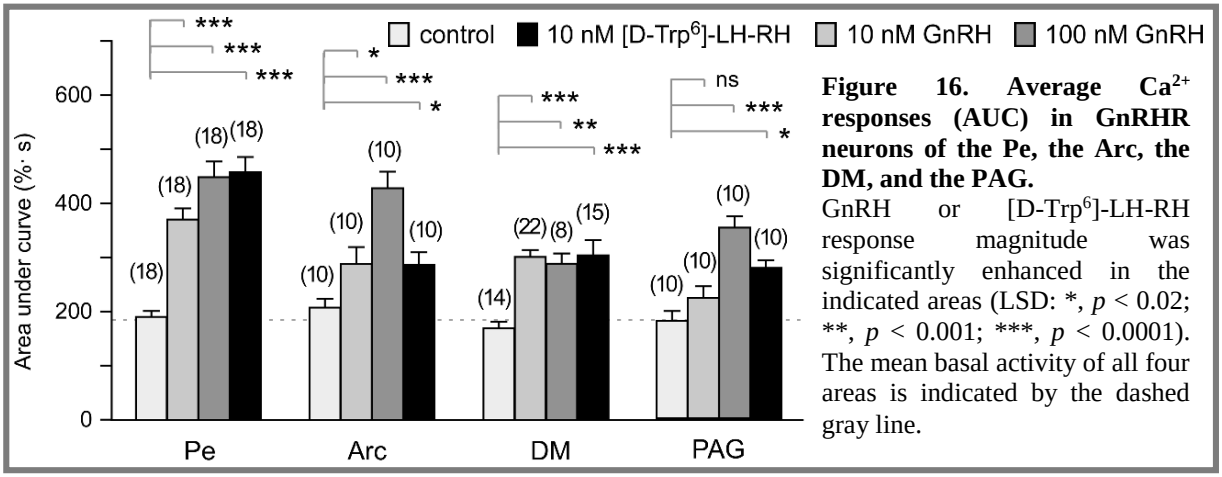

Figure 16. Average Ca^{2+} responses (AUC) in GnRHR neurons of the Pe, the Arc, the DM, and the PAG.
GnRH or [D-Trp^6]-LH-RH response magnitude was significantly enhanced in the indicated areas (LSD: *, $p < 0.02$; **, $p < 0.001$; ***, $p < 0.0001$). The mean basal activity of all four areas is indicated by the dashed gray line.

unstimulated arcuate GnRHR neurons indicated significantly elevated intracellular Ca^{2+} concentration ($[Ca^{2+}]_i$ = 0.95 ± 0.13 µM, n = 5) compared with the periventricular GnRHR neurons ($[Ca^{2+}]_i$ = 0.21 ± 0.06 µM, n = 12; unpaired t test, $p < 0.0001$). Saturation of the Ca^{2+} indicator dye would produce a relative increase of ~27%. These high values were not reached in our experiments, ruling out the possibility that dye saturation posed a significant problem.

4.3.4. GnRH-induced Ca^{2+} signals are not dependent on network activity

To exclude and prevent network activity that could influence and stimulate τGFP neurons, we repeated the stimulations with 10 nM GnRH in the presence of the sodium channel blocker TTX (10 µM; Figure 17). Inhibiting the network activity with 10 µM TTX decreased the basal Ca^{2+} signals by only 5%, suggesting foremost a dependence on intrinsic cellular processes. The inhibition of the action potential network activity was significantly hampered after TTX

treatment (70 - 100%) as could be monitored by the loss of depolarization-induced Ca^{2+} signals (Figure 17). Under these conditions the GnRH-induced Ca^{2+} signals were still clearly present, indicating that GnRH was the initial activator of the Ca^{2+} signals. Therefore, GnRH has a direct effect on τGFP neurons, providing compelling evidence that the labeled GnRHR neurons contain functional GnRHRs.

In summary, τGFP-marked GnRHR neurons in the different brain regions are able to respond to GnRH. These neurons use different Ca^{2+} signals for stimulus detection, which differ in waveform depending on stimulus strength and area. Our data suggest that GnRH, like dopamine, could pose as a neurotransmitter in the brain besides being a hormone.

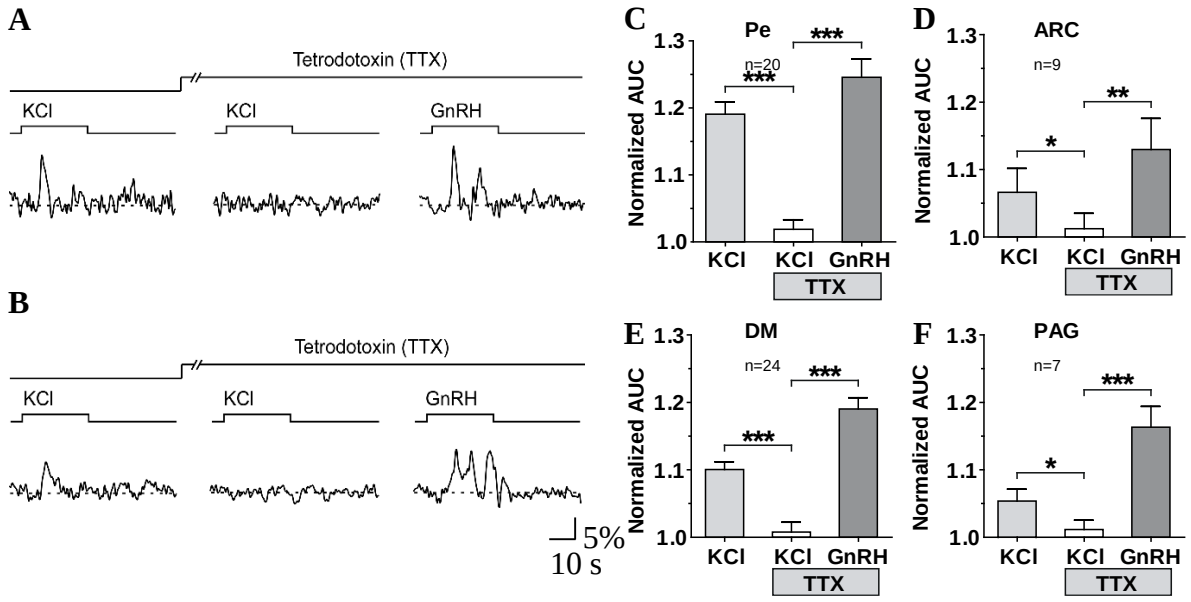

Figure 17. Somatic Ca^{2+} responses from an individual GnRHR neuron located in (A) the Pe and (B) the DM. Each neuron was subsequently stimulated with 60 mM KCl before and in the presence of 10 µM TTX treatment. After establishing a loss of depolarization-induced Ca^{2+} signal, the neurons were stimulated with 10 nM GnRH in the presence of 10 µM TTX. C-F, Bar histogram of AUC responses to KCl and GnRH normalized to their respective control AUC (either extracellular saline solution or saline solution supplemented with 10 µM TTX) (LSD: *, $p < 0.05$; ** < 0.001, ***, $p < 0.0001$). Data are expressed as means ± SEM.

4.4. Discussion

All GnRHR neurons tested in this study responded to GnRH application even under reduced synaptic activity because of blockage of the action potential network activity. These data provide compelling evidence that these genetically identified cells express functional GnRHR at the time of analysis.

The Ca^{2+} imaging results also indicate the existence of various populations of GnRHR neurons showing different response pattern due to the stimulation with GnRH. The different activity of

the neurons may indicates specific pattern of innervation of the individual nuclei, suggesting different integrative capacities.

The identification of direct GnRH target neurons in various brain regions suggests that GnRH could function as a neurotransmitter and –modulator besides being a hormone. In the past, different laboratories have postulated this idea (Samson et al., 1980; Dyer and Dyball, 1974; Pan et al., 1988; Renaud et al., 1975; Rothfeld et al., 1985). Still, GnRH is mainly considered a hormone and has not yet been classified differently. Like dopamine, GnRH is produced in several areas of the brain (Herbison, 2006) and is mainly released by the hypothalamus. Its main function as a hormone is to stimulate LH and FSH from the anterior lobe of the pituitary. Several circumventricular nuclei are sensitive to blood borne substances, substances delivered by cerebrospinal fluid or to both kind of substances (Duvernoy and Risold, 2007). The capitalization from the median eminence, which leaks a blood brain barrier, might deliver GnRH to hypothalamic areas (Wislocki, 1937; Page, 1982; Page et al., 1978; Cottrell and Ferguson, 2004). For several other areas around the third ventricle, it remains unclear if they may lack an effective blood–brain barrier (Saper, 2004; Herde et al., 2011). Alternatively to a direct communication via capillary contact, it has being hypothesized that GnRH, which is released in large quantities to the cerebrospinal fluid, may be transported in this way to brain regions located close to the third ventricle where it can bind to GnRHR neurons (Yoshioka et al., 2001). In several studies the effect of intracerebroventricular GnRH injections on reproductive behavior such as lordosis (Sirinathsinghji, 1983; Moss and Foreman, 1976), compensation of sexual behavior deficits by VNO removal (Meredith and Howard, 1992) or in male rats a decreases the latency to intromission and ejaculation (Moss and McCann, 1973) could be shown. Furthermore, microiontophoretic GnRH injections induced an increase of firing rate in many neurons recorded in this area (Samson et al., 1980).

Taken together, GnRH signaling may directly modulate the animal's sensitivity toward certain pheromones. In humans, GnRH signaling equally has been implicated in modulating the detection of odors relevant for reproduction (Wirsig-Wiechmann, 2001) and may thus cause variations in the olfactory performance during the menstrual cycle (Hummel et al., 1991).

Statement of copyright:
Figures 13 to 17 were adapted from (Wen et al., 2011) Copyright 2011, The Endocrine Society. Permission of usage see Chapter 7.

4.5. References

1 BOEHM, U., ZOU, Z. & BUCK, L. B. 2005. Feedback loops link odor and pheromone signaling with reproduction. *Cell,* 123**,** 683-95.

2 COTTRELL, G. T. & FERGUSON, A. V. 2004. Sensory circumventricular organs: central roles in integrated autonomic regulation. *Regul Pept,* 117**,** 11-23.

3 DUVERNOY, H. M. & RISOLD, P.-Y. 2007. The circumventricular organs: An atlas of comparative anatomy and vascularization. *Brain Research Reviews,* 56**,** 119-147.

4 DYER, R. G. & DYBALL, R. E. 1974. Proceedings: Inhibition of hypothalamic unit activity by iontophoretically applied luteinizing hormone releasing factor and thyrotrophin releasing factor. *J Endocrinol,* 63**,** 35P.

5 GORE, A. C. 2002. *GnRH: The master molecule of reproduction*, Kluwer Academic Publishers.

6 HERBISON, A. E. 2006. Chapter 28 - Physiology of the Gonadotropin-Releasing Hormone Neuronal Network. *In:* NEILL, J. D., PLANT, T. M., PFAFF, D. W., CHALLIS, J. R. G., KRETSER, D. M. D., RICHARDS, J. S. & WASSARMAN, P. M. (eds.) *Knobil and Neill's Physiology of Reproduction (Third Edition).* St Louis: Academic Press.

7 HERDE, M. K., GEIST, K., CAMPBELL, R. E. & HERBISON, A. E. 2011. Gonadotropin-releasing hormone neurons extend complex highly branched dendritic trees outside the blood-brain barrier. *Endocrinology,* 152**,** 3832-41.

8 HUMMEL, T., GOLLISCH, R., WILDT, G. & KOBAL, G. 1991. Changes in olfactory perception during the menstrual cycle. *Experientia,* 47**,** 712-5.

9 MERCHENTHALER, I., GORCS, T., SETALO, G., PETRUSZ, P. & FLERKO, B. 1984. Gonadotropin-releasing hormone (GnRH) neurons and pathways in the rat brain. *Cell Tissue Res,* 237**,** 15-29.

10 MEREDITH, M. & HOWARD, G. 1992. Intracerebroventricular LHRH relieves behavioral deficits due to vomeronasal organ removal. *Brain Res Bull,* 29**,** 75-9.

11 MOSS, R. L. & FOREMAN, M. M. 1976. Potentiation of lordosis behavior by intrahypothalamic infusion of synthetic luteinizing hormone-releasing hormone. *Neuroendocrinology,* 20**,** 176-81.

12 MOSS, R. L. & MCCANN, S. M. 1973. Induction of mating behavior in rats by luteinizing hormone-releasing factor. *Science,* 181**,** 177-9.

13 NAOR, Z. 2009. Signaling by G-protein-coupled receptor (GPCR): studies on the GnRH receptor. *Front Neuroendocrinol,* 30**,** 10-29.

14 PAGE, R. B. 1982. Pituitary blood flow. *Am J Physiol,* 243**,** E427-42.

15 PAGE, R. B., LEURE-DUPREE, A. E. & BERGLAND, R. M. 1978. The neurohypophyseal capillary bed. II. Specializations within median eminence. *Am J Anat,* 153**,** 33-65.

16 PAN, J. T., KOW, L. M. & PFAFF, D. W. 1988. Modulatory actions of luteinizing hormone-releasing hormone on electrical activity of preoptic neurons in brain slices. *Neuroscience,* 27**,** 623-8.

17 PAXINOS, G. & FRANKLIN, K. B. J. 2001. *The mouse brain in stereotaxic coordinates,* San Diego, Academic Press.

18 RENAUD, L. P., MARTIN, J. B. & BRAZEAU, P. 1975. Depressant action of TRH, LH-RH and somatostatin on activity of central neurones. *Nature,* 255**,** 233-5.

19 ROTHFELD, J. M., CARSTENS, E. & GROSS, D. S. 1985. Neuronal responsiveness to gonadotropin-releasing hormone and its correlation with sexual receptivity in the rat. *Peptides,* 6**,** 603-8.

20 SAMSON, W. K., MCCANN, S. M., CHUD, L., DUDLEY, C. A. & MOSS, R. L. 1980. Intra- and extrahypothalamic luteinizing hormone-releasing hormone (LHRH) distribution in the rat with special reference to mesencephalic sites which contain both LHRH and single neurons responsive to LHRH. *Neuroendocrinology,* 31**,** 66-72.

21 SAPER, C. B. 2004. Chapter 17 - Hypothalamus. *In:* PAXINOS, G. & MAI, J. K. (eds.) *The Human Nervous System (Second Edition).* San Diego: Academic Press.

22 SHERWOOD, N. M., LOVEJOY, D. A. & COE, I. R. 1993. Origin of mammalian gonadotropin-releasing hormones. *Endocr Rev,* 14**,** 241-54.

23 SIRINATHSINGHJI, D. J. 1983. GnRH in the spinal subarachnoid space potentiates lordosis behavior in the female rat. *Physiol Behav,* 31**,** 717-23.

24 TIRINDELLI, R., DIBATTISTA, M., PIFFERI, S. & MENINI, A. 2009. From pheromones to behavior. *Physiol Rev,* 89**,** 921-56.

25 TSUTSUMI, R., MISTRY, D. & WEBSTER, N. J. 2010. Signaling responses to pulsatile gonadotropin-releasing hormone in LbetaT2 gonadotrope cells. *J Biol Chem,* 285**,** 20262-72.

26 WEN, S., GOTZE, I. N., MAI, O., SCHAUER, C., LEINDERS-ZUFALL, T. & BOEHM, U. 2011. Genetic identification of GnRH receptor neurons: a new model for

studying neural circuits underlying reproductive physiology in the mouse brain. *Endocrinology,* 152**,** 1515-26.

27 WEN, S., SCHWARZ, J. R., NICULESCU, D., DINU, C., BAUER, C. K., HIRDES, W. & BOEHM, U. 2008. Functional characterization of genetically labeled gonadotropes. *Endocrinology,* 149**,** 2701-11.

28 WIRSIG-WIECHMANN, C. R. 2001. Function of gonadotropin-releasing hormone in olfaction. *Keio J Med,* 50**,** 81-5.

29 WISLOCKI, G. B. 1937. The vascular supply of the hypophysis cerebri of the cat. *The Anatomical Record,* 69**,** 361-387.

30 YOON, H., ENQUIST, L. W. & DULAC, C. 2005. Olfactory inputs to hypothalamic neurons controlling reproduction and fertility. *Cell,* 123**,** 669-82.

31 YOSHIOKA, K., SUZUKI, C., ARAI, S., IWAMURA, S. & HIROSE, H. 2001. Gonadotropin-releasing hormone in third ventricular cerebrospinal fluid of the heifer during the estrous cycle. *Biol Reprod,* 64**,** 563-70.

5. Endogenous GnRH determines GnRHR neuron spike code activity during female cyclicity

5.1. Abstract

As indicated in the previous chapters, GnRH plays an essential role in reproduction and has been implicated to regulate different hormonal and physiological signals in the brain. Its role in neuronal excitability and expected changes in neuronal activity during the female reproductive cycle have not been elucidated. Therefore, we started to investigate action potential discharges of hypothalamic GnRHR neurons in gonadally-intact female mice. The neurons exhibit distinct basic spike activity modes dependent on the stage within the estrous cycle. High-frequency clusters of action potentials, characteristic of a burst firing mode, are observed during reproductive stages associated with elevated GnRH or in the presence of externally applied GnRH, whereas the discharges change to a regular temporal pattern in the presence of a GnRHR antagonist. Information regarding GnRH concentration to a pulsed stimulation is encoded in the response latency to the first spike, indicating that GnRHR neurons can respond timely to GnRH changes, and more substantially with a long-lasting conversion in spike activity detected by the latency and duration of the modified variance in instantaneous spike frequency. A complete transformation in action potential firing pattern as seen during the estrous cycle is triggered by prolonged GnRH stimulation, manifesting this regulatory hormone as a strong neuromodulator. Taken together, GnRHR neurons seem to be ideally attuned to vascular changes in GnRH during the estrous cycle firing with brief action potential bursts after GnRH stimulation, potentially to be more effective in transmitter release and therefore enhance communication between neurons to optimize reproductive success.

5.2. Introduction

GnRH secreting neurons originate in the nasal placode and migrate to the anterior hypothalamus during embryonic development (Schwanzel-Fukuda and Pfaff, 1989; Wray et al., 1989). Interestingly, GnRH neurons in sexually mature animals remain connected to the olfactory system (Boehm et al., 2005; Yoon et al., 2005), which processes a variety of sensory signals (Leinders-Zufall et al., 2000; Leinders-Zufall et al., 2004; Leinders-Zufall et al., 2009; Haga et al., 2010; Del Punta et al., 2002) influencing numerous behaviors, including reproduction (Insel and Fernald, 2004; Tirindelli et al., 2009).

To maintain fertility, GnRH is released into the vascular system at regular intervals ensuring central control of reproduction via the Hypothalamic-Pituitary-Gonadal (HPG) axis. In female rodents, GnRH release occurs pulsatile from axon terminals at the median eminence and substantially during the late phase of proestrus (Moenter et al., 1992). The intensity of the GnRH release during this surge is highly elevated (Sisk et al., 2001; Moenter et al., 2003). Secreted GnRH then binds to GnRH receptors (GnRHRs) on gonadotrope cells of the anterior pituitary to regulate reproduction via the HPG axis. GnRH has also been implicated in regulating reproductive physiology independent of gonadotropin release (Moss and McCann, 1973; Moss and Foreman, 1976; Pfaff, 1973). Consistent with this, GnRH fibers project to brain areas influencing sexual behavior that contain GnRHR neurons (Wen et al., 2011b), raising the possibility that GnRH modulates the activity of its target neurons directly. Altering reproductive physiology in the brain will ultimately depend on the function of the target neurons whose axons carry spike-encoded information to different areas in the central nervous system.

To begin to define the circuitry of GnRH/GnRHR signaling in the brain, we started to investigate the excitability of GnRHR neurons located in the periventricular hypothalamic nucleus (Pe). The Pe is a thin sheet of small neurons located in the wall of the third ventricle (Figure 18). It is located in the rostral, intermediate, and caudal regions of the hypothalamus and may not have an effective blood–brain barrier (Saper, 2012; Herde et al., 2011). It is not clear how GnRH influences its target neuron expressing GnRHR. Therefore, a source of GnRH for modulating GnRHR neurons can come from either GnRH-secreting neuronal fibers, third ventricular cerebrospinal fluid or the cerebrovascular system (Skinner et al., 1997; Caraty and Skinner, 2008). In this chapter, we examined whether the neural activity of GnRHR neurons in the Pe changes during the female reproductive cycle and whether their activity depends on endogenous GnRH.

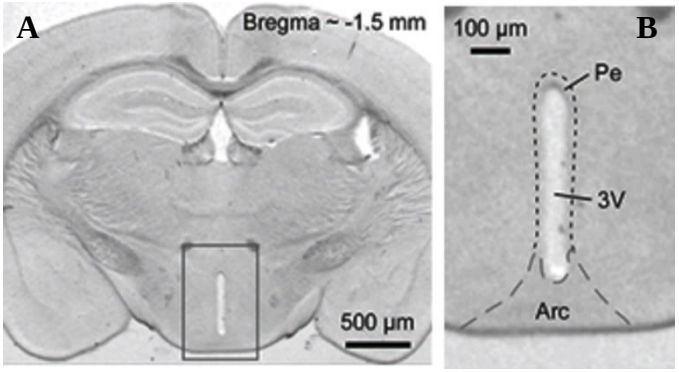

Figure 18. Coronal brain slice showing the location of the periventricular nucleus. A, overview and higher magnification (B) of a (Pe) and the arcuate nucleus (Arc) of the hypothalamus next to the third ventricle (3V).

5.3. Results

5.3.1. GnRHR neurons are spontaneously active and change their spike activity patterns depending on the female's reproductive stage

It is suggested that GnRH in the Pe is predominantly supplied by blood capillaries or the third ventricle. Thereby GnRHR neurons in this area might be susceptible to changes in GnRH levels during the estrous cycle. Therefore, we started to examine the basal excitability of Pe GnRHR neurons during the four stages of the mouse reproductive cycle.

We performed extracellular loose-patch recordings to register neuronal activity from optically identified GnRHR neurons in acute coronal brain tissue slices using a combination of fluorescence and infrared differential interference contrast (IR-DIC) illumination (Figure 19). The brain slices were prepared using an adapted version of our protocol for hypothalamic mouse brain slices (Chapter 3) (Schauer and Leinders-Zufall, 2012; Wen et al., 2011b). This adapted version includes an additional cooling as well as an incubation step (see Chapter 2.2.4.1 to .2.2.4.3) which facilitates an improved survival duration of patched neurons.

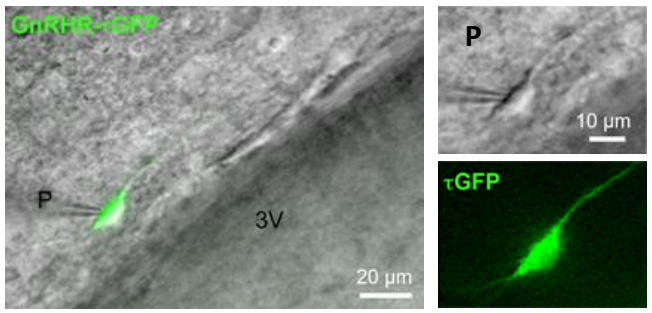

Figure 19. Overlay of a fluorescence image on top of an infrared-differential interference contrast (IR-DIC) micrograph of a live brain tissue slice identifying a GnRHR neuron in the Pe, which is located next to the third ventricle. The somata of the GnRHR neurons are clearly visible in the IR-DIC image (right top panel) and expresses τGFP (right lower panel). P, patch electrode, 3V third ventricle.

GnRHR neurons (n = 88) recorded in 50 gonadally intact female mice exhibit spontaneous spike activity recorded as action-potential-driven, capacitive currents. Neurons showed generally tonic or burst firing patterns, occasionally irregular firing (Figure 20).

To classify these neuronal spike activity patterns, various parameters established in the field of neuronal spike analysis where analyzed. The analysis of the parameters individual suitability and independency indicated the following parameters as essential: Coefficient of the Variation of the InterSpike Interval (CV_{ISI}) (Robin et al., 2009; Grace and Bunney, 1984), Percentage of Spikes in Bursts (PSiB) (Dahan et al., 2007; Grace and Bunney, 1984) and Mean number of Spikes in each Burst (MSiB) (Jackson et al., 2004; Gariano and Groves, 1988).

To enable the calculation of these various parameters in an unbiased manner, an interspike interval threshold had to be determined to help define the start and end of an action potential

burst. We used a quantitative approach from (Selinger et al., 2007). A burst was then classified as an event with at least three spikes that had a rate below 1.3 s. By applying the criteria of Robin et al., 2009 (Robin et al., 2009) a CV_{ISI} < 0.8 was calculated as threshold to define neurons as tonic firing neurons (n1 in Figure 20).

Neurons firing in bursts (= periods of time with a high spike rate separated by periods with a much lower spike rate (n2 in Figure 20) and irregular firing neurons (n3 in Figure 20), both having a CV_{ISI} > 0.8. Based on this approach the two parameters percentage of spikes in bursts (PSiB) and mean number of spikes in a burst (MSiB) could be calculated.

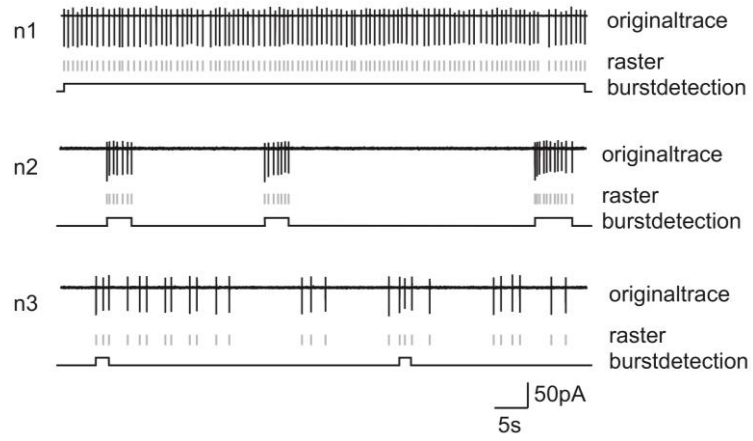

Figure 20. Example recordings of trains of extracellularly recorded, action-potential-driven capacitive currents of three different GnRHR neurons (n1 – n3). Pipette potential was 0 mV. Below the original recording the corresponding raster plot, indicating the time point of the occurrence of an action potential, and the burst patterns using an automated unbiased process (Selinger et al., 2007) are outlined.

By plotting the PSiB logarithmic, a threshold of 80% spikes in burst was provided. Neurons with a PSiB > 80% (and a CV_{ISI} > 0.8) are classified as bursting, neurons with a PSiB < 80% (and a CV_{ISI} > 0.8) as irregular firing respectively. The 2D scatter plots (Figure 21A-C), CV_{ISI} versus PSiB, CV_{ISI} versus MSiB and PSiB versus MSiB, visualize the impact of the obtained threshold levels to classify the neurons by firing pattern.

Considering the properties of GnRHR neurons (n = 88) we identified 34% of the neurons as firing tonically, 55% in a burst pattern and only 11% as irregular firing. Combining all three parameters used for classifying firing pattern in a 3D scatterplot (Figure 21D) tonic, bursting and irregular neurons form three independent non-overlapping clouds. The statistic comparison of the CV_{ISI} of tonic, bursting and irregular firing neurons confirms the importance of CV_{ISI} as parameter to distinguish tonic firing neurons from bursting and irregular neuron, as well as the significance of the threshold (Figure 22A, ANOVA: $F_{2,85} = 33.79$, $p < 0.0001$; Tukey: tonic vs. bursting: p = <0.0001, tonic vs. irregular: p = 0.0088).

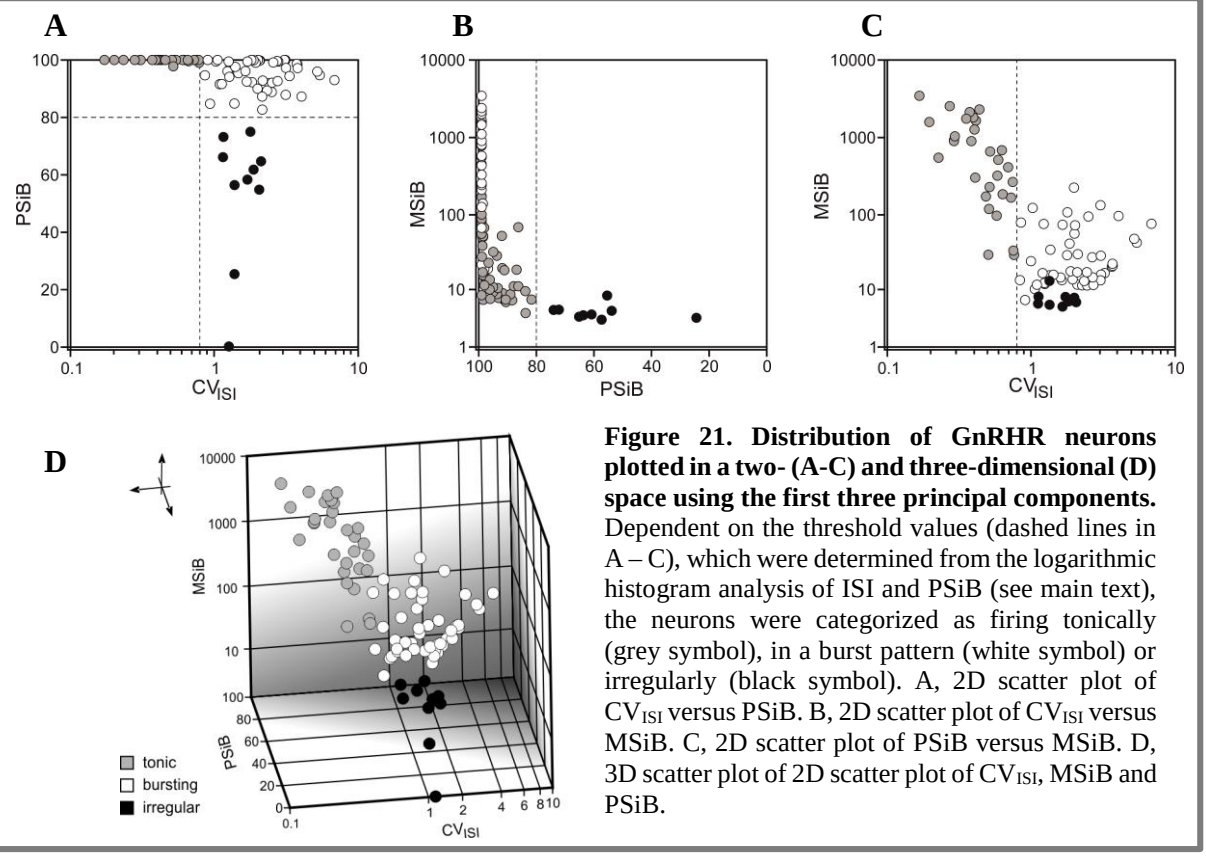

Figure 21. Distribution of GnRHR neurons plotted in a two- (A-C) and three-dimensional (D) space using the first three principal components. Dependent on the threshold values (dashed lines in A – C), which were determined from the logarithmic histogram analysis of ISI and PSiB (see main text), the neurons were categorized as firing tonically (grey symbol), in a burst pattern (white symbol) or irregularly (black symbol). A, 2D scatter plot of CV_{ISI} versus PSiB. B, 2D scatter plot of CV_{ISI} versus MSiB. C, 2D scatter plot of PSiB versus MSiB. D, 3D scatter plot of 2D scatter plot of CV_{ISI}, MSiB and PSiB.

Similar results are obtained by statistically analyzing (ANOVA with Tukeys multiple comparison) the MSiB of tonic, bursting and irregular firing neurons (Figure 22B, ANOVA: $F_{2,85} = 24.54$, $p < 0.0001$; Tukey: tonic vs. bursting: $p < 0.0001$, tonic vs. irregular: $p = 0.0001$).

Comparing statistically (ANOVA with Tukeys multiple comparison) the PSiB of the three groups of neurons, a highly significant difference especially between irregular firing neurons and the two regular firing pattern (tonic and bursting) were observed. Tonic and bursting neurons show as well a significant difference in the PSiB (Figure 22C, ANOVA: $F_{2,85} = 122.0$, $p < 0.0001$; Tukey: tonic vs. bursting: $p = 0.0466$, tonic vs. irregular: $p < 0.0001$, bursting vs. irregular $p < 0.0001$).

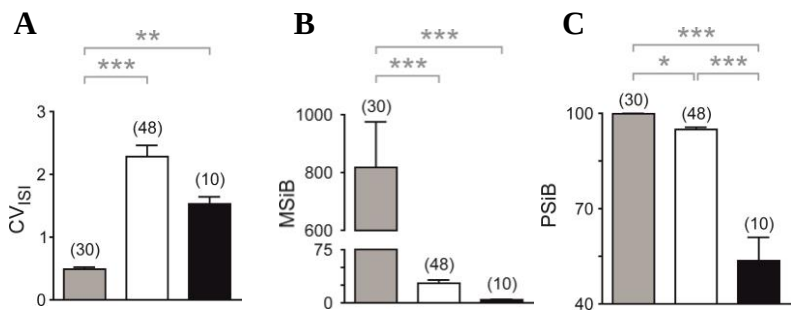

Figure 22. Bar histogram of the CV_{ISI} (A), the MSiB (B) and the PSiB (C) dependent on the spike activity classification of GnRHR neurons. Number of neurons is plotted in brackets above each bar. CV_{ISI}, coefficient of variation of the interspike interval; PSiB percentage of spikes in bursts; MSiB, mean number of spikes in a burst.

To determine if the spontaneous spike activity is linked to the female reproductive cycle, we characterized GnRHR neuron firing patterns during the four stages of the estrous cycle: metestrus, diestrus, proestrus and estrus. Vaginal cytology provided a means to establish the female's reproductive stage and revealed that GRIC/eR26-τGFP mice display normal 4-5 day length cycles (4.5 ± 0.2 days, n = 6) (Figure 23).

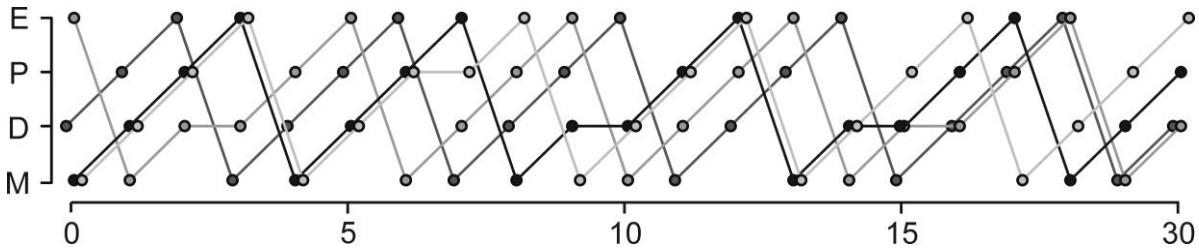

Figure 23. GnRHR neurons change their spontaneous spike activity pattern during the reproductive cycle. Representative plot of the estrous cycle from four GRIC/eR26-τGFP mice. The females display a normal 4-5 day length cycle. M, metestrus; D, diestrus; P, proestrus; E, estrus.

Analyzing the spontaneous firing of GnRHR neurons showed a dramatic increase in the mean spike frequency (Figure 24D) with a peak at 4.0 ± 0.7 Hz (n = 33) in proestrus compared to rates of 1.3 ± 0.2 Hz (n = 16) and 2.5 ± 0.5 Hz (n = 19) during metestrus and estrus, respectively (Tukey´s: $p < 0.0001$). An increase in the mean firing frequency suggests the presence of tonically firing neurons. In addition, the PSiB, the CV_{ISI} and the MSiB indicated shifts in firing behavior of the GnRHR neurons during the female's estrous cycle (Figure 24A-C). The rise in the PSiB and MSiB as well as the simultaneous reduction in CV_{ISI} is indicative of increasing numbers of tonically firing neurons during proestrus. Using the previously determined thresholds for classifying the GnRHR neurons, we could indeed confirm that a majority of tonically firing neurons are present during this reproductive stage (61%; Figure 24E). Virtually no GnRHR neurons fire tonically at metestrus (1 out of 16 cells), but this number increases by almost 30% during diestrus (7 out of 20 cells) with another 25% rise during proestrus (20 out of 33 cells) to dramatically decrease back to almost no tonically firing GnRHR neurons during estrus (2 out of 19 cells). A similar, but inverse, cyclicity is seen for the occurrence of bursting GnRHR neurons with most cells being observed during metestrus (12 out of 16 cells, 75%). The number of bursting neurons decline over the next stages to a low of 12 out of 33 cells (36%) to dramatically increase again on the day of estrus (13 out of 19 cells, 68%). Irregular firing neurons (n = 10) are rarely found at any stage during the reproductive cycle.

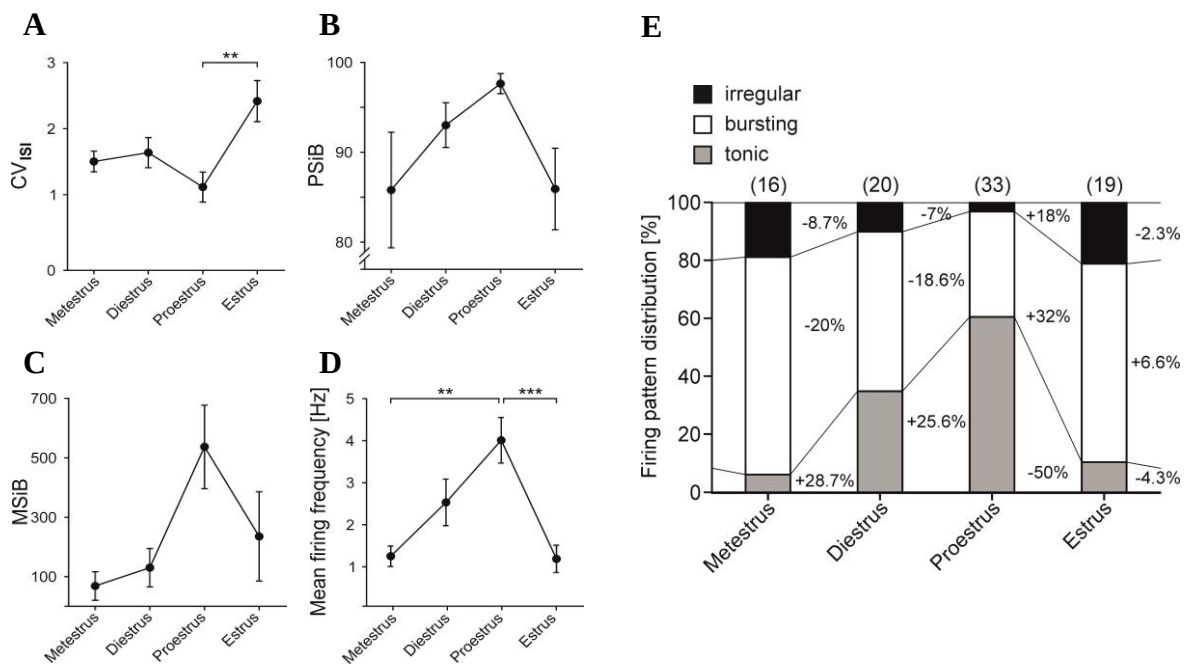

Figure 24. Distribution of firing pattern in GnRHR neurons depends on reproductive stage. A - C, The increased value in PSiB and MSiB at proestrus together with the reduced value in CV_{ISI} points to a rise in the number of tonically firing neurons. Metestrus: PSiB, 85.8 ± 6.4; CVISI, 1.5 ± 0.2; MSiB, 68.6 ± 47.9; Diestrus: PSiB, 93.0 ± 2.5; CVISI, 1.6 ± 0.2; MSiB, 130.3 ± 64.7; Proestrus: PSiB, 97.6 ± 1.1; CVISI, 1.1 ± 0.2; MSiB, 537.0 ± 140.4; Estrus: PSiB, 85.9 ± 4.5; CVISI, 2.4 ± 0.3; MSiB, 235.4 ± 150.4 F, The distribution of firing pattern (tonic, burst, irregular) of GnRHR neurons separated by the reproductive stage. Most tonically firing neurons are observed during proestrus. During the other stages of the reproductive cycle GnRHR neurons fire mainly in a bursting pattern. Reductions or rather increases in the number of GnRHR neurons modifying the spike pattern behavior between two reproductive stages are indicated between the bars. Number of neurons is plotted in brackets above each bar.

The dependence of the spontaneous firing pattern on the female reproductive cycle suggests communication between GnRHR neurons and either blood capillaries containing GnRH or GnRH-secreting fibers that follow the same pulsatility as measured in the HPG axis. The amplitude and frequency of GnRH levels near the median eminence is reported to be highly elevated during the second phase of proestrus (Sisk et al., 2001). We therefore speculated that after GnRH stimulation tonically firing GnRHR neurons, mainly present in proestrus, are compelled to change their neuronal spike activity to fire in bursts during estrus. Neurons firing with brief high-frequency bursts have been indicated to be more effective in increasing transmitter release and therefore communication between neurons. This would suggest that during the other phases of the reproductive cycle GnRHR neurons in the brain receive input from GnRH.

5.3.2. Dose-dependent modulation of action potential firing by GnRH

First, we examined tonically firing GnRHR neurons (n = 55) recorded in 21 gonadally intact female mice during proestrus to determine whether they can vary their action potential firing to stimulations with 1 s pulses of various GnRH concentrations as well as solution without GnRH (control). GnRHR neurons responded reproducibly and repeatably to GnRH with an increase in the mean spike frequency as can be noted by the more narrowly spaced lines in the raster plot (Figure 25A). To reveal if the spatio-temporal pattern of the GnRH-induced change in the action potential sequence contains information regarding the deterministic component for encoding GnRH concentrations, the mean spike frequency after GnRH stimulation was assessed. Compared to the control, the mean spike frequency ratio increased with the GnRH concentration, but not significantly (Figure 25B, ANOVA: $F_{4,56} = 0.81$, $p = 0.52$). Alternatively, the timing of the first spike after the GnRH stimulation may encode information regarding the GnRH concentration, as has been reported in various sensory modalities (Rospars et al., 2003; Robin et al., 2009). We found a dose-dependent change in the first-spike latency independent of the noise caused by spontaneous action potential activity of the neurons (Figure 25C), With increasing GnRH concentration the latency decreases having a $K_{1/2}$ value of 0.71 ± 0.41 nM (mean ± SD) indicating that GnRHR neurons are able to respond timely to a changes in GnRH concentration.

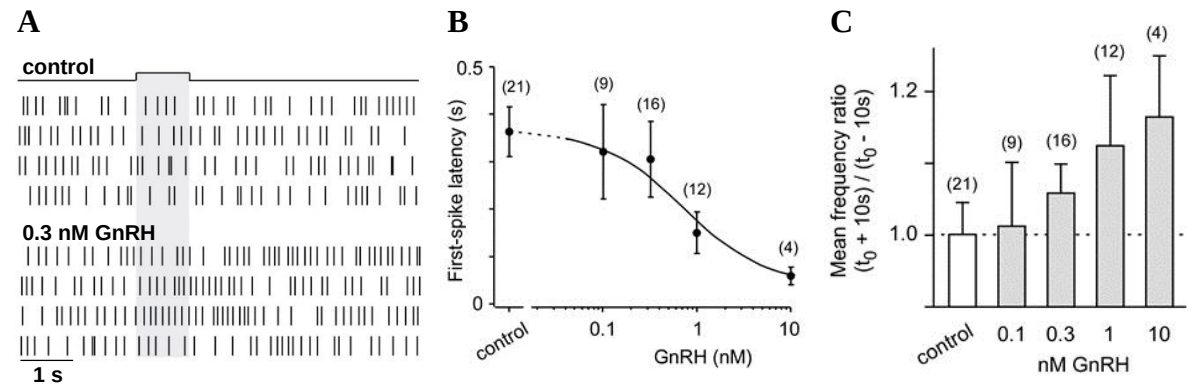

Figure 25. GnRH modulates the neuronal activity of GnRHR neurons dose-dependently. A, Raster diagram of an individual GnRHR neuron consecutively stimulated with a 1-s pulse (grey) of a solution containing either no GnRH (control) or 0.3 nM GnRH. B, The mean spike frequency ratio rises with the GnRH concentration, but is not statistically significant due to the high variance in the data set. C, The first-spike latency decreases with increasing GnRH concentration having a $K_{1/2}$ value of 0.71 ± 0.41 nM and a Hill coefficient of -1.2 ± 1.0. The curve is a fit of the Hill equation.

Neurons in the hypothalamus are embedded in a network of dissimilar cells, whereby each cell is subjected to a bombardment of incoming synaptic input. Therefore, it is debatable if this spike code information can effectively influence the actions of the neuron for modulating social behavior dependent on the hormonal status of the animal. Therefore, hormonal modulation of

behaviors likely relies on neural firing over extended time periods.

Intriguingly, GnRHR neurons showed long-lasting changes in spike activity that persisted for 1-2 min, in addition to the short-lived responses (Figure 26). Analyzing the variance in instantaneous spike frequency (VARiF) revealed a dose-dependent change in both latency and duration of a 1 s GnRH-induced long-lasting conversion in spike activity (Figure 26, ANOVA: latency, $F_{3,36} = 36.35$, $p < 0.0001$; duration, $F_{3,36} = 11.24$, $p < 0.0001$). Both dose-dependent properties of long-lasting changes could be fitted with a Hill equation giving $K_{1/2}$ values (mean ± SD) of 0.48 ± 0.11 and 0.46 ± 0.17 nM for the latency and duration of the long-lasting conversion in spike activity, respectively.

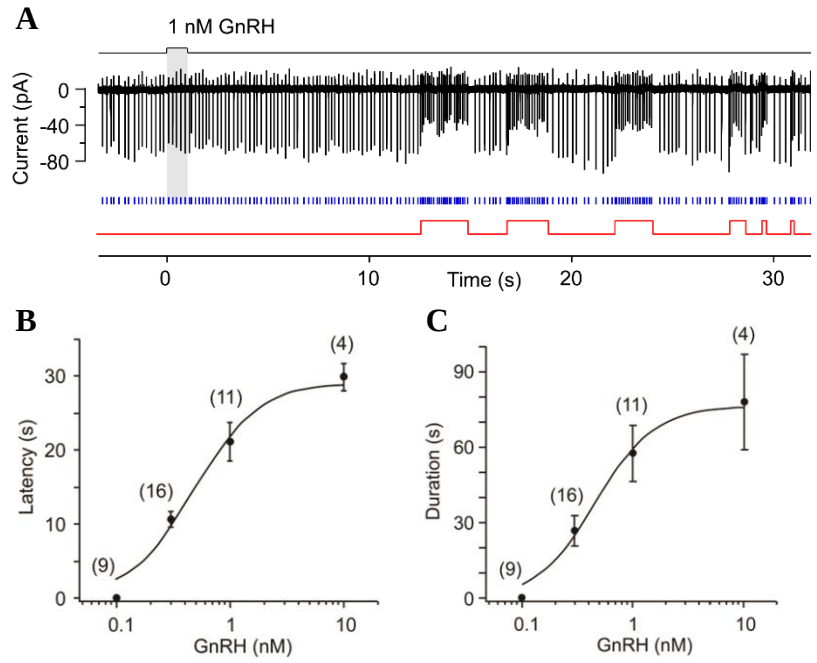

Figure 26. GnRHR neurons possess long-lasting changes in spike activity after a brief GnRH stimulation. A, Original recording (black), raster diagram (blue) and burst detection (red) of a GnRHR neuron stimulated by a 1 s application of GnRH. B - C, Dose-dependency of the latency (B) and duration (C) of the long-lasting conversion in spike activity. Both values increase with increasing GnRH concentration. Curves are fitted by the Hill, yielding $K_{1/2}$ values and Hill coefficients of 0.48 ± 0.11 nM, 1.5 ± 0.4 (latency, mean ± SD) and 0.46 ± 0.17 nM, 1.6 ± 0.7 (duration, mean ± SD), respectively.

Interestingly, the $K_{1/2}$ values obtained by analyzing GnRH-induced short- and long-duration effects are in close proximity to values published previously for the GnRHR in immortalized gonadotrope-like cells (Conn and Hazum, 1981; Barran et al., 2005; Lu et al., 2005).

In addition, the similar $K_{1/2}$ values for the GnRH-induced spike activity (Figure 25 and 26) give reason to speculate that the observed modulations in spike activity are all due to the activation of the receptor itself, which may consecutively stimulated different G-proteins or second messenger pathways generating dual effects on the intrinsic activity of the cell (Naor and Huhtaniemi, 2013; Naor, 2009). Our results demonstrate that GnRH can act as a strong modulator of the firing activity of GnRHR neurons. The long-lasting increase in the variance in instantaneous spike frequency following a short pulse of GnRH could be a first step in modulating the initiation of action potential plasticity that leads to the transformation of a tonic firing pattern to a burst or irregular pattern.

5.3.3. Endogenous GnRHR activity regulates the neuronal spike code

During proestrus, GnRH levels are elevated in the hypophyseal portal blood and cerebrospinal fluid (Moenter et al., 1992; Moenter et al., 2003; Sisk et al., 2001). To explore the possibility that GnRHR neurons alter their firing pattern due to sustained GnRH stimulation, we assessed the action potential firing behavior of tonic GnRHR neurons continuously stimulated with 10 nM GnRH for 10 min up to 1½ hours (Figure 27). During these recordings the mean firing frequency and the two parameters of spike code classification (CV_{ISI} and PSiB) were evaluated every 220 s. All tonically firing GnRHR neurons from females in proestrus had a basic CV_{ISI} below the threshold of 0.8 (0.55 ± 0.24, n = 6) and a PSiB of 99.8 ± 0.21 (6). The mean spike frequency was 3.5 ± 0.3 Hz (n = 6; *pre* in Figure 27C) which dropped to 1.4 ± 1.1 Hz (n = 6; *post* in Figure 27C) after 10 min GnRH perfusion. The characteristic parameter CV_{ISI}, separating the tonic firing neurons from bursting and irregular firing neurons, changed to values above 0.8 (1.9 ± 0.8, n = 6; Figure 27D) without significantly changing the PSiB (77.1 ± 33.2; t-test: p = 0.17), reclassifying the initially tonic firing GnRHR neurons as firing in bursts (Figure 27). Therefore, prolonged GnRH stimulation triggers a transformation in action potential firing pattern.

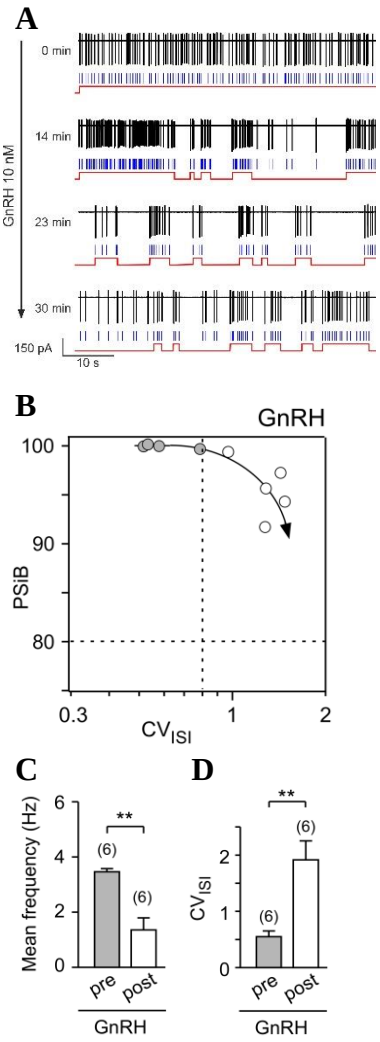

Figure 27. Long-term application of GnRH changes the firing pattern of GnRHR neurons. A, Example traces (original recording (black), raster diagram (blue), burst detection (red)) of trains of extracellularly recorded, action-potential-driven capacitive currents from the same GnRHR neuron of a proestrus mouse taken at various times after starting the 10 nM GnRH perfusion. B, GnRH-induced change in the spike activity from the same GnRHR neuron as shown in A. Dependent on the threshold values for the CV_{ISI} and the PSiB (dashed lines, see 5.4.1), the neuron can be categorized to fire first tonically (grey symbols), which changes to a burst pattern (white symbol) during the GnRH treatment. C – D, Bar histogram of the mean spike frequency (C) and the CV_{ISI} (D) 4 min before the start (pre) and the last 4 min of the GnRH treatment (post) of GnRHR neurons of mice in proestrus. T-test: ** $p < 0.01$. Bar and symbol coloring (grey and white) indicate to which category of firing pattern (tonic (grey), bursting (white)) the group of neurons belongs to.

These results suggest that GnRHR neurons firing in bursts might be prestimulated with GnRH as our data regarding the spontaneous burst activity during estrus, met- and diestrus indicated (Figure 28). To access this scenario, we repeated the previous experiment in the presence of a

competitive antagonist for the GnRHR, namely 10 µM Cetrorelix (Halmos et al., 1996; Reissmann et al., 2000).

Idle GnRHR activity, as predicted for tonic firing GnRHR neurons during proestrus, should not be affected by the treatment with the GnRHR antagonist. Applying 10 µM Cetrorelix to tonically firing GnRHR neurons for at least 10 min did not induce any change in either the $CV_{ISI,}$ PSiB or the mean frequency during proestrus (t-test: p = 0.15 - 0.42), suggesting that the GnRHR is not activated under these circumstances (Figure 28A, B). However, bursting GnRHR neurons recorded during the three other reproductive stages and also treated for approximately 10 min with Cetrorelix, convert their originally burst firing pattern towards tonic firing. The mean spike frequency for the non-proestrus GnRHR neurons was 1.3 ± 0.7 Hz (n = 5; Figure 28C), similar to the values of the originally measured bursting GnRHR neurons (Figure 24; t-test: p = 0.07). As predicted for

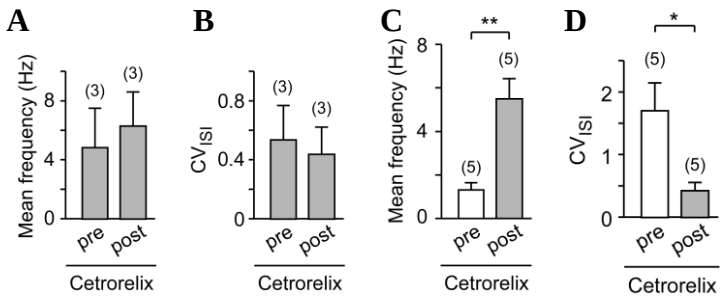

Figure 28. Effect of GnRH long-term application depends on reproductive state. A – D, Bar histogram of the mean spike frequency (A, C) and the CV_{ISI} (B, D) 4 min before the start (pre) and the last 4 min of the 10 µM Cetrorelix treatment (post) of a tonically firing GnRHR neurons during proestrus (A, B) or during estrus, met- or diestrus (C, D). T-test: ** $p < 0.01$, * $p < 0.05$. Bar coloring (grey and white) indicate to which category of firing pattern (tonic (grey), bursting (white)) the group of neurons

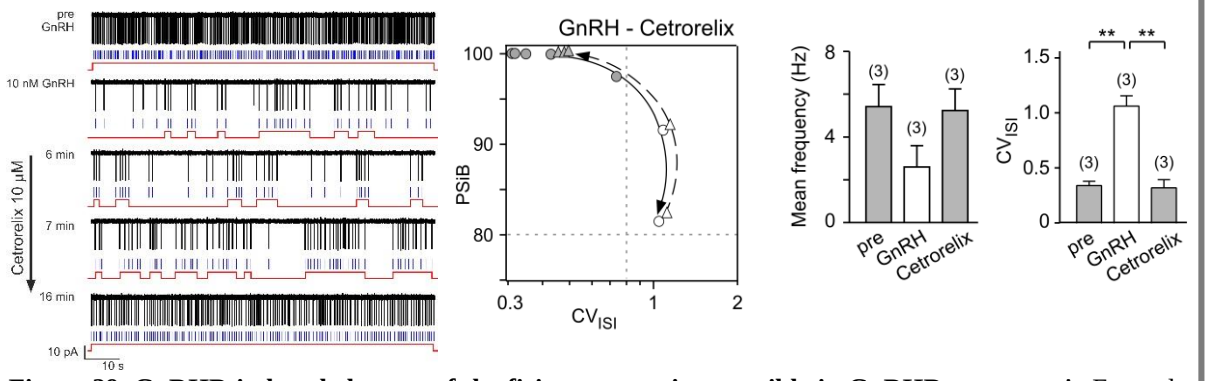

Figure 29. GnRHR induced changes of the firing pattern is reversible in GnRHR neurons. A, Example traces (original recording (black), raster diagram (blue), burst detection (red)) of trains of extracellularly recorded, action-potential-driven capacitive currents from the same GnRHR neuron of a proestrus mouse taken before GnRH stimulation (pre GnRH), 10 min after GnRH treatment and at various times after starting the 10 µM Cetrorelix perfusion. B, GnRH- and Cetrorelix-induced change in the spike activity from the same GnRHR neuron as shown in A. Dependent on the threshold values for the CV_{ISI} and the PSiB (dashed lines, see 5.4.1), the neuron fired first tonically (grey circles) and changed to a burst pattern (white circles) during the GnRH treatment. This change can be reversed by the Cetrorelix treatment whereby the burst pattern (white triangles) reverts to a tonic spike activity (grey triangles). C – D, Bar histogram of the mean spike frequency (C) and the CV_{ISI} (D) 4 min before the start (pre) and the last 4 min of either the GnRH or the Cetrorelix treatment of GnRHR neurons of mice in proestrus. The values of pre and Cetrorelix are not significantly different (Tukey: p = 0.97 and 0.98 for K and L, respectively). Tukey: ** $p < 0.01$. Bar and symbol coloring (grey and white) indicate to which category of firing pattern (tonic (grey), bursting (white)) the group of neurons belongs to.

tonic firing GnRHR neurons, the mean spike frequency increased to 5.5 ± 2.1 Hz (n = 5; Figure 29C) and the CV_{ISI} dropped from 1.7 ± 0.99 (n = 5; *pre* in Figure 29C) to 0.43 ± 0.29 (n = 5; *post* in Figure 29D).

Moreover, stimulating proestrus GnRHR neurons firing tonically with GnRH triggered the neurons to fire in bursts that could be reversed after Cetrorelix treatment (Figure 29). As seen with the innately tonic proestrus GnRHR neurons (Figure 29) these neurons reduced their mean spike frequency from 5.4 ± 1.8 Hz to 2.6 ± 1.7 Hz (n = 3; Figure 29C) and increased their CV_{ISI} from 0.34 ± 0.07 to 1.1 ± 0.16 (n = 3; Figure 29D) during the GnRH treatment (10 nM). The firing pattern changed back to their original values after 10 min Cetrorelix application (10 µM) having now a mean spike frequency of 5.2 ± 1.7 Hz and a CV_{ISI} of 0.32 ± 0.13 (n = 3; Figure 29C, D). Consequently, endogenous receptor activity regulates the neuronal spike code of GnRHR neurons even in acute brain slices. The neurons appear to be under endogenous GnRH control leading to a transformation of tonic high frequency firing to a state of bursting lower frequency firing. Moreover, it seems that endogenous GnRH has to be present during the non-proestrus stages of the reproductive cycle to induce the observed burst-firing pattern.

5.4. Discussion

GnRH plays an essential role in reproduction, is used to assist in various reproductive techniques and treatment of hormone-dependent diseases (Millar et al., 2004; Brioude et al., 2010). Modulating reproductive physiology using a central regulator, like GnRH, is contingent on the function of its target neurons expressing GnRHR. Potentially, GnRH agonists and antagonists could have undesirable effects during therapeutic applications due to the multiple brain areas containing its target neurons (Wen et al., 2011a). To investigate if the hormone GnRH could alter the neuronal activity in the central nervous system as a neurotransmitter or -modulator of GnRHR neurons and to define how GnRH stimulation may alter the function of these neurons, we started to investigate action potential discharges of hypothalamic neurons in intact female mouse brain slices during their reproductive cycle.

Our results reveal that the activity of GnRHR neurons changes and depends on endogenous GnRH. GnRHR neurons are spontaneously active and fire action potentials in three different modes: tonic, bursting or irregular. The pattern of activity depends on the female reproductive cycle. GnRHR with tonically firing are mainly present during proestrus and bursting/irregular firing GnRHR neurons during either estrus or metestrus, respectively. Tonically firing GnRHR neurons are able to respond dose-dependently to short pulses of GnRH by reducing the latency to the first spike after GnRH stimulation and by increasing the duration of a long-lasting change

in spike activity pattern. The GnRHRs in tonic firing neurons are not occupied by GnRH, since the competitive GnRH antagonist Cetrorelix has no effect on the spike behavior of these neurons. Prolonged stimulation with GnRH initiates a form of action potential plasticity, whereby tonically firing neurons are transformed to fire with a pattern of action potential bursts. Conversely, bursting GnRHR neurons seem to receive input from GnRH, which can be prevented using Cetrorelix. This causes the neurons to reset their spiking behavior to tonic. These results indicate that GnRHR neurons are ideally attuned to vascular changes in GnRH during the estrous cycle firing with brief high-frequency action potential bursts after GnRH stimulation, potentially to be more effective in transmitter release and therefore enhance communication between neurons.

5.4.1. Involvement of GnRH or estradiol

Hypothalamic GnRH is released approximately every 30 min with an increase in frequency and intensity in the late phase of proestrus (Radovick et al., 2012; Sisk et al., 2001). Estradiol levels rise during the estrous cycle peaking during proestrus (Butcher et al., 1974) and affect differentially GnRH-secreting neurons (Otani et al., 2009; Roy et al., 1999; Abe and Terasawa, 2005; Chu et al., 2009; Christian and Moenter, 2010). GnRH secretion decreases in the presence of low estradiol concentration, but is augmented at high concentrations. Interestingly, the increase in the number of tonically firing GnRHR neurons correlates with the estradiol levels during the female reproductive cycle (Figure 24), suggesting that decreased GnRH release due to estradiol alleviates GnRHR neuronal bursting activity. A direct effect of estradiol generating the tonicity of GnRHR neuron firing could be caused by preventing the activity of intrinsic cascades known to induce oscillatory spike behavior (Chu et al., 2010; Bal et al., 1995) or by estradiol modulating the local network activity (Christian and Moenter, 2007; Veliskova and Velisek, 2007). Estradiol is however more known to be an initiator of burst activity (Abe and Terasawa, 2005; Chu et al., 2009), but this seems unlikely here. The amount of bursting neurons decreases (Figure 24) with reported increase in estradiol levels (Butcher et al., 1974). In addition, non-proestrus GnRHR neurons firing in bursts can be modulated to fire tonically with the help of a GnRH antagonist for the receptor. Likewise, originally tonically firing neurons from proestrus, which are prestimulated with GnRH and therefore firing in bursts, will reverse their activity in the presence of the antagonist indicating that activation of the GnRHR causes the change in spike activity.

5.4.2. Possible role of receptor expression or internalization during the estrous cycle

Estrogen regulates gene expression and has been reported to be an important regulator of GnRHR, increasing the amount of receptors in ewe pituitary cells during estradiol treatment (Gregg et al., 1990; Turzillo et al., 1998). With increasing estradiol concentration the number of GnRHR in cultured ovine pituitary cells rise (Gregg et al., 1990). The decrease in bursting GnRHR neurons during metestrus to proestrus could hint to a loss of GnRHR in Pe neurons. The estradiol levels are however increasing during this time (Butcher et al., 1974) and would argue against an effect of estradiol on the expression of GnRHR in Pe neurons.

Internalization or desensitization of the G-protein-coupled receptor (GPCR) in response to agonist activation could account for the reduction in GnRHR activity-induced spike bursting behavior in Pe neurons and therefore cause the increase in tonic firing GnRHR neurons. However, agonist-induced GnRHR internalization, as indicated in Finch et al. (Finch et al., 2009), can be excluded, since a GnRH upsurge has to be present to induce this process. Our data correspond more with a reduction in the total amount of GnRH up to the late phase of proestrus during the estrous cycle. Moreover, type I mammalian GnRHR, which is the only GnRHR expressed in mice (Reinhart et al., 1992; Stewart et al., 2009), does not desensitize due to the lack of arrestin binding (Millar et al., 2004; Finch et al., 2009; Naor, 2009). Still, no definitive conclusion can be drawn regarding the GnRHR internalization/desensitization effect in these Pe neurons during the estrous cycle, since other not-yet identified regulatory elements or hormones may affect this process.

All lines of reasoning indicate that GnRH is the main regulator for the change in spike activity in Pe GnRHR neurons. Then again, the half-life of circulating GnRH (serum GnRH) is approximately 2-6 min (Pimstone et al., 1977), which may not be prolonged enough to induce the different action potential pattern as observed in the recordings obtained in acute slice preparations. GnRH mRNA levels have been reported to have a half-life of 22-30 hours (Gore and Roberts, 1997). If GnRH-secreting fibers are still active, even when they have been severed from their cell bodies, they may still release GnRH into the vascular system or 3V. On the other hand, GnRH could be stable for an extended period in the brain. Human patients with liver or renal dysfunction have GnRH half-life times up to 20 min (Pimstone et al., 1977), indicating that plasma GnRH levels depend on the degradation and clearance of GnRH by the liver and kidney, respectively.

5.4.3. Mechanisms underlying GnRHR-induced spike code modulation

The mechanism by which GnRH modulates and triggers the action potential pattern in a concentration-dependent manner is not yet known. GnRH acts via $Ga_{q/11}$-coupled GnRHR to activate phospholipase C (PLC) resulting in the mobilization of Ca^{2+}, but the involvement of other second messenger pathways as well as G-proteins have also been proposed [reviewed in: (Naor, 2009; Naor and Huhtaniemi, 2013)]. Using calcium imaging we observed two types of somatic Ca^{2+} transients in periventricular hypothalamic GnRHR neurons having a 25 s delay between the responses at 10 nM GnRH (Wen et al., 2011b). The latency of the GnRH-induced long-lasting change in spike activity is in a similar range, being approximately 29 s at 10 nM GnRH (Figure 26), suggesting that the underlying mechanism of the altered spike activity depends on the intracellular Ca^{2+} concentration. A possible mechanism could involve initial Ca^{2+} entry through depolarization-dependent ion channels explaining the first Ca^{2+} rise in the calcium imaging data set (Wen et al., 2011b) and the GnRH-dependent shortening of the first-spike latency (Figure 25). A secondary process that could depend on the same PLC-signaling cascade in combination with Ca^{2+} stores could initiate the pronounced change in spike activity. Possible candidates for the hyperpolarizing Ca-dependent or PLC-dependent pathways could be channels of the Trp superfamily and of the Ca_v family (Lee et al., 2008; Fowler et al., 2007; Kunert-Keil et al., 2006). Future experiments need to clarify the involvement of these pathways in regulating the GnRHR neuron activity.

5.5. References

1 ABE, H. & TERASAWA, E. 2005. Firing pattern and rapid modulation of activity by estrogen in primate luteinizing hormone releasing hormone-1 neurons. Endocrinology, 146, 4312-20.

2 BAL, T., VON KROSIGK, M. & MCCORMICK, D. A. 1995. Role of the ferret perigeniculate nucleus in the generation of synchronized oscillations in vitro. J Physiol, 483 (Pt 3), 665-85.

3 BARRAN, P. E., ROESKE, R. W., PAWSON, A. J., SELLAR, R., BOWERS, M. T., MORGAN, K., LU, Z. L., TSUDA, M., KUSAKABE, T. & MILLAR, R. P. 2005. Evolution of constrained gonadotropin-releasing hormone ligand conformation and receptor selectivity. J Biol Chem, 280, 38569-75.

4 BOEHM, U., ZOU, Z. & BUCK, L. B. 2005. Feedback loops link odor and pheromone signaling with reproduction. Cell, 123, 683-95.

5 BRIOUDE, F., BOULIGAND, J., TRABADO, S., FRANCOU, B., SALENAVE, S., KAMENICKY, P., BRAILLY-TABARD, S., CHANSON, P., GUIOCHON-MANTEL, A. & YOUNG, J. 2010. Non-syndromic congenital hypogonadotropic hypogonadism: clinical presentation and genotype-phenotype relationships. Eur J Endocrinol, 162, 835-51.

6 BUTCHER, R. L., COLLINS, W. E. & FUGO, N. W. 1974. Plasma concentration of LH, FSH, prolactin, progesterone and estradiol-17beta throughout the 4-day estrous cycle of the rat. Endocrinology, 94, 1704-8.

7 CARATY, A. & SKINNER, D. C. 2008. Gonadotropin-releasing hormone in third ventricular cerebrospinal fluid: endogenous distribution and exogenous uptake. Endocrinology, 149, 5227-34.

8 CHRISTIAN, C. A. & MOENTER, S. M. 2007. Estradiol induces diurnal shifts in GABA transmission to gonadotropin-releasing hormone neurons to provide a neural signal for ovulation. J Neurosci, 27, 1913-21.

9 CHRISTIAN, C. A. & MOENTER, S. M. 2010. The neurobiology of preovulatory and estradiol-induced gonadotropin-releasing hormone surges. Endocr Rev, 31, 544-77.

10 CHU, Z., ANDRADE, J., SHUPNIK, M. A. & MOENTER, S. M. 2009. Differential regulation of gonadotropin-releasing hormone neuron activity and membrane properties by acutely applied estradiol: dependence on dose and estrogen receptor subtype. J Neurosci, 29, 5616-27.

11 CHU, Z., TAKAGI, H. & MOENTER, S. M. 2010. Hyperpolarization-activated currents in gonadotropin-releasing hormone (GnRH) neurons contribute to intrinsic excitability and are regulated by gonadal steroid feedback. J Neurosci, 30, 13373-83.

12 CONN, P. M. & HAZUM, E. 1981. Luteinizing hormone release and gonadotropin-releasing hormone (GnRH) receptor internalization: independent actions of GnRH. Endocrinology, 109, 2040-5.

13 DAHAN, L., ASTIER, B., VAUTRELLE, N., URBAIN, N., KOCSIS, B. & CHOUVET, G. 2007. Prominent burst firing of dopaminergic neurons in the ventral tegmental area during paradoxical sleep. Neuropsychopharmacology, 32, 1232-41.

14 DEL PUNTA, K., LEINDERS-ZUFALL, T., RODRIGUEZ, I., JUKAM, D., WYSOCKI, C. J., OGAWA, S., ZUFALL, F. & MOMBAERTS, P. 2002. Deficient pheromone responses in mice lacking a cluster of vomeronasal receptor genes. Nature, 419, 70-4.

15 FINCH, A. R., CAUNT, C. J., ARMSTRONG, S. P. & MCARDLE, C. A. 2009. Agonist-induced internalization and downregulation of gonadotropin-releasing hormone receptors. Am J Physiol Cell Physiol, 297, C591-600.

16 FOWLER, M. A., SIDIROPOULOU, K., OZKAN, E. D., PHILLIPS, C. W. & COOPER, D. C. 2007. Corticolimbic expression of TRPC4 and TRPC5 channels in the rodent brain. PLoS One, 2, e573.

17 GARIANO, R. F. & GROVES, P. M. 1988. Burst firing induced in midbrain dopamine neurons by stimulation of the medial prefrontal and anterior cingulate cortices. Brain Research, 462, 194-198.

18 GORE, A. C. & ROBERTS, J. L. 1997. Regulation of gonadotropin-releasing hormone gene expression in vivo and in vitro. Front Neuroendocrinol, 18, 209-45.

19 GRACE, A. A. & BUNNEY, B. S. 1984. The control of firing pattern in nigral dopamine neurons: burst firing. J Neurosci, 4, 2877-90.

20 GREGG, D. W., ALLEN, M. C. & NETT, T. M. 1990. Estradiol-induced increase in number of gonadotropin-releasing hormone receptors in cultured ovine pituitary cells. Biol Reprod, 43, 1032-6.

21 HAGA, S., HATTORI, T., SATO, T., SATO, K., MATSUDA, S., KOBAYAKAWA, R., SAKANO, H., YOSHIHARA, Y., KIKUSUI, T. & TOUHARA, K. 2010. The male mouse pheromone ESP1 enhances female sexual receptive behaviour through a specific vomeronasal receptor. Nature, 466, 118-22.

22 HALMOS, G., SCHALLY, A. V., PINSKI, J., VADILLO-BUENFIL, M. & GROOT, K. 1996. Down-regulation of pituitary receptors for luteinizing hormone-releasing hormone (LH-RH) in rats by LH-RH antagonist Cetrorelix. Proc Natl Acad Sci U S A, 93, 2398-402.

23 HERDE, M. K., GEIST, K., CAMPBELL, R. E. & HERBISON, A. E. 2011. Gonadotropin-releasing hormone neurons extend complex highly branched dendritic trees outside the blood-brain barrier. Endocrinology, 152, 3832-41.

24 INSEL, T. R. & FERNALD, R. D. 2004. How the brain processes social information: searching for the social brain. Annu Rev Neurosci, 27, 697-722.

25 JACKSON, M. E., HOMAYOUN, H. & MOGHADDAM, B. 2004. NMDA receptor hypofunction produces concomitant firing rate potentiation and burst activity reduction in the prefrontal cortex. Proc Natl Acad Sci U S A, 101, 8467-72.

26 KUNERT-KEIL, C., BISPING, F., KRÜGER, J. & BRINKMEIER, H. 2006. Tissue-specific expression of TRP channel genes in the mouse and its variation in three different mouse strains. BMC Genomics, 7, 1-14.

27 LEE, S., HAN, T. H., SONNER, P. M., STERN, J. E., RYU, P. D. & LEE, S. Y. 2008. Molecular characterization of T-type Ca2+ channels responsible for low threshold spikes in hypothalamic paraventricular nucleus neurons. Neuroscience, 155, 1195-1203.

28 LEINDERS-ZUFALL, T., BRENNAN, P., WIDMAYER, P., S, P. C., MAUL-PAVICIC, A., JAGER, M., LI, X. H., BREER, H., ZUFALL, F. & BOEHM, T. 2004. MHC class I peptides as chemosensory signals in the vomeronasal organ. Science, 306, 1033-7.

29 LEINDERS-ZUFALL, T., ISHII, T., MOMBAERTS, P., ZUFALL, F. & BOEHM, T. 2009. Structural requirements for the activation of vomeronasal sensory neurons by MHC peptides. Nat Neurosci, 12, 1551-8.

30 LEINDERS-ZUFALL, T., LANE, A. P., PUCHE, A. C., MA, W., NOVOTNY, M. V., SHIPLEY, M. T. & ZUFALL, F. 2000. Ultrasensitive pheromone detection by mammalian vomeronasal neurons. Nature, 405, 792-6.

31 LU, Z. L., GALLAGHER, R., SELLAR, R., COETSEE, M. & MILLAR, R. P. 2005. Mutations remote from the human gonadotropin-releasing hormone (GnRH) receptor-binding sites specifically increase binding affinity for GnRH II but not GnRH I: evidence for ligand-selective, receptor-active conformations. J Biol Chem, 280, 29796-803.

32 MILLAR, R. P., LU, Z. L., PAWSON, A. J., FLANAGAN, C. A., MORGAN, K. & MAUDSLEY, S. R. 2004. Gonadotropin-releasing hormone receptors. Endocr Rev, 25, 235-75.

33 MOENTER, S. M., ANTHONY DEFAZIO, R., PITTS, G. R. & NUNEMAKER, C. S. 2003. Mechanisms underlying episodic gonadotropin-releasing hormone secretion. Frontiers in Neuroendocrinology, 24, 79-93.

34 MOENTER, S. M., BRAND, R. M., MIDGLEY, A. R. & KARSCH, F. J. 1992. Dynamics of gonadotropin-releasing hormone release during a pulse. Endocrinology, 130, 503-10.

35 MOSS, R. L. & FOREMAN, M. M. 1976. Potentiation of lordosis behavior by intrahypothalamic infusion of synthetic luteinizing hormone-releasing hormone. Neuroendocrinology, 20, 176-81.

36 MOSS, R. L. & MCCANN, S. M. 1973. Induction of mating behavior in rats by luteinizing hormone-releasing factor. Science, 181, 177-9.

37 NAOR, Z. 2009. Signaling by G-protein-coupled receptor (GPCR): studies on the GnRH receptor. Front Neuroendocrinol, 30, 10-29.

38 NAOR, Z. & HUHTANIEMI, I. 2013. Interactions of the GnRH receptor with heterotrimeric G proteins. Front Neuroendocrinol, 34, 88-94.

39 OTANI, H., OTSUKA, F., TAKEDA, M., MUKAI, T., TERASAKA, T., MIYOSHI, T., INAGAKI, K., SUZUKI, J., OGURA, T., LAWSON, M. A. & MAKINO, H. 2009. Regulation of GNRH production by estrogen and bone morphogenetic proteins in GT1-7 hypothalamic cells. J Endocrinol, 203, 87-97.

40 PFAFF, D. W. 1973. Luteinizing hormone-releasing factor potentiates lordosis behavior in hypophysectomized ovariectomized female rats. Science, 182, 1148-9.

41 PIMSTONE, B., EPSTEIN, S., HAMILTON, S. M., LEROITH, D. & HENDRICKS, S. 1977. Metabolic clearance and plasma half disappearance time of exogenous gonadotropin releasing hormone in normal subjects and in patients with liver disease and chronic renal failure. J Clin Endocrinol Metab, 44, 356-60.

42 RADOVICK, S., LEVINE, J. E. & WOLFE, A. 2012. Estrogenic regulation of the GnRH neuron. Front Endocrinol (Lausanne), 3, 52.

43 REINHART, J., MERTZ, L. M. & CATT, K. J. 1992. Molecular cloning and expression of cDNA encoding the murine gonadotropin-releasing hormone receptor. J Biol Chem, 267, 21281-4.

44 REISSMANN, T., SCHALLY, A. V., BOUCHARD, P., RIETHMIILLER, H. & ENGEL, J. 2000. The LHRH antagonist cetrorelix: a review. Hum Reprod Update, 6, 322-31.

45 ROBIN, K., MAURICE, N., DEGOS, B., DENIAU, J. M., MARTINERIE, J. & PEZARD, L. 2009. Assessment of bursting activity and interspike intervals variability: a case study for methodological comparison. J Neurosci Methods, 179, 142-9.

46 ROSPARS, J. P., LANSKY, P., DUCHAMP, A. & DUCHAMP-VIRET, P. 2003. Relation between stimulus and response in frog olfactory receptor neurons in vivo. Eur J Neurosci, 18, 1135-54.

47 ROY, D., ANGELINI, N. L. & BELSHAM, D. D. 1999. Estrogen directly respresses gonadotropin-releasing hormone (GnRH) gene expression in estrogen receptor-alpha (ERalpha)- and ERbeta-expressing GT1-7 GnRH neurons. Endocrinology, 140, 5045-53.

48 SAPER, C. B. 2012. Chapter 16 - Hypothalamus. In: MAI, J. K. & PAXINOS, G. (eds.) The Human Nervous System (Third Edition). San Diego: Academic Press.

49 SCHAUER, C. & LEINDERS-ZUFALL, T. 2012. Imaging calcium responses in GFP-tagged neurons of hypothalamic mouse brain slices. J Vis Exp, e4213.

50 SCHWANZEL-FUKUDA, M. & PFAFF, D. W. 1989. Origin of luteinizing hormone-releasing hormone neurons. Nature, 338, 161-4.

51 SELINGER, J. V., KULAGINA, N. V., O'SHAUGHNESSY, T. J., MA, W. & PANCRAZIO, J. J. 2007. Methods for characterizing interspike intervals and identifying bursts in neuronal activity. J Neurosci Methods, 162, 64-71.

52 SISK, C. L., RICHARDSON, H. N., CHAPPELL, P. E. & LEVINE, J. E. 2001. In vivo gonadotropin-releasing hormone secretion in female rats during peripubertal development and on proestrus. Endocrinology, 142, 2929-36.

53 SKINNER, D. C., CARATY, A., MALPAUX, B. & EVANS, N. P. 1997. Simultaneous measurement of gonadotropin-releasing hormone in the third ventricular cerebrospinal fluid and hypophyseal portal blood of the ewe. Endocrinology, 138, 4699-704.

54 STEWART, A. J., KATZ, A. A., MILLAR, R. P. & MORGAN, K. 2009. Retention and silencing of prepro-GnRH-II and type II GnRH receptor genes in mammals. Neuroendocrinology, 90, 416-32.

55 TIRINDELLI, R., DIBATTISTA, M., PIFFERI, S. & MENINI, A. 2009. From pheromones to behavior. Physiol Rev, 89, 921-56.

56 TURZILLO, A. M., NOLAN, T. E. & NETT, T. M. 1998. Regulation of gonadotropin-releasing hormone (GnRH) receptor gene expression in sheep: interaction of GnRH and estradiol. Endocrinology, 139, 4890-4.

57 VELISKOVA, J. & VELISEK, L. 2007. Beta-estradiol increases dentate gyrus inhibition in female rats via augmentation of hilar neuropeptide Y. J Neurosci, 27, 6054-63.

58 WEN, J., FENG, Y., BJORKLUND, C. C., WANG, M., ORLOWSKI, R. Z., SHI, Z. Z., LIAO, B., O'HARE, J., ZU, Y., SCHALLY, A. V. & CHANG, C. C. 2011a. Luteinizing Hormone-Releasing Hormone (LHRH)-I antagonist cetrorelix inhibits myeloma cell growth in vitro and in vivo. Mol Cancer Ther, 10, 148-58.

59 WEN, S., GOTZE, I. N., MAI, O., SCHAUER, C., LEINDERS-ZUFALL, T. & BOEHM, U. 2011b. Genetic identification of GnRH receptor neurons: a new model for

studying neural circuits underlying reproductive physiology in the mouse brain. Endocrinology, 152, 1515-26.

60 WRAY, S., GRANT, P. & GAINER, H. 1989. Evidence that cells expressing luteinizing hormone-releasing hormone mRNA in the mouse are derived from progenitor cells in the olfactory placode. Proc Natl Acad Sci U S A, 86, 8132-6.

61 YOON, H., ENQUIST, L. W. & DULAC, C. 2005. Olfactory inputs to hypothalamic neurons controlling reproduction and fertility. Cell, 123, 669-82.

6. Discussion

GnRH has been implicated to regulate different hormonal and physiological signals in the brain. This master molecule of reproduction and its analogs are used in various types of assisted reproductive techniques, treatment of hormone-dependent diseases and several cancer therapies (Millar et al., 2004; Brioude et al., 2010; Naor, 2009; Limonta et al., 2012). Nevertheless, the functional role of its target receptor, the GnRHR, in the central nervous system has been remained unclear due to the absence of models that permit the identification of GnRHR expressing neurons in live brain tissue.

To overcome this problem, a genetic strategy to identify GnRHR neurons was used. Therefore, GnRHR-internal ribosome entry site-Cre (GRIC) mice were crossbred to ROSA26-CAGS-tauGFP (eR26-τGFP) mice leading to the generation of GnRHR/eR26-τGFP offspring, which show an irreversible Cre-mediated activation of the τGFP reporter in GnRHR positive cells under the control of the enhanced ROSA26 promoter (Wen et al., 2011; Wen et al., 2008). However, due to the breeding scheme, GnRHR could have been expressed during development and just due to the original activation of the promoter Cre is being expressed, activating the expression of τGFP. It was unclear if these genetically marked neurons in this model still express the receptor for GnRH. Normally, antibody staining could have been used, but unfortunately, the antibody against GnRHR is very unreliable and another approach was necessary to check if GnRHR/eR26-τGFP mice express a functional GnRHR in hypothalamic neurons. To facilitate this effort we developed a novel protocol for the preparation of coronal hypothalamic brain slices and Ca^{2+} imaging in GFP-labelled neurons. The red-shifted Ca^{2+} indicator dye fura-red, which allows imaging both, Ca^{2+} signals as well as the GFP-labelling of the neurons, synchronously, was used. The huge difference in the stokes shift of fura-red/AM and GFP permits the parallel real time analysis of both emission signals using one single excitation wavelength. Using this approach, we could show that τGFP-labeled GnRHR neurons responded reproducibly to the extracellular application of GnRH and its analog. This confirms that the tested neurons express a functional GnRH receptor. Even under reduced synaptic activity, caused by blocking action potential network activity, GnRHR neurons respond in similar manner.

Interestingly the GnRHR neurons respond in nucleus specific manner to the stimulation with GnRH. The duration and form of the Ca^{2+} response relates on the nucleus, as well on the applied concentration of GnRH. This indicates the existence of various populations, which may differ by specific pattern of innervation. Furthermore different signal transduction pathways might be

activated depending on area, stimulus duration and stimulus concentration (Naor, 2009; Tsutsumi et al., 2010).

The level of endogenous GnRH in the brain changes during the estrus cycle. It is released in a pulsatile way, but before estrus GnRH release intensifies. This increase in GnRH is needed for the induction of ovulation. To investigate if the change of endogenous GnRH level in the brain alters the neuronal activity of GnRHR neurons, we started to investigate spontaneous action potential discharges of hypothalamic neurons in intact female mouse brain slices during their reproductive cycle. The analysis of possible firing properties for characterizing the basic activity pattern of GnRHR neurons allowed us to identify the Variation of the InterSpike Interval (CV_{ISI}), Percentage of Spikes in Bursts (PSiB) (Dahan et al., 2007; Grace and Bunney, 1984), Mean number of Spikes in each Burst (MSiB) (Jackson et al., 2004; Gariano and Groves, 1988) and mean spike frequency (mf) as the principal properties. A combination of these properties permits an unambiguous classification of firing activity pattern in tonically, bursting and irregular firing neurons in GnRHR.

Interestingly the distribution of firing pattern changes during the reproductive stages equal as the levels endogenous GnRH change. The pattern of activity depends on the female reproductive cycle with mainly tonically firing GnRHR neurons being present during proestrus, and bursting/irregular firing GnRHR neurons during either estrus or metestrus, respectively. Tonically firing GnRHR neurons respond dose-dependently to short pulses of GnRH by reducing the latency to the first spike after GnRH stimulation and by increasing the duration of a long-lasting change in spike activity pattern. The GnRHRs in tonic firing neurons are not occupied by GnRH, since the competitive GnRH antagonist Cetrorelix has no effect on the spike behavior of these neurons. Prolonged stimulation with GnRH initiates a form of action potential plasticity, whereby tonically firing neurons are transformed to fire with a pattern of action potential bursts. Conversely, bursting and irregular GnRHR neurons seem to receive input from GnRH, which can be prevented using Cetrorelix. This causes the neurons to reset their spiking behavior to tonic.

Mimicking the changes of endogenous GnRH levels in brain by the stimulation of GnRHR neurons with longtime exposure to GnRH could change the firing pattern as well as the exposure to the competitive GnRH antagonist Cetrorelix can reverse this effect. These results reveal that the firing activity of GnRHR neurons changes and depends on endogenous GnRH. These results indicate that GnRHR neurons are ideally attuned to vascular changes in GnRH during the estrous cycle firing with brief high-frequency action potential bursts after GnRH

stimulation, potentially to be more effective in transmitter release and therefore enhance communication between neurons.

The influence of other hormones like estradiol remains unclear. Estradiol is known to be an initiator of burst activity (Abe and Terasawa, 2005; Chu et al., 2009), but the reported estradiol levels during reproductive cycle (Butcher et al., 1974) – showing a peak during proestrus - and the amount of bursting neurons observed behave contrary. Furthermore, it has been published, that estradiol regulates by gene expression the amount of GnRHR expressed in hypothalamic neurons. In cultured ovine pituitary cells increasing estradiol concentration induced an increased number of GnRHR (Gregg et al., 1990), which would result in an tendency to tonic firing behavior. However, during metestrus to proestrus estradiol level increases (Butcher et al., 1974) what would contrary to our results lead to an decrease o tonic firing neurons.

Internalization or desensitization of the G-protein-coupled receptor (GPCR) in response to agonist activation could account for the reduction in GnRHR activity-induced spike bursting behavior in Pe neurons and therefore cause the increase in tonic firing GnRHR neurons. However, agonist-induced GnRHR internalization, as indicated in Finch et al. (Finch et al., 2009), can be excluded, since a GnRH upsurge has to be present to induce this process. Our data correspond more with a reduction in the total amount of GnRH up to the late phase of proestrus during the estrous cycle. Still, no definitive conclusion can be drawn regarding the GnRHR internalization/desensitization effect in these Pe neurons during the estrous cycle, since other not-yet identified regulatory elements or hormones may affect this process.

All lines of reasoning indicate that GnRH is the main regulator for the change in spike activity in Pe GnRHR neurons, butthe source of GnRH in the periventricular hypothalamic nucleus (Pe) remains unclear. Many cerebral capillaries are observed in the Pe, which is located next to the third ventricle. At this point, it cannot be excluded that GnRHR neurons are synaptically innervated by GnRH-secreting neurons, but the dependence of the action potential activity on the estrous cycle suggests that the activity of periventricular hypothalamic GnRHR neurons is modified by the GnRH released into blood and cerebrospinal fluid. More detailed studies regarding the source of GnRH using high resolution imaging techniques and immunohistochemic techniques are necessary to clarify this question.

6.1. References

1 ABE, H. & TERASAWA, E. 2005. Firing pattern and rapid modulation of activity by estrogen in primate luteinizing hormone releasing hormone-1 neurons. Endocrinology, 146, 4312-20.

2 BRIOUDE, F., BOULIGAND, J., TRABADO, S., FRANCOU, B., SALENAVE, S., KAMENICKY, P., BRAILLY-TABARD, S., CHANSON, P., GUIOCHON-MANTEL, A. & YOUNG, J. 2010. Non-syndromic congenital hypogonadotropic hypogonadism: clinical presentation and genotype-phenotype relationships. Eur J Endocrinol, 162, 835-51.

3 BUTCHER, R. L., COLLINS, W. E. & FUGO, N. W. 1974. Plasma concentration of LH, FSH, prolactin, progesterone and estradiol-17beta throughout the 4-day estrous cycle of the rat. Endocrinology, 94, 1704-8.

4 CHU, Z., ANDRADE, J., SHUPNIK, M. A. & MOENTER, S. M. 2009. Differential regulation of gonadotropin-releasing hormone neuron activity and membrane properties by acutely applied estradiol: dependence on dose and estrogen receptor subtype. J Neurosci, 29, 5616-27.

5 FINCH, A. R., CAUNT, C. J., ARMSTRONG, S. P. & MCARDLE, C. A. 2009. Agonist-induced internalization and downregulation of gonadotropin-releasing hormone receptors. Am J Physiol Cell Physiol, 297, C591-600.

6 GREGG, D. W., ALLEN, M. C. & NETT, T. M. 1990. Estradiol-induced increase in number of gonadotropin-releasing hormone receptors in cultured ovine pituitary cells. Biol Reprod, 43, 1032-6.

7 LIMONTA, P., MONTAGNANI MARELLI, M., MAI, S., MOTTA, M., MARTINI, L. & MORETTI, R. M. 2012. GnRH receptors in cancer: from cell biology to novel targeted therapeutic strategies. Endocr Rev, 33, 784-811.

8 MILLAR, R. P., LU, Z. L., PAWSON, A. J., FLANAGAN, C. A., MORGAN, K. & MAUDSLEY, S. R. 2004. Gonadotropin-releasing hormone receptors. Endocr Rev, 25, 235-75.

9 NAOR, Z. 2009. Signaling by G-protein-coupled receptor (GPCR): studies on the GnRH receptor. Front Neuroendocrinol, 30, 10-29.

10 TSUTSUMI, R., MISTRY, D. & WEBSTER, N. J. 2010. Signaling responses to pulsatile gonadotropin-releasing hormone in LbetaT2 gonadotrope cells. J Biol Chem, 285, 20262-72.

11 WEN, S., GOTZE, I. N., MAI, O., SCHAUER, C., LEINDERS-ZUFALL, T. & BOEHM, U. 2011. Genetic identification of GnRH receptor neurons: a new model for

studying neural circuits underlying reproductive physiology in the mouse brain. Endocrinology, 152, 1515-26.

12 WEN, S., SCHWARZ, J. R., NICULESCU, D., DINU, C., BAUER, C. K., HIRDES, W. & BOEHM, U. 2008. Functional characterization of genetically labeled gonadotropes. Endocrinology, 149, 2701-11.

7. Publications

2014 **SCHAUER, C.,** TONG, T.**,** PETITJEAN, H., MAI, O., BOEHM, U. & LEINDERS-ZUFALL, T. 2014. Hypothalamic GnRH-Receptor neuron activity alternates during female reproductive cycle: GnRH generates burst firing behavior prior to ovulation. In preparation

2012 **SCHAUER, C.** & LEINDERS-ZUFALL, T. 2012. Imaging calcium responses in GFP-tagged neurons of hypothalamic mouse brain slices. J Vis Exp, e4213.

2011 WEN, S., GOTZE, I. N., MAI, O., **SCHAUER, C.**, LEINDERS-ZUFALL, T. & BOEHM, U. 2011. Genetic identification of GnRH receptor neurons: a new model for studying neural circuits underlying reproductive physiology in the mouse brain. Endocrinology, 152, 1515-26

PERMISSION TO USE COPYRIGHTED WORKS IN A PUBLICATION

Journal of Visualized Experiments (JoVE)

17 Sellers St., Cambridge, MA 02139

Dear Christian Schauer:

This letter is to confirm you are granted permission to use your JoVE publication, ID number 4213, in your dissertation.

The JoVE publication will need to be cited for the appropriate chapters/sections:

Schauer, C., Leinders-Zufall, T. Imaging Calcium Responses in GFP-tagged Neurons of Hypothalamic Mouse Brain Slices. J. Vis. Exp. (66), e4213, doi:10.3791/4213 (2012).

Best wishes, and many congratulations on your dissertation,

Adria Gottesman-Davis

PERMISSION GRANTED FOR THE USE REQUESTED ABOVE:

By: Adria Gottesman-Davis
Title: Deputy Content Director, Journal of Visualized Experiments
Date: 12/19/12

The Endocrine Society
8401 Connecticut Avenue, Suite 900
Chevy Chase, MD 20815-5817
Telephone: 301-941-0200
Fax: 301-941-0259
www.endo-society.org
TIN Number: 73-0531256
Original author to publish in a Dissertation.
Date: December 18, 2012

Name: Christian Schauer
Organization: University of Saarland
Department: Physiology
Address: Kirrbergerstrasse1, Geb. 45.2
City, State and Postal Code: Homburg, 66421
Country: Germany
Phone: +49 6841 1626576

Journal: Endocrinology
Author Name: C Schauer
Title: Genetic Identification of GnRH Receptor Neurons: A New Model for Studying Neural Circuits Underlying Reproductive Physiology in the Mouse Brain
Year: 2011
Volume: 152
Page Range: 1515-1526
Figure Reproduction:
Figure Number(s): Fig.1, Fig.2, Fig.3, Fig.4, Fig.5, Fig.6, Fig.7, Table 1.

Where will the figures appear:
Dissertation
Title: GnRH-induced calcium signals and spike activity in GnRHR neurons: Change in activity during reproductive cycle?
Publisher: Schauer, Christian

The Endocrine Society grants permission to reproduce tables/figures Fig.1, Fig.2, Fig.3, Fig.4, Fig.5, Fig.6, Fig.7 and Table 1. from the selected article stated above contingent upon the following conditions: 1) That you give proper credit to the author(s) and to include in your citation, the title of journal, title of article, volume, issue number, date, and page numbers. 2) That you include the statement Copyright 2011, The Endocrine Society. Please understand that permission is granted for one-time use only. Permission must be requested separately for future editions, revisions, translations, derivative works, and promotional pieces.

Title: Journal Publications Coordinator
Date: December 18, 2012

8. Acknowlegements

First, I like to thank to Prof. Trese Leinders-Zufall for trusting in my scientific competence and giving me the opportunity to realize this work in her laboratory. She gave me the possibility to develop myself scientifically in a positive and highly professional environment, always being attendant without limiting the space necessary to create own ideas, strategies and solutions and to work independently, to develop my own individual way to do science. In addition, I want to thank Prof. Ulrich Boehm who walked with me a long way in bad and in good days, from a to o, trusted in my abilities and always supported me scientifically as well as personally.

I would also like to thank to Prof. Frank Zufall for his positive input and his critic view because only critics help to improve. A special thank goes to Mrs. Tong Tong, who collaborated with me in an excellent and indefatigable way in developing the electrophysiologic part of this project, as well as in recording and analyzing the obtained data. As well, I want to thank Gabriele Mörschbächer for all her help and the organizational work she did. Additionally, I want to thank to Iris Goetze for her help in creating the Ca2+ Imaging data.

I want to thank to the Deutsche Forschungsgemeinschaft for supporting this work financially as a part of the Schwerpunktprogramm 1392 - “Integrative analysis of olfaction”.

Furthermore, I want to thank to Micheal Konzmann, Katherin Bleymehl, Thomas Blum and Anabel Perez-Gomez for motivating and being responsible for a happy and positive atmosphere in the laboratory, what allows one to see work not as an obligation and necessary part of life, but as a happy and nice part. I would like to acknowledge all members of the Leinder-Zufall/Zufall Labs who always had time and voluntariness to help if necessary. A special thank goes to PD Andreas Schmid, who apart from his useful advices in neurophysiologic questions as well taught me a lot about classic disciplines of biology, especially entomology and ornithology.

Finally, I want to thank my wife and my family for supporting me always without any doubts and motivating me to my own way.

Last, but not least, goes a big thanks to Timo and Eva Schuman and Katherin Bleymehl, because without them the Saarland and Rocklands would be a lonely and sad place.